

https://dspace.org/

The laboratory determination of young's modulus for an expansive clay with particular reference to stiffened raft foundation design

David, Richard

2015-01-19
http://hdl.handle.net/10539/16601

Downloaded from a DSpace repository. https://dspace.org/



THE LABORATORY DETERMINATION OF YOUNG'S MODULUS FOR AN EXPANSIVE CLAY WITH PARTICULAR REFERENCE TO STIFFENED RAFT FOUNDATION DESIGN.

declaration

I declare that this project report is my own unaided work. It is being submitted for the Degree of Master of Science in Engineering in the University of the Witwatersrand, Johannesburg. It has not been submitted before for any degree or examination at any other University.

(Signature of Candidate)

29 day of May 1990

ABSTRACT

All methods of stiffened raft foundation design for expansive soils require an estimate of the underlying soil stiffness albeit that this parameter is expressed in different ways depending on the design parameters employed. However, there is no generally accepted method to determine soil stiffness, either in the laboratory or in the field.

In this work oedometer and triaxial tests were conducted on highly expansive Onderstepoort clay to determine the range of modulus values that the different tests would give. The triaxial tests were as follows: drained and undrained triaxial tests and confined and unconfined triaxial tests on samples held at constant moisture contents. The oedometer tests conducted were as follows : swell under load tests, compression at constant moisture content tests, swell under load tests with subsequent unloading and reloading and constant rate of strain oedometer tests.

The criterion that is used to evaluate which is the best test depends on how closely the field stress path is followed in the laboratory. A recommended test is consequently the swell under load test because this test models, fairly closely, the interaction of the raft with the soil once the soil beneath it begins to swell. Further, modulus values from this test correlate very well with the modulus required to predict actual raft behaviour using a finite element program. Triaxial tests on saturated samples were considered to be unrealistic because of the small strains involved.

To Ami, Leon and Sara

Acknowledgements

I believe that writing a report of this nature is very much like scaling a peak of a large mountain. Usually only one person is remembered for being the first to reach the top, but in reality, the feat would not have been possible without the support of many different people and organisations.

In this case my Supervisor, Professor Blight, was an invaluable source of encouragement and assistance. He not only proposed the topic, but he also arranged for generous financial support.

This work was predominantly funded by grants from the local consulting firm Steffen Robertson and Kirsten and the Foundation for Research and Development of the CSIR. I would therefore like to extend my thanks to these two organisations for their assistance.

I would also like to thank Graeme Bailey for building some of the equipment used in this project. Lastly, much gratitude is also due to Norman Alexander who, with great patience, coached me in the laboratory testing techniques.

1.0 Table of Contents

2.0 List of Illustrations **10**

3.0 List of Tables. **13**

4.0 Introduction. **14**

LITERATURE SURVEY **16**

5.0 General Principles in Expansive Soil Technology. **17**

5.1 Effective Stresses in Partially Saturated Soils 17

5.2 Soil Suction in Partially Saturated Soils 19

5.3 The Axis-Translation Technique 24

5.4 Mechanism of Swell Below Buildings and Associated Structural Measures. 27

5.5 Summary 28

6.0 The Equivalent E-Value in Stiffened Raft Foundation Design. **30**

6.1 Introduction to Stiffened Raft Foundation Design. 30

6.2 Definition of Soil Stiffness in raft design techniques 32

6.2.1 Lytton's design method (1971): 32

6.2.2 Design method proposed by Walsh (1978): 33

6.2.3 Design method proposed by Mitchell (1980): 35

6.2.4 Finite element program developed by Fraser and Wardle (1975): 36

6.2.5 The Post Tensioning Institute Method: 36

6.2.6 Design method proposed by Pidgeon (1988). 37

6.3 Equilibrium conditions below raft foundations 41

6.4 Summary 44

7.0 Young's Modulus as Determined by the Triaxial Apparatus. **46**

7.1 Introduction. 46

7.2 The use of triaxial apparatus to determine the stiffness of saturated clays. 46
7.3 Testing of Partially Saturated Soils in the Triaxial Apparatus 51
7.3.1 Introduction 51
7.3.2 Modifications to the Triaxial Apparatus 52
7.3.3 Testing procedures for partially saturated soils 53
7.3.4 Additional problems associated with triaxial testing of partially saturated soils 55
7.4 Summary 56

8.0 The use of Consolidometers in Expansive Soils Technology. 57
8.1 Introduction. 57
8.2 The Membrane Oedometer: 58
8.3 Consolidometer developed by Escario and Saez (1973): 60
8.4 Controlled suction consolidometer developed by Chu and Mou (1973): 61
8.5 Suction controlled consolidometer developed by Richards, Peter and Martin (1984). 64
8.6 Constant-rate-of-strain consolidometers: 68
8.7 Corrections to be applied to the Consolidometer results. 71
8.8 Summary 72

PRESENTATION OF THE EXPERIMENTAL RESULTS 74

9.0 Explanation of the Experimental Design. 75

10.0 Material Description. 76

11.0 Triaxial Tests. 81
11.1 Introduction 81
11.2 Triaxial Tests on Saturated Samples 82
11.2.1 Experimental technique 82
11.2.2 Discussion of the stress-strain curves. 83
11.2.3 Discussion of the p-q plots 85
11.3 Triaxial Tests on Partially Saturated Samples. 94

11.3.1 Experimental Procedure. 94
11.3.2 Discussion of the results 94
11.4 Measured Triaxial Moduli Related to Stiffened Raft Design 99

12.0 The Oedometer Test. 100
12.1 Introduction 100
12.2 Swell under load tests. 101
12.2.1 Introduction 101
12.2.2 Experimental Technique 102
12.2.3 Discussion of the results 102
12.3 Oedometer tests on saturated samples 110
12.3.1 Test Objective. 110
12.3.2 Experimental Procedure 110
12.3.3 Discussion of the results. 110
12.4 Oedometer Compression Tests at Constant Moisture Content 114
12.4.1 Experimental Technique 114
12.4.2 Discussion of the Results 114
12.5 Constant Rate of Strain Oedometer. 120
12.5.1 Experimental Procedure. 120
12.5.2 Presentation of the results 120
12.6 Measured Oedometer Moduli Related to Raft Design. 125

CONCLUSIONS AND RECCOMENDATIONS. 126

13.0 Laboratory and Field Moduli Compared. 127

14.0 Reccomended Procedure to Determine the Modulus. 128

15.0 Other General Conclusions 130

16.0 Suggestions For Further Research 131

16.0 REFERENCES. 132

2.0 List of Illustrations

Figure 1. Curve for the swelling of partly saturated sand held under constant isotropic load 18

Figure 2. Action of pore-water in partially saturated soils (After Burland 1965). 20

Figure 3. Suction - water content relationships for an expansive clay 22

Figure 4. Suction - dry density relationships for an expansive clay 22

Figure 5. Changes in the soil suction of compacted soil specimens with curing time (Mou 1981) 23

Figure 6. Percent swell initial suction relationship for an expansive clay. (Mou 1981). 24

Figure 7. Pressure Plate Cell (Olson and Langfelder 1965) 26

Figure 8. Influence of air pressure on the measured pore-water pressure (Olson and Langfelder (1965). 26

Figure 9. Likely long-term distortion modes for rafts on expansive soils (Holland and Richards 1984). 31

Figure 10. Idealised initial mound shape-centre doming (Williams et al 1985). 31

Figure 11. Pressure versus swell deficit (O'Neill and Poormoayed 1980). 32

Figure 12. Swell-pressure curves for Dooen clay. This is a clay found in Victoria, Australia (Walsh 1978). 34

Figure 13. Swell-pressure curve for idealised foundation (Walsh 1978). 34

Figure 14. Effect of a change in swell stiffness while all other design parameters are held constant (Mitchell 1984). 35

Figure 15. The combined effect of edge distance and soil modulus on deflection ratio (Pidgeon 1980a). 36

Figure 16. A chart showing the percentage additional cost for a 7m*8m raft. 38

Figure 17. Modulus from SUL towers, plate and pressuremeter tests. 40

Figure 18. Equilibrium suction beneath the centre of sealed road pavements in terms of Thornthwaite moisture index (Pellisier 1987). 42

Figure 19. Idealised initial and final soil suction profile beneath a covered area in a semi-arid environment (Hamberg and Nelson 1984) 43

Figure 20. The effect of trees planted near a house sited on expansive clays in Adelaide, Australia (Pile 1984). 44

Figure 21. Stress-strain curve for undrained test on NC clay (Lee, White and Ingles 1983) 47

Figure 22. Contours of equal strain for normally consolidated Amua clay (Whitman and Lambe 1969). 48

Figure 23. Stress-strain curves from triaxial tests on five normally consolidated clays (Ladd 1964). ... 49

Figure 24. Sources of error in external strain measurements (Jardine et al 1984) 50

Figure 25. The construction of the electrolevel capsule used to measure local axial strains (Jardine et al 1984). 51

Figure 26. Stress-strain data for a sample of undisturbed North Sea clay 52

Figure 27. Modified triaxial cell for unsaturated soils (Fredlund and Ho 1982). 54

Figure 28. Ideal stress versus strain curves for a multistage test using the cyclic loading procedure (Fredlund and Ho 1982). 54
Figure 29. Stress versus strain curves for decomposed granite (Fredlund and Ho 1982). 55
Figure 30. Different stress paths that can be defined by using the conventional consolidometer (After Brackley 1971). 58
Figure 31. Cross-section of membrane oedometer (Aitchison and Martin 1973). 59
Figure 32. Cross-section of a modified consolidometer developed by Escario and Saez (1973). 60
Figure 33. Swelling under constant load and controlled negative pore-water pressure of remoulded clay (Escario and Saez 1973). 61
Figure 34. Controlled suction consolidometer developed by Chu and Mou (1973). 62
Figure 35. Relationship between suction and swell determined by controlled suction tests (Chu and Mou 1973). 63
Figure 36. Percent swell vs soil suction relationship for specimens under nominal surcharge (Mou 1981). 64
Figure 37. Schematic diagram of suction controlled oedometer developed by Richards, Peter and Martin (1984). 65
Figure 38. Experimental results from tests on Riverina clay. The results from a finite element analysis have also been included. 66
Figure 39. Results of consolidometer tests on pleistocene clay varying the concentration of NaCl in the equilibrating solution. 67
Figure 40. Results of consolidometer tests on pleistocene clay for 68
Figure 41. Comparison of stress-strain relations as obtained from incremental loading test and CRS test (Wissa et al 1971). 69
Figure 42. Comparison of constrained moduli. 69
Figure 43a Typical consolidation-swell test results (Porter and Nelson 1980). 70
Figure 43b Typical strain controlled swell tests (Porter and Nelson 1980). 70
Figure 43c Comparison of controlled strain and consolidation swell test results (Porter and Nelson 1980). 71
Figure 44 Typical soil profile at Onderstepoort (Brink 1979) 78
Figure 45 Grading curve 79
Figure 46 Soil suction versus moisture content 80
Figure 47 Compaction curve 80
Figure 48 Triaxial sample mould. 88
Figure 49. Undrained triaxial test results 88
Figure 50 Undrained triaxial test results 89
Figure 51 Undrained triaxial test results with load cycling 89
Figure 52 Undrained triaxial test with load cycling 90

Figure 53. Drained triaxial test results 90
Figure 54 Drained triaxial test results 91
Figure 55 Undrained triaxial test results: Stage loading 91
Figure 56 Drained triaxial test results : Stage loading 92
Figure 57 P-Q plot 92
Figure 58 P-Q plot : stage loading 93
Figure 59 Unconfined triaxial test. 97
Figure 60 Unconfined triaxial test 97
Figure 61 Confined triaxial test 98
Figure 62 Sketch of mould for oedometer samples 107
Figure 63 Oedometer correction curve 107
Figure 64 Swell versus time curve 108
Figure 65 Swell versus log pressure 108
Figure 66 Swell versus log pressure 109
Figure 67 Oedometer compression of saturated samples 112
Figure 68 Oedometer compression of saturated samples : log scale 112
Figure 69 Oedometer compression of saturated samples 113
Figure 70 Oedometer compression of saturated samples 113
Figure 71 Consolidation curves : Water content 25% 117
Figure 72 Consolidation curves : Water content 33% 117
Figure 73 Oedometer compression at constant moisture content 118
Figure 74 Oedometer compression at constant moisture content 118
Figure 75 Consolidation curve : water content 33% 119
Figure 76 Constant rate of strain oedometer test 123
Figure 77 Constant rate of strain oedometer test : Slurry specimen 123
Figure 78 Constant rate of strain oedometer test 124
Figure 79 Modulus versus applied stress. 132

3.0 List of Tables.

TABLE 1 : Material classification data. 79

TABLE 2 : Sample preparation data for triaxial tests on saturated samples. 86

TABLE 3 : Strain rates and degrees of saturation for triaxial tests. 86

TABLE 4 : Tangent and secant moduli from triaxial tests on saturated samples. 87

TABLE 5 : Comparison of triaxial moduli from stage loaded and standard tests. 87

TABLE 6 : Confined triaxial test data. 96

TABLE 7 : Unconfined triaxial test data 96

TABLE 8 : Moduli from unconfined and confined triaxial tests. 96

TABLE 9 : Sample preparation data and percent swell from swell under load tests. 105

TABLE10 : Sample preparation data and percent swell from swell under load tests. Material was initially oven dried. 105

TABLE11 : Equations of best-fit lines for swell under load tests. 106

TABLE12 : Predicted swelling pressure and free swell from best fit lines 106

TABLE13 : Comparison of predicted swell and measured swell. 106

TABLE14 : Sample preparation data for oedometer tests on saturated samples 111

TABLE15 : Summary of oedometer modulus D from oedometer compression of saturated samples. 111

TABLE16 : Sample preparation data for compression at constant moisture content. 116

TABLE17 : Oedometer modulus D from oedometer compression at constant moisture content 116

TABLE18 : Sample preparation data for constant rate of strain oedometer. 122

TABLE19 : Moduli values determined from constant rate of strain oedometer tests. 122

4.0 Introduction.

Expansive clay profiles are found in many areas of South Africa and, as a result, the local building industry has often been faced with the challenge of building light structures (such as houses) in these areas. As is now well known, if the foundation for these houses are not carefully designed to withstand differential movements caused by heave, then severe distress can occur in the structure.

The Division of Building Technology of the CSIR in Pretoria (formerly the National Building Research Institute) has long been involved in helping the building industry overcome some of these problems. Their approach has been one of conducting research into the behaviour of stiffened raft foundations with the object of developing a suitable design package. This design package is based on a linear elastic finite element model which adopts the 'plate on mound' approach. Very briefly, this method models the swell occurring under light structures by assuming that a slab is placed on an already formed mound of known geometry. For a known raft stiffness, the edge deflection and stresses in the raft can then be calculated.

One of the input parameters required for this package is the stiffness of the underlying soil and it is here that much research into the correct assessment of this factor has been done by the Division of Building Technology. In this research, emphasis has been placed on the determination of the modulus from field tests (such as plate tests and pressuremeter tests) as well as from the back analysis of full scale raft foundations constructed at Onderstepoort.

The aim of this project therefore, is to continue this work by supplying moduli values from different laboratory tests on Onderstepoort clay so as to gain a complete picture of the range in moduli values that can be expected from different tests. From the back analysis mentioned previously, the modulus values which allow for the correct raft simulation are now known and consequently, the laboratory tests which give moduli values within the required range and which model the field stress path most closely can be highlighted. In addition, the combination of the field and laboratory data will also prove interesting in itself and could be useful in applications other than in stiffened raft design (such as road construction).

Note that the emphasis of this report lies in the laboratory testing of the material and not so much in the theory of stiffened raft foundations.

This report is divided into three main parts: the first section deals with a very broad literature survey which discusses the general concepts of expansive clay technology, the concept of soil stiffness in various stiffened raft foundation packages and the laboratory techniques used in expansive soil technology. The second part

contains a description of the laboratory tests performed and a presentation of the results. This section is divided into two parts which deal with the triaxial and oedometer tests respectively. Lastly, in the third section, the moduli values from all the laboratory tests are reviewed and the best laboratory technique to determine the modulus is discussed.

With regard to the literature survey, it must be borne in mind that this section has been written from a point of view of gaining a feel for the vast subject of expansive soil technology. Thus, many lines of thought are presented in the literature survey which are not further developed in the laboratory work. A good example of this is the axis-translation technique which was not attempted in the laboratory because of the limitation of time. The material in the literature survey was also collected over a lengthy period of time and thus, in some cases, the experimental techniques used differ slightly from those suggested in the literature survey.

In conclusion, the value of the soil stiffness determined by the method recommended in this work should lead to more economical stiffened raft foundation designs when used in conjunction with computer design programs.

LITERATURE SURVEY

5.0 General Principles in Expansive Soil Technology.

5.1 Effective Stresses in Partially Saturated Soils

For saturated soils the principle of effective stress originally proposed by Terzaghi in 1923 has proved to be of fundamental importance in understanding the mechanical behaviour of saturated soils. The principle of effective stress simply states that: 'for saturated soils all measurable effects of a change in stress such as compression, distortion and a change in shearing resistance are exclusively due to changes in the effective stress'(Burland 1965). For saturated soils the effective stress is defined as the difference between the total stress σ and the pore-water pressure u.

The question now arises as to whether or not the principle of effective stress applies to unsaturated soils as well. A modified form of the effective stress equation was first proposed by Bishop in 1959 and can be stated in a mathematical form as follows:

$$\sigma' = (\sigma - u_a) - \chi(u_a - u_w) \quad (1)$$

σ' = Effective Stress

σ = Total Stress

u_a = Pore-air Pressure

u_w = Pore-water Pressure

χ = An empirical factor

$(u_a - u_w)$ = Soil Suction

To prove the validity of equation 1 Bishop and Donald (1961) performed drained triaxial tests in a modified triaxial apparatus whereby σ_3, u_a and u_w could be controlled. In these tests the absolute values of σ_3, u_a and u_w were all varied in such a way so as to keep $(\sigma_3 - u_a)$ and $(u_a - u_w)$ constant. The results showed that in spite of the variations in σ_3, u_a and u_w no significant change in the axial stress-strain response was noted.

Burland (1965) has however, contested the assumption that the use of the effective stress principle for partially saturated soils is always valid because, on wetting, some partially saturated soils (especially sands) collapse. He claimed that this is a violation of the effective stress principle because, due to wetting, there is a reduction in the effective stress (the suction term is reduced) which should result in a volume increase. On the other hand, Blight (1965) has postulated that this behaviour is due to a structural breakdown of the soil skeleton (or fabric) and therefore cannot be related to the principle of effective stress. Blight (1965) has also shown that this collapse behaviour is only limited to a small critical range of suctions. For values of suction outside this range the collapsing sand expands upon effective stress decrease (Figure 1). Hence the collapse phenomenon applies a limitation to the use of the effective stress principle, but occurs as a consequence of the principle (Blight 1965).

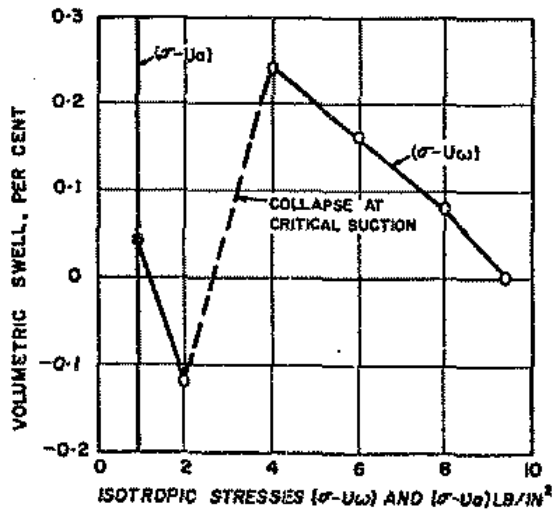

Figure 1. Curve for the swelling of partly saturated sand held under constant isotropic load $(\sigma - u_a)$: Swelling took place under decreasing values of $(\sigma - u_w)$ until a critical effective stress was reached, whereupon collapse took place (Blight 1965).

There are however many other problems associated with the direct use of equation 1. One major problem involves determining a suitable value of χ because it is most often not known and is difficult to determine. This is because χ is not a constant over a particular stress range due to its dependence on soil suction, as well as the fact that it is dependent on the stress-path being followed (Blight 1965).

To simplify the analysis of partially saturated soil behaviour, a stress-path analysis has been proposed (Aitchison 1973). This entails performing laboratory tests on undisturbed samples whereby the sample is subjected to the various stress components in the correct order in which they would occur in the field. Thus the relevant soil properties may be quantified even though the actual values of effective stress remain unknown (Aitchison 1973).

5.2 *Soil Suction in Partially Saturated Soils*

The concept of soil suction has already been mentioned in the section dealing with effective stresses. However, this concept is very important when it comes to expansive soil behaviour because it is often found that it is the dominant term determining the stress-strain response of the soil in the longer term (ie. over a period of years). For this reason the concept of soil suction will be explained in more detail.

Soil suction can be evaluated from the following two points of view:

- Soil suction contributes directly to the effective stress in the sample, as already indicated in equation 1. Menisci form at grain to grain contacts which, due to their very small radii of curvature, develop large negative pressures in the pore-fluid (Figure 2).

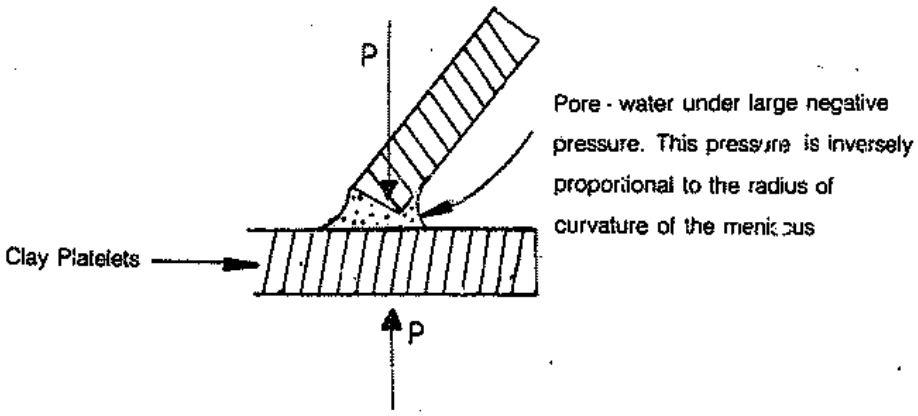

Figure 2. Action of pore-water in partially saturated soils (After Burland 1965).

This results in a large increase in the normal force P (and hence the effective stress) acting between particles. On the other hand, removal of the suction in the soil causes these large internal forces to be released, resulting in swell (Brackley 1983).

- Soil suction can alternatively be viewed as a measure of the free energy available in the soil-water relative to a pool of pure water located outside the soil at the same elevation (Snethen 1980). Hence, if the pure water is brought into contact with a soil having a suction component, an energy gradient will be set up causing water to flow into the soil until the system is in equilibrium. In so doing, an amount of energy is dissipated which is numerically equal to the work done on the soil to create a suction in the soil in the first place. This energy is dissipated by means of overcoming friction and by expanding the soil lattice (Snethen 1980). In this context soil suction can also be seen as a 'soil's affinity for water' (Peter 1979) and can be regarded as the basic driving force behind moisture changes in partially saturated soils.

Soil suction is the result of the following 3 factors (Peter 1979):

1. Surface tension effects: As has already been discussed, the small radii of curvature of the menisci at the air/water interface causes large negative pressures in the pore-fluid between grains. If a sufficiently large

external load is applied, this component of suction could reduce as the soil tends towards a higher degree of saturation. Also, the smaller the water content, the greater the surface tension effects.

2. Adsorption: Clay particles possess a net negative surface charge which attracts the bipolar water molecules constituting the pore-fluid.

3. Osmotic imbibition: The pore-water of a soil can contain large quantities of dissolved salts. These dissolved salts create an osmotic suction which can be substantial even when the soil is saturated.

Matrix suction is denoted as the sum of adsorption and surface tension effects, while osmotic imbibition is simply denoted as osmotic suction. Total suction then becomes the sum of matrix and osmotic suctions and is sometimes measured in terms of the pF scale where:

$$pF = \log_{10}(\text{suction in cm water})$$

For any given soil, the value of total suction is dependent on the following factors (Bishop and *Blight 1963*, Mou 1981):

a)Dry density

b)Water content

c)The stress difference $(\sigma - u_a)$

d)The concentration of ions in the pore-water; and

e)*The nature of the soil fabric.*

As a consequence, it is difficult to relate water content directly to suction, which implies that water content should not be used as a descriptor of the state of a partially saturated soil.

Tests done by Mou (1981) on an expansive soil (PI = 32) indicate the relative magnitude of the influence of dry density and water content on the matrix suction of a s: specimen (Figure 3and Figure 4). The results were obtained from a modified suction controlled oedometer which will be described in a later section. These figures clearly indicate that the water content of a soil is the predominant contributor to a particular value of matrix suction. Also, as shown in these two figures, the type of soil compaction used in the laboratory can influence the value of suction measured. Mou (1981) ascribes this phenomenon to the different types of soil fabric which are produced by these two methods of compaction. Another factor influencing the value of suction measured in a remoulded laboratory specimen is the length of time elapsed between sample preparation and suction determination. *Typical curves for an expansive clay* with a PI of 19 is shown in Figure 5 and is denoted as sample A. The curve for kaolin has been included to show that the trend of suction development with time is independent of the soil type for statically compacted material. From this

curve Mou (loc. cit.) concluded that for this particular material, the curing period should last for a minimum of four days.

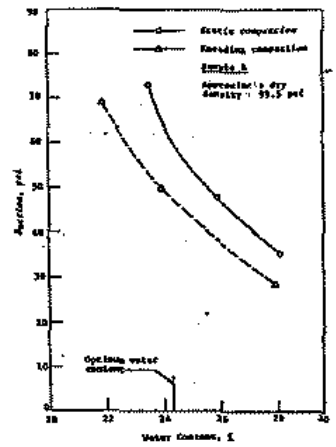

Figure 3. Suction - water content relationships for an expansive clay: This clay had a PI of 32 (Mou 1981).

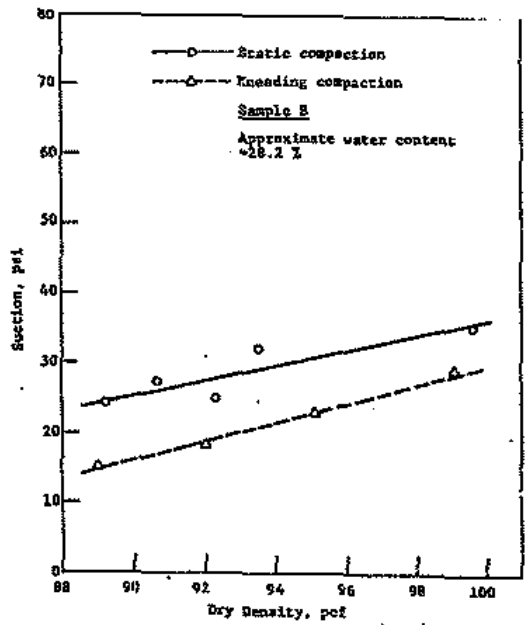

Figure 4. Suction - dry density relationships for an expansive clay: Plasticity index of 32 (Mou 1981).

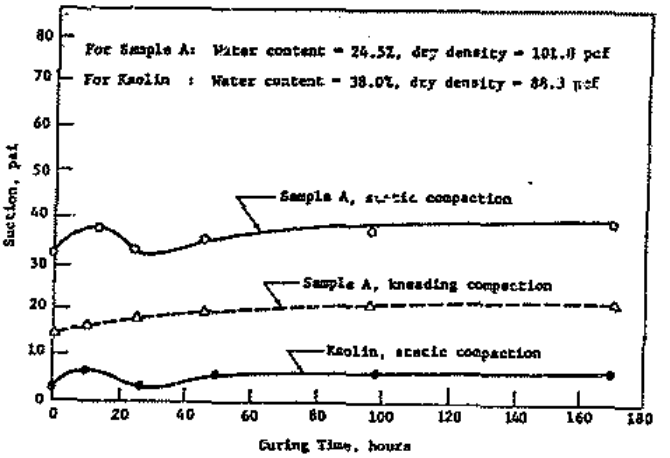

Figure 5. Changes in the soil suction of compacted soil specimens with curing time (*Mou 1981*)

Mou (1981) has also shown that there is a unique relationship between the initial suction of a specimen, percent swell and swelling pressure regardless of the cause of the suction which may be due to variations in the initial dry density or in the initial water content. The relationship between initial suction and percent swell is shown in Figure 6.The points on the graph all have differing values of initial water content and dry density, but due to the fact that all the points lie on a relatively smooth curve, one can only conclude that the initial suction is the controlling factor in determining swell behaviour.

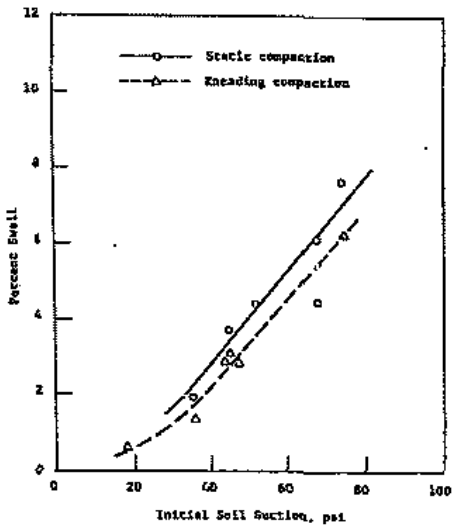

Figure 6. Percent swell initial suction relationship for an expansive clay. (Mou 1981).

5.3 The Axis-Translation Technique

It it is impossible to work directly with suctions greater than 80kPa in the laboratory because the water in the pore-water pressure measuring system cavitates (Bishop and Blight 1963). To measure greater suctions, the axis-translation technique is used. The basic principle is to raise the pore-air pressure of the sample and, assuming that all the voids are interconnected, the pore-water pressure should increase by the same amount, thus leaving the suction in the sample unchanged. If the pore-air pressure is elevated sufficiently, a stage will be reached where the pore-water pressure is zero. At this point the pore-air pressure can be regarded as being equal to the suction in the sample (Olson and Langfelder 1965). The axis-translation technique is so named because it translates the origin of reference for the pore-water pressure measurement, from standard atmospheric conditions to the final air pressure value (Bocking and Fredlund 1980). Through the use of this technique Bishop and Blight (1963) managed to measure suctions as large as 430kPa (pF3,69).

An instrument used to measure suctions, using the axis-translation technique, is the pressure plate cell (Figure 7). Results showing the pore-water response to applied air pressure are shown in Figure 8. Notice

that the slope of the line is close to 45 degrees as is to be expected, which implies that the final applied air pressure is equal to the extrapolated negative pore-water pressure.

One of the problems that arises when using the axis-translation technique occurs when samples with very large suctions are initially placed on the porous stone. It has been noted that, due to this large suction, there is a tendency for the water in the pore water pressure measuring system to cavitate almost immediately (Olson and Langfelder 1965). A possible solution to this problem is to either assemble the cell very rapidly and apply a large air pressure as quickly as possible, or to open the flushing valve momentarily (Figure 7) while the cell is being assembled. The latter solution has been successfully used by Olson and Langfelder (1965), but it induces a time lag of approximately 30 minutes before the full suction can be measured. The former solution causes the air pressure to 'overshoot' the actual suction value because the sample has finite air permeability, which means that a very large air pressure is required initially to penetrate to the base of the sample (Olson and Langfelder 1965).

Another problem that may arise, if longer testing times are required, is the diffusion of air through the porous stone. This will cause the actual suction valve to be underestimated (Bocking and Fredlund 1980). To remedy this problem, an elevated positive pore-water pressure can be used (ie. not zero) and therefore the estimated suction becomes the applied pore-air pressure less the measured pore-water pressure.

Usually the maximum suction that can be measured by means of the axis-translation technique is determined by the air-entry value of the porous disc placed below the sample. The air-entry value corresponds to the maximum air pressure that can be applied before air is forced through the disc.

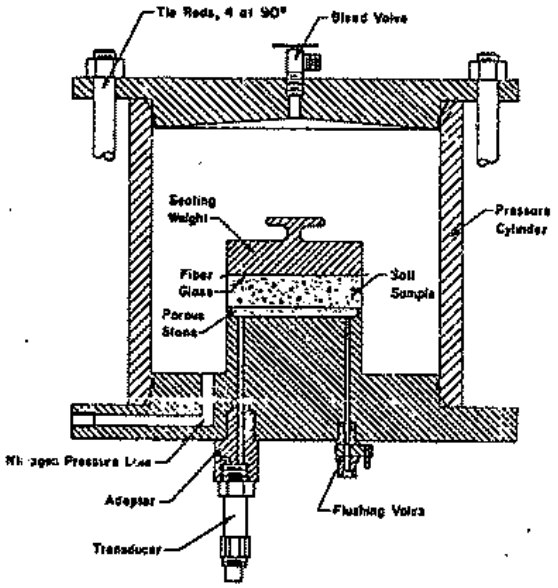

Figure 7. Pressure Plate Cell (Olson and Langfelder 1965)

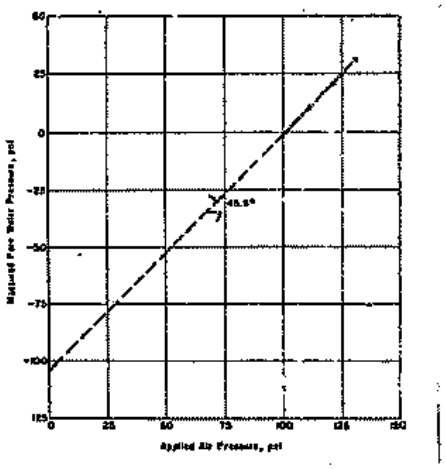

Figure 8. Influence of air pressure on the measured pore-water pressure (Olson and Langfelder (1965).

5.4 *Mechanism of Swell Below Buildings and Associated Structural Measures.*

The mechanism of swell below buildings is best illustrated by experiments conducted by De Bruin (1973) who investigated the behaviour of different surface covers placed on expansive profile over a period of five years. Two of these covers consisted of a plastic cover and a fallow area respectively. The fallow area was prepared by means of a defoliant. Surprisingly, the heave of the fallow area was very similar to that of recorded under the plastic cover. This led Williams and Pidgeon (1983) to conclude that "the most significant change in loading made to a building site, ie to the stress change in the soil, is considered to be the the removal of the vegetation - all other effects such as imposed foundation loads, drainage or lowering of the ground water table, relief of stress on excavation are of secondary importance". In other words, the placement of a surface cover implies the elimination of transpiration which fundamentally disturbs the original moisture equilibrium between the soil and the atmosphere. As a consequence, moisture gradually accumulates beneath the cover causing a reduction in suction resulting in swell.

The special construction techniques employed to reduce damage caused by heaving soil are briefly listed below (Louw 1988, Williams et al 1985):

1. Excavation of expansive soil under the foundation and replacement with non-expansive soil material which is well compacted. This technique is only applicable in areas where expansive profile is shallow.

2. *Articulated or "open joint" construction which divides the house into smaller,* stable units by means of movement joints or window openings of full height. Sections between the movement joints should be provided with both vertical and horizontal reinforcement. Generally, open joint construction should not be used in areas were the total heave is expected to exceed 30mm.It must also be realised that structures build by this technique will still require occasional maintenance such as the patching of cracks during the life of the structure.

3. Stiffened raft foundations consisting of reinforced slab and beams which are stiff enough to reduce differential deflections. It is generally uneconomical to provide a raft stiff enough to allow for the use of solid brickwork (ie no joints) and therefore, articulated brickwork is usually employed in conjunction with stiffened rafts. This method has been used extensively in Australia, the USA and South Africa no doubt due to its low cost relative to other construction techniques.

4. Anchor piles founded in the stable soil layer beneath the layer of heaving soil. The structure is then erected on a slab or beam on top of the piles in such a way that it is isolated entirely from the soil surface and the heaving clay. The piles must be either designed to resist tensile forces generated by heaving or, alternatively, the piles must be isolated from the surrounding soil. In the case of augered piles, this can be achieved by drilling an oversize hole through the expansive layer, casting the pile within a permanent casing and then filling the annular void with vermiculite. The cost of forming the void below light structures is usually expensive so this technique is best used in heavy structures.

5. Pre-wetting is applied to allow the profile to expand before the structure is build. It generally works better for larger structures because seasonal moisture changes below smaller structures prevent the moisture content from stabilising. Differential heaves are therefore not eliminated.

After the building has been erected, further care should be taken to ensure that the moisture content of the soil below the structure remain as stable as possible. This can be achieved by allowing no trees or shrubs to be planted near the structure and by permitting no garden watering too close to the structure.

5.5 *Summary*

1. The effective stress equation proposed by Bishop (equation 1) identifies two stress state variables which effects partially saturated soil behaviour. These two variables are the total stress $(\sigma - u_a)$ and the matrix suction $(u_a - u_w)$. In the laboratory, the exact effective stress operative in a sample is not quantified but rather, as far as possible, the correct stress path as occurring in the field is emulated.

2. Matrix suction or soil suction is a measure of the potential energy within a soil. Dissipation of this energy through wetting causes soil lattice expansion. In this context, soil suction can also be regarded as the basic driving force behind moisture changes in partially saturated soils.

3. Besides the water content, the soil suction is also influenced by other factors such as dry density, the concentration of ions in the pore water and by the nature of the soil fabric. Therefore, water content should not be used as a descriptor of the state of of a partially saturated soil. Further, there is a unique relationship between the initial suction of a sample, percent swell and swelling pressure regardless of the cause of the suction which may be due to variations in the initial dry density or in the initial water content.

4. The axis translation technique is a powerful tool for achieving large suctions in the laboratory, but the maximum suction that can be measured by this technique is limited by the air entry value of the porous stone placed below the sample.

5. The most significant change in loading made to a building site, ie to the stress change in the soil, is considered to be the the removal of the vegetation - all other effects such as imposed foundation loads, drainage or lowering of the ground water table, relief of stress on excavation are of secondary importance. The special construction techniques employed to reduce damage by heaving soil to light structures include excavation and replacement, articulated construction, stiffened rafts, pre-wetting and anchor piles. On a relative cost basis, stiffened rafts have been shown to be one of the cheaper techniques.

6.0 The Equivalent E-Value in Stiffened Raft Foundation Design.

6.1 Introduction to Stiffened Raft Foundation Design.

At present there are at least 17 different methods and/or approaches used for the design of stiffened rafts on expansive soil (Pellisier 1987). For all of these procedures, the basic principle is to recognise that the changing support offered by swelling or shrinking soil is unpredictable in character due to extraneous circumstances such as garden watering and desiccation by trees. Consequently, these design procedures are based on the most likely mechanism of soil distortion (Lytton and Meyer 1971 and Pile 1987).

Figure 9 displays two likely long term slab distortion modes which are recognised in design. They are the edge heave mode (sagging condition) or the centre heave mode (hogging condition). In South Africa only centre heaving is considered in design because it has been found to be by far the major cause of cracking in buildings located on expansive soil profiles in this country (Pidgeon 1980a).

Most of the above mentioned design procedures use the 'plate-on-mound' approach. This approach assumes that an elastic footing is placed on an already formed mound which is taken to be that which would occur under an impermeable membrane of the same size as the proposed foundation (Williams et al 1985). Figure 10 shows how this centre-heave mode is idealised in a typical design procedure with some of the as-*sociated design input parameters.*

The stiffened raft assumes to deflect towards the shape of the soil surface while at the same time 'sinking' slightly into the soil (Woodburn 1979). Obviously, this design procedure significantly simplifies the true situation in the field because, in practice, the mound would form only after the foundation was cast due to the elimination of transpiration as has already been discussed.

In this section, the major design procedures will be reviewed in terms of their recommendations concerning the correct E-value. Where possible, actual values will be given and the relative importance of estimating the correct E-value will be discussed. Finally, please note that in this section, E-value subgrade modulus and swell stiffness will be used interchangeably. It is felt that this is justifiable because they all refer to the soil mound's response to load, even though they have differing precise definitions.

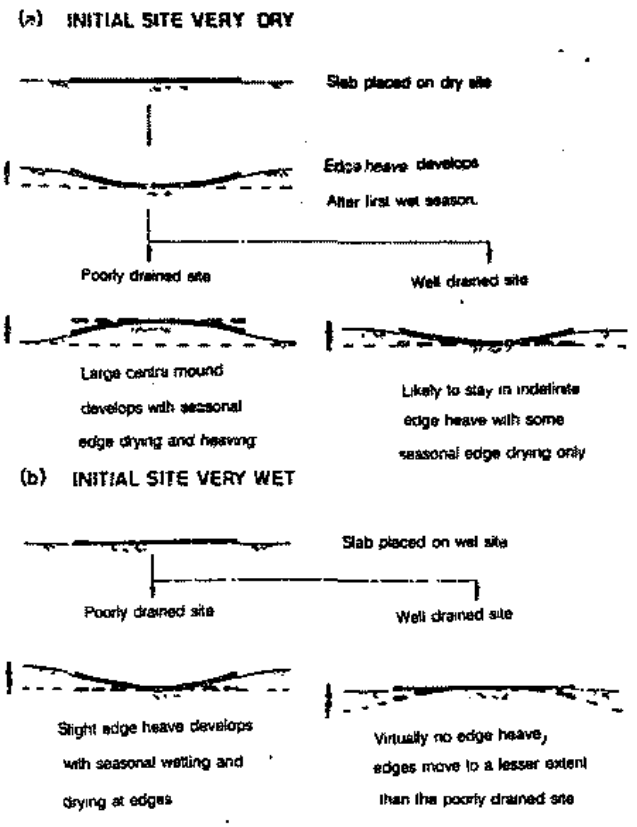

Figure 9. Likely long-term distortion modes for rafts on expansive soils (Holland and Richards 1984).

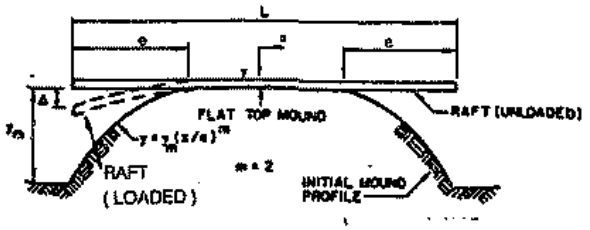

Clay Platelets
Definition of design parameters:
a) L= Slab length
b) δ= Edge deflection
c) y_m=Differential heave
d) m= Mound exponent (defines the shape of the mound).
e) k_s or E = Mound stiffness (not shown on sketch)
f) e or e_m = Edge distance

Figure 10. Idealised initial mound shape-centre doming (Williams et al 1985).

6.2 *Definition of Soil Stiffness in raft design techniques*

6.2.1 Lytton's design method (1971):

Lytton defines a 'subgrade modulus' to describe the elastic properties of the soil mound. This modulus is defined in the following way (Lytton and Meyer 1971): 'If there is no pressure on its surface, the soil will swell xmm. If b units of pressure are applied, the soil will swell x-a mm. The pressure swell deficit modulus b/a is the modulus to be used. O'Neill and Poormoayed (1980), in their review of foundation design on expansive soil, define the subgrade modulus from an unloading curve (Figure 11). This curve is obtained by allowing a soil sample to develop a maximum swell pressure under zero volume change in the oedometer. The sample is then unloaded in increments *until full swell is reached under zero load.*

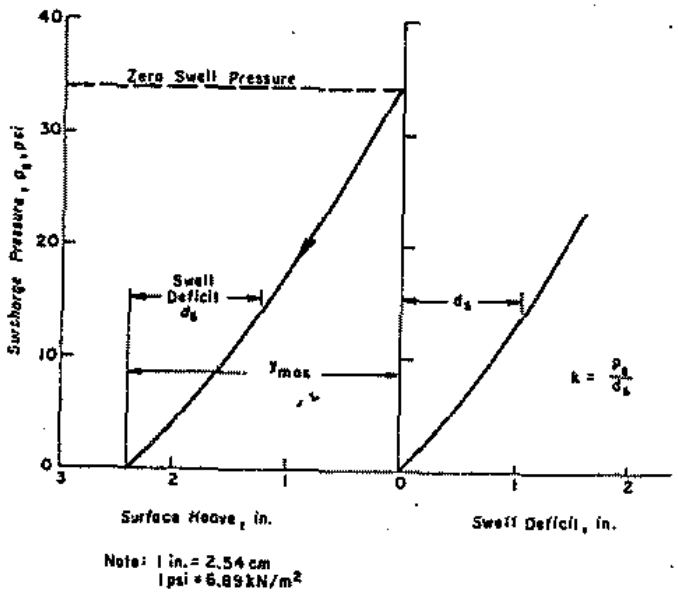

Figure 11. Pressure versus swell deficit (O'Neill and Poormoayed 1980).

The subgrade modulus can then be defined as shown in Figure 11. One gets the impression that Lytton, O'Neill and Poormoayed are trying to define the same modulus, but whether or not these two definitions yield similar results has yet to be investigated.

In a recent paper presented by Williams et al (1985), the method of obtaining the subgrade modulus, as proposed by Lytton, was questioned. It was felt that a 'deformation under load' parameter should rather be used because it simulates the long-term stiffness of the soil after mound formation more closely.

Lytton and Meyer (1971) also recommended that in the shrinkage condition 'the subgrade modulus to be used, would be a slope or secant of a long-term pressure-deformation curve for a soil column down to a depth of negligible movement'. Lastly, for the Lytton method, an accurate measure of the subgrade modulus is not required because the final output is relatively insensitive to changes in the value of the subgrade modulus (Pidgeon 1980b).

6.2.2 Design method proposed by Walsh (1978):

Walsh (1978), states that the swell-stiffness (k) correctly models the footing/soil interaction. His definition of k is the same as that used by Lytton to describe the subgrade modulus and can be expressed in a mathematical form as follows:

$$P = k(y-\delta) \qquad \text{---------- (2)}$$

P = Soil pressure on base of footing (MPa).

k = Subgrade modulus (MPa/m).

y = Free swell of soil with no vertical load (m).

δ = Equilibrium position after load has been applied (m).

Walsh (loc.cit.) does however, have the following additional comments to make:

1. A linear relationship between P and (δ) should not be assumed.

2. The swell-stiffness, as defined in equation 2, does not 'suggest any superposition of pressure on a mound that has developed its full swell y'.

3. Swell-stiffness cannot be related to the elastic property of the soil because it is related more to swell sensitivity. However, the conventional modulus of subgrade reaction may be taken as an upper limit to the value of k.

Walsh (1978), suggests the following method for finding the swell-stiffness:

- Various samples are taken from a profile and are tested in the oedometer. The initial condition of the specimens correspond to the correct in-situ density and have a water content similar to that which would occur when the profile was in a 'dry' state.

- The samples are allowed to swell to 'wet' profile conditions, which then allows one to plot out a graph as shown in Figure 12.

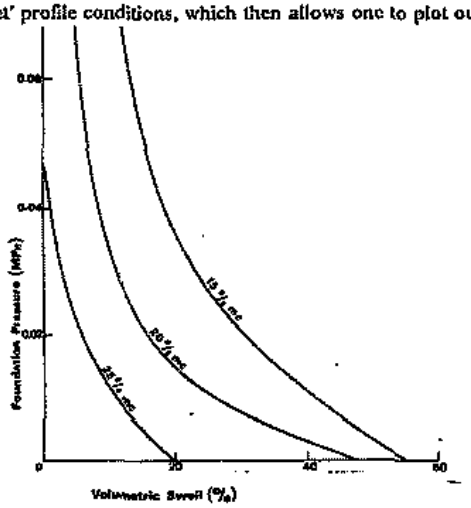

Figure 12. Swell-pressure curves for Dooen clay. This is a clay found in Victoria, Australia (Walsh 1978).

- Under a given foundation pressure, the overall vertical heave for the profile is then calculated by summing the component heaves for each layer in the profile (Figure 13). Account is taken of heave reduction caused by overburden pressures.

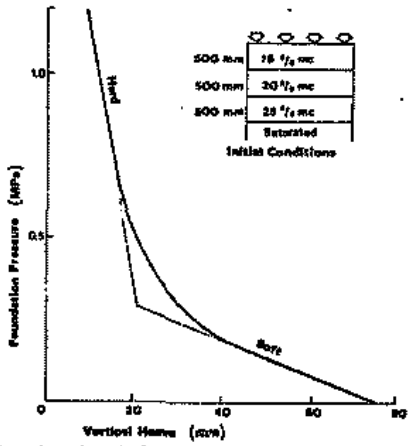

Figure 13. Swell-pressure curve for idealised foundation (Walsh 1978).

This analysis led Walsh to believe that two types of stiffness were applicable: one for lightly loaded structures and another for heavily loaded structures, which he called soft and hard mound stiffness respectively. From the data shown in Figure 12 and Figure 37 Walsh calculated a soft mound stiffness of 0,5 MPa/m. In another paper Walsh (1984), suggests that the expected stiffness should lie in the range of 0,1-2 MPa/m.

An interesting observation regarding the subgrade modulus as defined in equation 2 is that it is dependent on the depth of the profile considered to make a contribution to the total heave. Also, it should be noticed that the term 'wet profile' is used very loosely here because a possible final moisture content is not mentioned at all by Walsh (1978) although in the quoted tests a final condition of full saturation was most probably used. Thus it is clear that the value of the final moisture content chosen will also have an influence on the value of k calculated.

6.2.3 Design method proposed by Mitchell (1980):

Mitchell defines the subgrade modulus in exactly the same way as Lytton and Walsh (equation 2). This equation is then used to build up vertical and moment equilibrium equations for the footing as a whole which when combined with a compatibility equation (between the soil surface and the footing base), establish the basic design equations for this method. Most importantly, however, is the fact that these equations demonstrated that large variations in the choice of subgrade modulus do not significantly alter the final design moments (Mitchell 1984). In fact, if the modulus varies by a factor of 8, little variation in the final design moment, as calculated by this method, can be noticed (Figure 14).

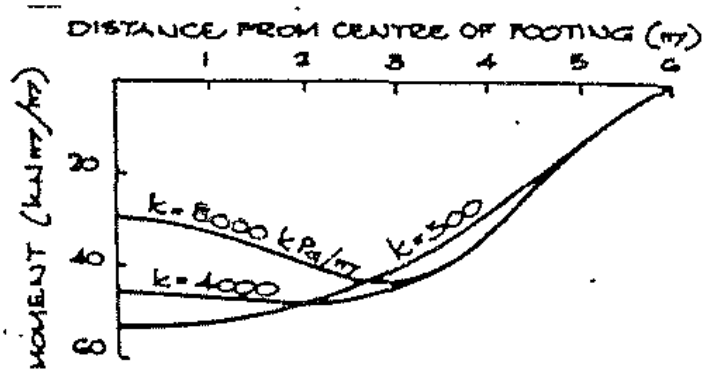

Figure 14. Effect of a change in swell stiffness while all other design parameters are held constant (Mitchell 1984).

6.2.4 Finite element program developed by Fraser and Wardle (1975):

Fraser and Wardle (1975) describe a sophisticated finite element program called FOCALS to model the plate-on-mound approach more accurately. Their findings, with regard to subgrade modulus, is that 'if the modulus value of the elastic mound increases, it is of minor importance - an increase of 300% requires only a small change in beam size'. Pidgeon (1980a), while using this program, concluded that at large values of edge penetration distance (e_m) and differential mound heave (y_m) the soil modulus is sufficiently significant to be taken into consideration (Figure 15).

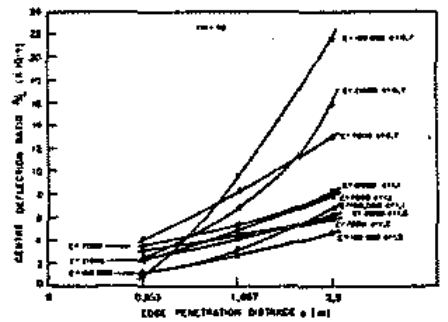

Figure 15. The combined effect of edge distance and soil modulus on deflection ratio (Pidgeon 1980a).

However, it should be pointed out that on larger edge distances (e_m), only deeper beams can be used to keep the deflection ratio within tolerable limits. Therefore, Figure 15 may over-emphasise the importance of soil modulus on stiffened raft foundation design (Pidgeon 1980a).

6.2.5 The Post Tensioning Institute Method:

This method uses equations derived from a finite element package and models the condition of a slab superimposed on an already formed mound (Pidgeon 1980). Young's modulus is set to a constant value of 7 MPa and is therefore not one of the input variables. Walsh (1980), in his detailed description of the assumptions inherent in this method, makes very little mention of the Young's modulus for the mound, except to point out that it effects the position of the maximum moment in the slab. One can only assume that the modulus was not considered important enough, relative to the other input variables, to be included as a variable. Pidgeon (1980a), considers the value of 7 MPa to be too low for South African conditions and thus suggests that a value of 21 MPa is a more realistic value of the soil modulus.

6.2.6 Design method proposed by Pidgeon (1988).

This method is computer based and essentially consists of a modified and improved version of the FOCALS program mentioned earlier. For the purposes of raft design the soil is idealised as a single isotropic soil layer 3 metres thick with a poisson's ratio of 0,3. The elastic modulus is the only soil variable and it is called the Equivalant Elastic Mound Modulus (EEMM) and is defined as follows:

$$EEMM = \frac{C_d\, w\, B\,(1-\nu^2)}{\delta_e} \qquad (4)$$

C_d = A factor which depends on the shape and stiffness of the foundation and the thickness of the elastic half space. For this design method a soil thickness of 3m is always used. Values for this factor are quoted by Pidgeon (1988).

w = The average contact pressure of the raft, assumed to be uniformly distributed.

B = The length of the short side of the raft.

ν = The poisson's ratio of the half space. It can be taken as 0.3.

δ_e = The reduction in heave in the centre of a loaded area caused by the weight of the raft alone.

The parameter δ_e is calculated by assuming that the soil profile is divided into a number of discreet layers. To each layer the Generalised Heave equation is applied (see equation 4 below) to compute the free swell occurring under an impermeable cover taking into account overburden pressures. Total free swell then is simply the sum of all the heaves of the layers. This calculation is repeated assuming that the foundation is placed on the surface and the associated stress distribution through the soil layer is now taken into account. The difference between the total free swell and the swell occurring when the foundation is in place is then the parameter δ_e. The Generalised Heave equation is given as follows:

$$\Delta H_L = \frac{Free\ swell(\%)}{100}(1 - logp/logp_s)H \qquad (4)$$

H = The thickness of the layer.

ΔH_L = Heave of the soil layer

p = The vertical stress acting at the centre of the soil layer due to the overburden pressure and the foundation pressure.

p_s = The swelling pressure.

Further simplifying assumptions regarding the EEMM include the following:

1. The lateral variation of moisture content and hence elastic modulus should be ignored.

2. The stiffness of the the foundation and hence the distribution of the contact pressure should be ignored, and a uniform contact pressure assumed instead.

3. *It should be assumed that the contact area remains* constant during mound development and is equal to the surface area of the foundation without any lift-off. The applied pressure should then be taken as *the* total load divided by the area.

4. The initial elastic settlement prior to mound development should be ignored where this is due to centre heave.

Essentially the factor EEMM is the same as *the factor k given by equation 2. However,* in contrast to the previous methods, the design output is significantly more sensitive to the value of EEMM used. For example, *Figure 16 shows the impact of small changes* in EEMM in terms of additional cost for a 7m by 8m raft. This figure shows that if the EEMM increases from roughly 1.0 to 2.5, then the cost increases by a factor of 2.6 if one assumes a differential heave of 60mm. However, as one would expect, at lower differential heaves, the sensitivity of the program is reduced.

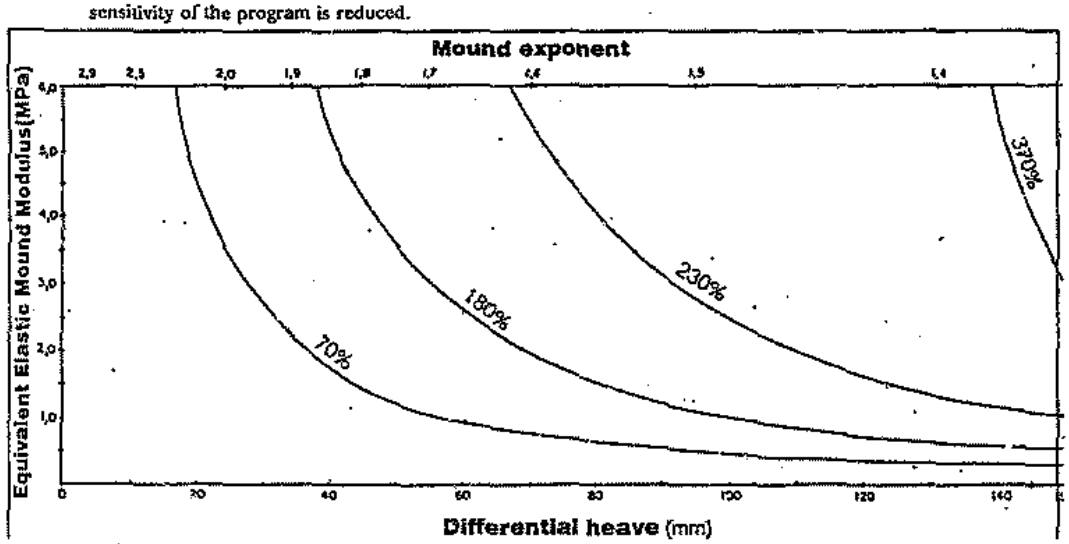

Figure 16. A chart showing the percentage additional cost for a 7m*8m raft.: (RPUG 1989).

It is also evident from equation 3 that the EEMM is not only a function of the type of soil, but it is also a function of *foundation size and shape as well as the* applied vertical stress.

By using the analytical technique method described above, typical values of EEMM have been shown to lie between 2 and 7 MPa for various sites in South Africa. These low values not only correspond with the values quoted by Walsh (1978) given previously, but also field tests as well as back analysis of full scale experimental rafts have shown the applicability of these values (Sanders 1989 and Pidgeon 1987).

Sanders (1989) conducted the following field tests at Onderstepoort and other sites, the aim of which was to determine the EEMM:

1. Full scale swell under load (SUL) tests: An area measuring 1.2m by 1.2m was loaded by means of concrete blocks to the required load. Over a long period of time, levels were taken on the surface of the concrete blocks and also on pegs driven into the soil surface nearby. All levels were taken relative to a stable benchmark which was socketed into bedrock and isolated from the surrounding soil. By means of this levelling exercise therefore, δ_e could be calculated directly from the field results.

2. Self boring pressuremeter test (SBPM test).

3. Plate jacking tests: This test can be further divided into the following categories:

   a. Vertical plate test

   b. Lateral maintained load test (abbreviated ML).

   c. Lateral constant rate of penetration test (CRP test).

In the ML test, a further load increment was only applied when the rate of deformation reduced to a chosen value.

The results from these tests are given in Figure 17. Note that the intermediate EEMM values from the SUL towers are plotted with time, while the plate and pressuremeter moduli have also been inserted with the associated stress at which the modulus was measured.

The point to note is that the final EEMM value from the SUL towers is very low and further, it is significantly lower than the pressuremeter and plate moduli. Obviously, differences in test duration, scale and test direction have a role to play. The ML plate test and the vertical plate test are the only test which give moduli close to the EEMM value, but on the other hand, this may be due to differing test conditions. For instance, in the case of the vertical plate test, the modulus is low because of bedding - in effects (Sanders 1989), while in the case of the ML test, the low modulus is as a result of the high applied stress.

Sanders (1989) also conducted laboratory swell under load oedometer tests on Onderstepoort clay (see stress path 5 in figure 18). The modulus from these tests agreed very well with the EEMM value from the SUL towers constructed at Onderstepoort if the inverse of the slope of the best fit line through the points was used to calculate the modulus. Thus it appears that a single swell under load test could give a reasonable estimate of the EEMM where there is a deep residual layer of expansive clay as is the case at Onderstepoort.

Pidgeon (1987a, 1987c) describes the behaviour of full scale experimental rafts build at Onderstepoort. The main aim of these experimental rafts among other things, was to determine how well the FOCALS pr .. m predicted actual raft behaviour . In the initial back analysis, a typically accepted soil modulus of 11.5 MPa was used in the program. The results showed that the program severely overestimated edge deflections mainly because the plate on mound approach is a gross simplification of the true situation and also because the program ignores slab membrane action, lateral restraint on beams due to the presence of soil between them

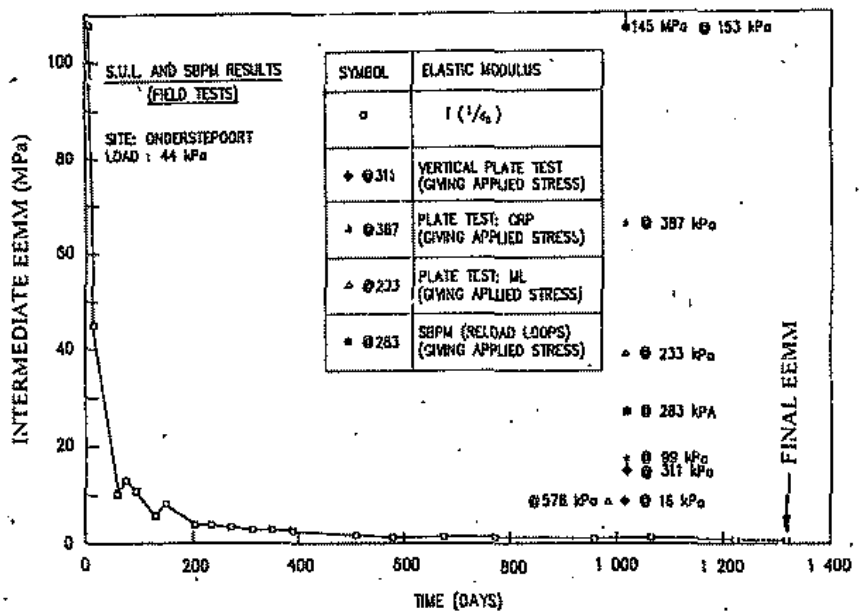

Figure 17. Modulus from SUL towers, plate and pressuremeter tests.

and the coupling rigidity of the beams (Pidgeon 1987a). However, it was found that if a much lower value of modulus was used (for example 2-3 MPa) then good correlation between actual behaviour and predicted behaviour could be attained.

6.3 *Equilibrium conditions below raft foundations*

There exists the possibility that the particular value of Young's Modulus, chosen for stiffened raft design, could be dependent on, amongst other things, the final suction under the raft. This could occur, for instance, if the material shows distinctly different values of stiffness at differing values of suction. This point will be elaborated on later, but for our present purposes a brief literature review will be conducted to determine suggested values of equilibrium suction.

Russam and Coleman (1961), proposed a relationship between Thornthwaite moisture index and possible values of suction below a pavement where no water table is present (Figure 18). The extra points on the curve (numbered) refer to road pavements in Australia. The fair degree of scatter is due to various simplifying assumptions used to calculate the climatic index (Aitchison and Richards 1965). Also of interest is the fact that values plotted from South Africa are fairly close to the Russam and Coleman line. Thus, according to Pellisier (1987), this curve can be used to predict the final suction value below a raft foundation in South Africa.

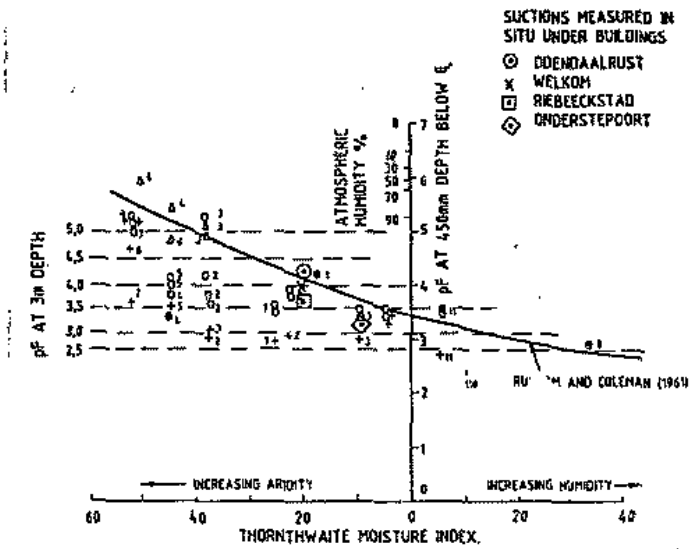

Figure 18. Equilibrium suction beneath the centre of sealed road pavements in terms of Thornthwaite moisture index (Pellisier 1987).

Peter (1979), maintains that if the water table exists close to the surface (ie. 6m in clay), then regardless of climate, the equilibrium suction profile will be that given by static equilibrium with the water table.

De Bruin (1973) has shown that, under a 7.2m diameter fibre glass cover constructed at Onderstepoort, the final condition was one of near saturation down to the water table which was at a depth of 8.5m.

Hamberg and Nelson (1984) assumed that the final suction profile varies linearly from pF2.5 at the surface to some stable suction value existing at the base of the active zone (Figure 19). A value of pF2.5 was chosen to represent the final suction at the surface because no volume changes were assumed to occur at suctions less than this value. For the clay profile that these authors were interested in, the suction value of pF2.5 corresponded to a water content roughly equal to the plastic limit. The initial suction profile shown in this figure represents the suction profile prior to construction. This profile has been truncated at the moisture content corresponding to the shrinkage limit because volume changes occurring below the shrinkage limit are insignificant.

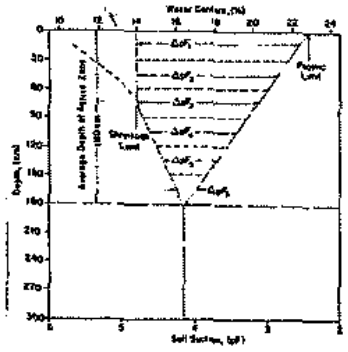

Figure 19. Idealised initial and final soil suction profile beneath a covered area in a semi-arid environment (Hamberg and Nelson 1984)

Pidgeon (1987d), observed that under experimental stiffened raft foundations at Onderstepoort near Pretoria, the final suction value was fairly constant with depth and had a value of pF3,1. This corresponds to a moisture content of 39%.

Snethen (1980) suggests that a realistic assumption regarding the final moisture content regime below a raft foundation corresponds to a condition of of full saturation. If the water content versus suction relationship for the soil is known, then the suction associated with the fully saturated moisture content can be determined. Note however that the saturated water content decreases with decreasing void ratio. Consequently, because the void ratio of the soil in-situ is lower than that of the laboratory specimen used to determine the suction versus moisture content relationship, the condition of full saturation does not imply zero suction.

Pile (1984) investigated houses sited on expansive profiles in Adelaide, Australia. He found that when trees were planted too close to a house, invariably shrinkage took place near the vicinity of the tree, inducing large differential settlements in the structure (Figure 20).

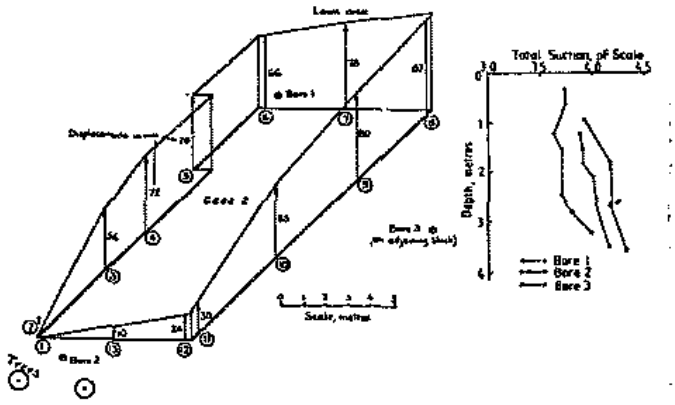

Figure 20. The effect of trees planted near a house sited on expansive clays in Adelaide, Australia (Pile 1984).

This case history has been included to show that often extraneous influences (especially trees and garden watering) can have a profound effect on the long term behaviour of expansive clays. Therefore, it is often very difficult to predict with certainty final suction values underneath a proposed structure in the long term.

Fissuring of the soil mass presents another major obstacle in the prediction of final suction values. This is because the fissures allow moisture to enter and leave the soil at a faster rate than that predicted by the classical diffusion theory (De Bruijn 1965).

6.4 *Summary*

1. At least 17 different methods and/or approaches have been devised for the design of stiffened raft foundation design. Most of the techniques model the raft/soil interaction by assuming that a raft is placed on an already formed mound, the dimensions of which correspond to a mound that would form under an impermeable cover.This cover has the same shape and size as the proposed foundation. The mound stiffness is then defined as the applied vertical pressure divided by the reduction in swell caused by the raft pressure. It has been shown that all previous design methods have been relatively insensitive

to the value of the mound stiffness used based on sensitivity analysis. However, in a recently developed design method by Pidgeon (1988), an accurate determination of the mound stiffness is of fundamental importance for the successful use of the method. Further, back analysis of experimental rafts at Onderstepoort has shown that the design program only models actual raft behaviour when a very low modulus of 2.6 MPa is used.

2. Moisture equilibrium conditions below a raft are difficult to determine due to the many extraneous influences such as adjacent vegetation, climatical conditions, degree of fissuring in the soil and the type of soil. In general though it has been shown that the final moisture content below a raft corresponds to one of full saturation to some significant depth below the raft. Alternatively, the Russman Coleman line given in this work can be used to predict the final suction values below a raft foundation.

7.0 Young's Modulus as Determined by the Triaxial Apparatus.

7.1 Introduction.

In this section the use of the triaxial apparatus to determine the stiffness of saturated clays will first be reviewed. It is assumed here that the general ideas relating to the behaviour of saturated soils can be extended to partially saturated soils as well, so that this section should also be viewed as providing the necessary background information for the testing of partially saturated soils. The second part of this section will then discuss the stress-strain behaviour of partially saturated clays with its added complexities.

7.2 The use of triaxial apparatus to determine the stiffness of saturated clays.

In the standard triaxial test, the sample is failed by means of an increasing vertical stress with a constant horizontal stress which gives a direct measurement of the stiffness of the clay. A problem does arise however, because clays display distinct non-linearity at strains greater than 0,5%, making it difficult to define any one value of Young's Modulus for the whole stress range. It is therefore possible to define a range of moduli, as shown in Figure 21. For example:

1. The initial Tangent Modulus, E_i

2. Secant Modulus at Failure, E_f equals the slope of the line between the origin and the point of failure.

3. The Secant Modulus which is the slope of the line drawn between the origin and any specified stress level (eg E_{50} in Figure 21).

The type of triaxial test to obtain the E-values previously described, can either be the unconsolidated undrained test (denoted the UU test) or the consolidated isotropically undrained test (denoted the CIU test) (Ladd 1964). Usually an E-value determined from triaxial tests is used in the calculation of immediate settlements which precludes the use of drained triaxial tests.

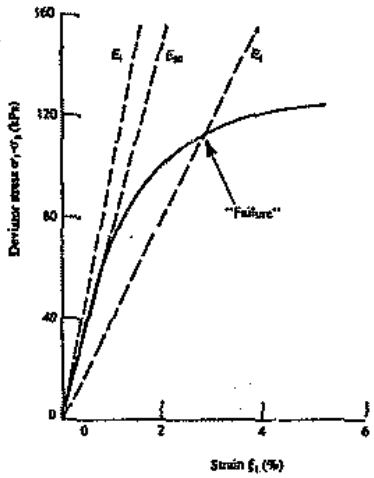

Figure 21. Stress-strain curve for undrained test on NC clay (Lee, White and Ingles 1983).

It is generally believed that the E-value from UU tests is too low due to the effects of sampling disturbance, while the value from the CIU test, consolidated to the in-situ effective stress, is too high (Ladd 1964). The degree of error can be up to 400% in either case, but the CIU test is recommended because it eliminates the effect of sampling disturbance (Ladd 1964). Hence, even in saturated soils where the understanding of the mechanical behaviour is quite well advanced, the standard techniques can only give very approximate values of the modulus.

It is now well known that effective stress governs the mechanical behaviour of saturated soil, as has been previously stated. Thus, in a CIU test, the larger the initial effective stress, the larger the stiffness and ultimate strength of the sample. Ladd (1964) maintains that for the clays he tested, the stress-strain curves could be normalized by dividing the deviator stress by the initial effective consolidation stress. This normalization procedure yields one stress-strain curve, making the E-value dependent on the initial effective consolidation stress (Lambe and Whitman 1969). This approach is particularly successful if the stress path for each initial consolidation stress is geometrically similar and if the strain contours are straight lines, as shown in Figure 22 For Amua clay.

Figure 23 shows the normalized stress-strain curve for Amua clay as well as for four other clays.

Although of great value, this approach may not be applicable to all types of soils because the peak strength is usually reached at differing axial strains. Usually the greater the initial effective stress, the greater the axial strain at failure. This point will be further discussed in the section dealing with the experimental results

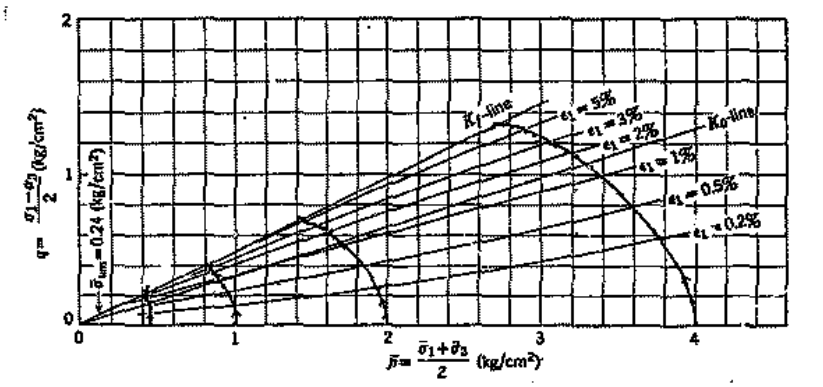

Figure 22. Contours of equal strain for normally consolidated Amua clay (Whitman and Lambe 1969).

Other factors which have an effect on the E-value, as determined from the triaxial test, can be listed as follows (*Lambe and Whitman* 1969):

1. Load cycling: The stress-strain modulus is greater on a second cycle of loading than on the initial one due to the elimination of seating errors and the closing of sample cracks. Generally the moduli differ by a factor of 1.5 for undrained loading.

2. Influence of time:

   a. Thixotropic effects: If a soil sample is stored for some time before testing, there is a possibility that it may be stiffer than if the sample were tested immediately after sample preparation. Thus, for certain soil types, a period of sample storage may be necessary before testing to give a more realistic value of the stiffness.

   b. Aging effects: This refers to the influence of the length of time that a sample is allowed to undergo secondary consolidation. In some cases an increase in aging, of approximately 60 days, can nearly double the stiffness of the sample.

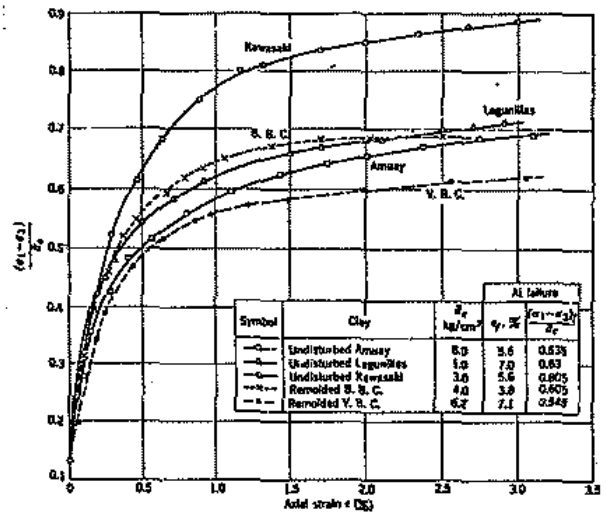

Figure 23. Stress-strain curves from triaxial tests on five normally consolidat i clays (Ladd 1964).

c. Strain rate effects: *Strain rate refers to the rate of strain (change in axial strain per unit time) that* is applied during undrained shear. For example, it has been shown that a reduction in strain rate from 1% per minute to 0.002% per minute caused a reduction in modulus of the order of 200% for a plastic clay.

3. Stress path: *Ladd (1964) subjected various samples of the same material to different stress paths.* For example, he took two samples and consolidated them anisotopically. He then increased the axial load in the one sample while he decreased it in the other. In both tests the horizontal stress was kept constant. The results show that the unloaded sample was more than twice as stiff as the loaded sample. This illustrates that when determining an E-value from laboratory tests, it is always important to follow the stress path which is anticipated in the field.

Recent research has shown that the measurement of soil stiffness in the triaxial test is in fact invalid if an unmodified triaxial apparatus is used (Jardine et al 1984). This is because it is impossible to measure the true sa..ple deformations by means of instruments extraneous to the sample (such as a dial gauge measuring overall chan..e in sample length). For example, Figure 24 shows all of the deformations which could be registered by such a device, but the sum of these deformations clearly does not correspond to the true sample

deformation. Thus, even when careful calibration of the ram deflections is undertaken, bedding in of the end platens and tilting of the sample are very difficult to correct for in the standard test.

To overcome this problem a special device was developed to measure actual sample strains (Jardine et al 1983) (Figure 25). The transducer consists of a capsule containing three coplanar electrodes which protrude into the capsule and are partially immersed in the electrolyte. As the transducer goes thro gh some angle of tilt, the impedance between the central electrode and the outer ones varies. A calibration curve relating the relative movement of points A and B (Figure 25) to the voltage output can then be easily established by mounting the gauges on a micrometer winding frame. Further, on this winding frame, an LVDT with a sensitivity of 0,2μm was attached to measure the displacement. Through the use of this technique, it was shown that the gauges could actually measure displacements less than 0.01mm.

The difference between the standard curve using corrected strain recordings (ε_a) and true axial strains is shown in Figure 26. From this figure one would normally conclude that the material was behaving in a linear elastic fashion, but obviously by comparison with the more accurate curve, the true behaviour is much stiffer and non-linear. In this case the initial tangent modulus of the apparent stress-strain line was 12 times smaller than for the true stress-strain curve (Jardine et al 1983).

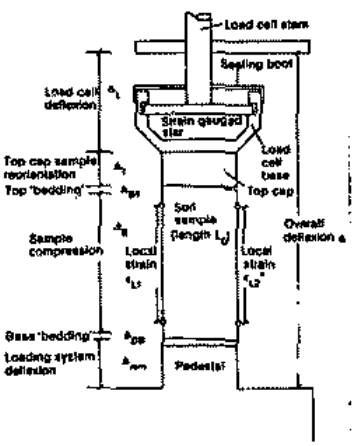

Figure 24. Sources of error in external strain measurements (Jardine et al 1984)

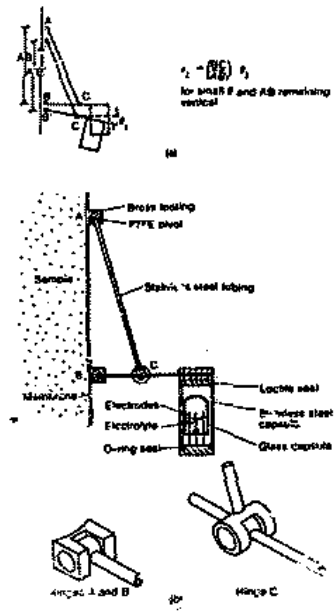

Figure 25. The construction [illegible] capsule [illegible] measuring local axial strains (Jardine et al 1984).

7.3 *Testing of Partially Saturated Soils in the Triaxial Apparatus*

7.3.1 Introduction

The testing of partially saturated soils in the laboratory is unfortunately rather complex due to the many variables involved. In this section the various modifications that have to be made to the triaxial apparatus will be examined while a few problems that arise in these tests will also be highlighted.

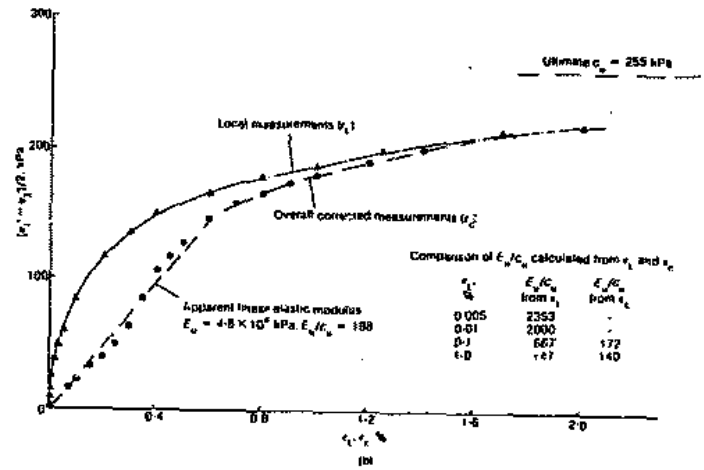

Figure 26. Stress-strain data for a sample of undisturbed North Sea clay tested unconsolidated undrained (Jardine et al 1984)

7.3.2 Modifications to the Triaxial Apparatus

Only a very brief description of the major modifications will be given here. For a more detailed treatment, refer to Ho and Fredlund (1982) and Bishop and Henkel (1962).

The major modifications can be listed as follows (Ho and Fredlund 1982):

1 *Pore-water* pressure control: Pore-water pressures are controlled through a porous ceramic disc sealed into the base of the pedestal (Figure 27). This disc usually consists of fired kaolinite which, by virtue of its very tiny pores, prevents the passage of air when saturated. The reason for this is to create a continuous column of water from the sample base to the pore water pressure measuring device. If air bubbles were allowed into the pore water pressure measuring system, then misleading measurements of pore pressure would result.

2. Pore-air pressure control: The pore-air pressure in the sample is controlled through an air pressure line connected to the loading cap (Figure 27). Between the loading cap and the sample a coarse grained

corundum stone is used as a drainage element for the air. The stone must be coarse grained to prevent the stone from imbibing water from the sample.

3. Flushing system: Although the ceramic disc does not allow the passage of free air, it is found that dissolved air is still able to diffuse through the disc and cause an air bubble to form at the base of the disc. A flushing system may have to be introduced to eliminate these bubbles. It consists of an added drainage line connected to the pore-water pressure transducer (*Figure* 27). To minimise the potential of the water in the pore-water pressure measuring system to dissolve air, the axis-translation technique is used with pore-water pressures greater than zero.

7.3.3 Testing procedures for partially saturated soils

As discussed previously, the effective stress in partially saturated soils is dependent on both $(\sigma - u_a)$ and $(u_a - u_w)$. This fact makes the testing of partially saturated soils difficult because of the number of permutations involved. For instance, for each value of $(\sigma - u_a)$ there can be a number of possible suction values depending on the stress range under consideration. To overcome this problem Fredlund and Ho (1982) have developed a multi-stage testing technique to reduce the number of tests. This technique will now be described in more detail.

The basic principle involved is to test the sample in various stages until the deviator stress levels off (Figure 28). After each stage the deviator stress is reduced to zero, the stress state variables (ie.$(\sigma - u_a)$ and/or $(u_a - u_w)$) are changed and the sample is reloaded again. The stress state variables for each stage are listed in Figure 28 which shows that the same values of $(\sigma_3 - u_a)$ are used for all the stages, but the value of the soil suction is increased at each subsequent stage.

It is worth mentioning that in cases where the initial value of the suction in the sample was greater than that needed for stage 1 loading, a special procedure had to be adopted to reduce the suction. Secondly, the deviator stress was reduced to zero at the end of stage 1 and 2 to prevent the accumulation of strain. The authors did in fact comment that at stage 3 loading, the accumulation of strain did adversely affect the shear strength of the sample.

Actual data generated by this technique is shown in Figure 29.

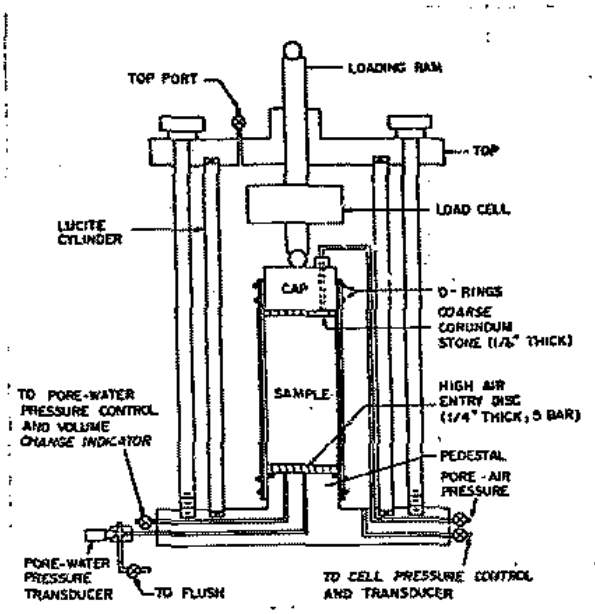

Figure 27. Modified triaxial cell for unsaturated soils (Fredlund and Ho 1982).

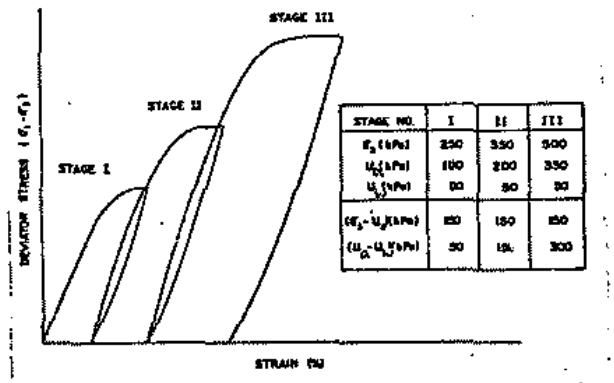

Figure 28. Ideal stress versus strain curves for a multistage test using the cyclic loading procedure (Fredlund and Ho 1982).

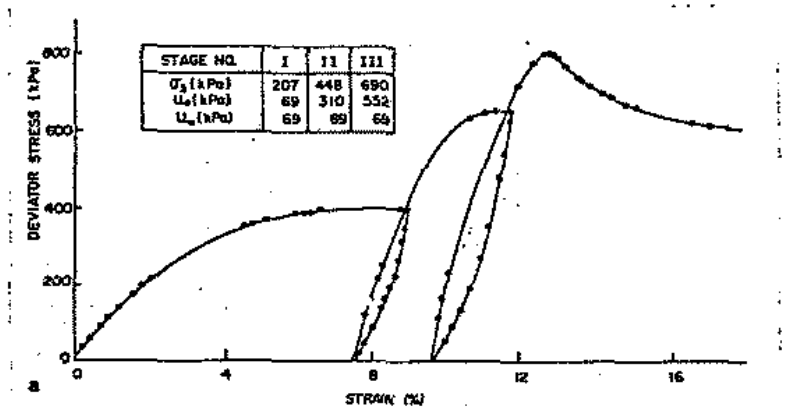

Figure 29. Stress versus strain curves for decomposed granite (Fredlund and Ho 1982).

7.3.4 Additional problems associated with triaxial testing of partially saturated soils

The in-situ stresses are very difficult to determine in clay profiles, so it is assumed that a K_o test usually best represents the in-situ conditions (Pile and McInnes 1984). This type of test is difficult to perform because, to prevent lateral strain, a large confining stress needs to be applied. Consequently, any free vertical strain occurring, due to swell, is severely reduced due to the associated large vertical stresses (Pile and McInnes 1984). However, if tension is applied to the top cap of a magnitude equal to the cell pressure, then the applied vertical stress can be reduced to zero. Note also that when saturating a partially saturated sample, the cell pressure must be kept above the swelling pressure of the clay so that the original sample dimensions can be used in the analysis.

Other problems include excessive testing times. Testing times in excess of 4 days are not uncommon (Blight 1963). Lastly, it has been found that air diffuses from the sample into the cell water through the rubber membrane causing an air-pressure drop of 5% over a 24hr period (Bishop and Henkel 1972). On the other hand, if u_a can be controlled than this should not be a serious problem.

7.4 Summary

1. Non-linearity displayed in stress strain curves from the triaxial test makes it difficult to define one characteristic modulus for a soil. In fact, three moduli can be defined, namely an initial tangent modulus, a secant modulus at failure and a secant modulus drawn between the origin and some specified stress level.

2. Many factors effect the modulus as determined in the triaxial apparatus. Most important of these factors is effective stress, but stress path, strain rate, thixotropic and aging effects as well as load cycling can measurably influence the modulus value measured. It has also been shown that the compliance of the apparatus itself causes the initial tangent modulus to be significantly underestimated.

3. Partially saturated soils can be tested in the triaxial apparatus provided a porous stone is placed in the pedestal with a high air entry value for the control of pore water pressure. Further, an air pressure line for the control of pore air pressure is connected to the top loading cap. A possible testing procedure entails stage loading the sample at different matrix suctions while the total stress variable $(\sigma - u_a)$ is held constant.

8.0 The use of Consolidometers in Expansive Soils Technology.

8.1 Introduction.

A review of the literature dealing with expansive soils shows that the standard consolidometer is the preferred instrument for testing these soils. The main reason is that it is a simple apparatus to use and the interpretation of the results is not very complex. Also, the oedometer allows one to follow a wide variety of stress-paths with respect to the applied vertical pressure as shown in Figure 30.

However, the main disadvantage of this instrument is that suction cannot be measured during the test. In a standard consolidometer test, the sample is usually saturated so that only the final value of suction is known (ie. final suction value is zero) and hence, the true stress path incorporating suction is unknown. Due to the fact that the mechanical behaviour of expansive clays is highly stress path dependent it is not sufficient to simply know the final boundary condition. The initial boundary condition, as well as the path taken towards this boundary condition, is also of vital importance (eg. refer to points A and B in Figure 30 which lie on stress paths with the same boundary conditions, but show different swell due to their differing stress paths). Another disadvantage of the standard consolidometer is that, because the sample is saturated at the end of the test, it gives overly conservative results if the final condition in the field is not one of full saturation (Mou 1981).

For these reasons suction controlled consolidometer tests have been developed by various authors, each of which will be described in this section. Please note however, that in this section much will be said about swelling potential and swelling pressures, while very little will be said directly about stiffness. The reason for this is twofold. Firstly, most research work in the past has gone into determining swelling potential and swelling pressure and secondly, a thorough understanding of these two factors lies at the base of an understanding of stiffness.

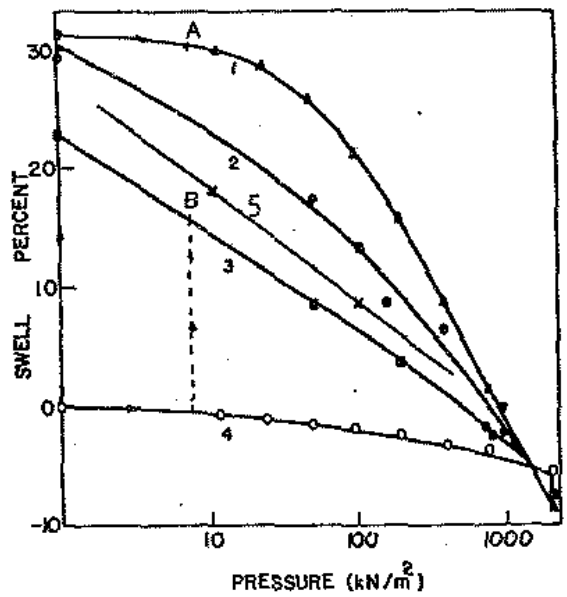

Legend: 1= Free swell curve (sample is allowed to swell under nominal load and then compressed).
2= The sample is allowed to swell to a chosen percent swell, then held.
3= Sample held at constant volume while being wetted, then unloaded after maximum swell pressure development.
4= Natural moisture content compression.
5= Sample allowed to swell under constant pressure.

Figure 30. Different stress paths that can be defined by using the conventional consolidometer (After Brackley 1971).

8.2 *The Membrane Oedometer:*

This instrument was developed by Aitchison and Martin (1973) and a cross-section is shown in Figure *31*.

The main modifications to the standard oedometer include the following:

1. The sample is enclosed in a cell so that u_a can be raised above atmospheric pressure. Hence, by varying u_a and keeping $(\sigma - u_w)$ constant, the matrix suction in the sample can be varied. This facility also allows one to determine the in-situ effective matrix suction of the sample. This is achieved by placing an undisturbed sample in the apparatus and allowing it to imbibe water (at atmospheric pressure) under an applied in-situ overburden pressure (this pressure is applied through the loading rod). Air pressure is then simultaneously applied to restrain the sample swelling and the final air pressure required to hold the sample at zero volume change is denoted as the effective matrix suction (Aitchison and Peter 1973). The range of suctions that can be determined in this way lie between pF2 and pF4.

2. If necessary, an electrolyte instead of water maintained at atmospheric pressure, can be circulated through the porous stone at the base of the sample. An automatic flushing system reverses the direction of flow periodically so as to prevent accumulation of air bubbles in the system.

Therefore, with these two major modifications any stress path can be followed with respect to total stress, matrix suction and . ate suction (Peter 1973).

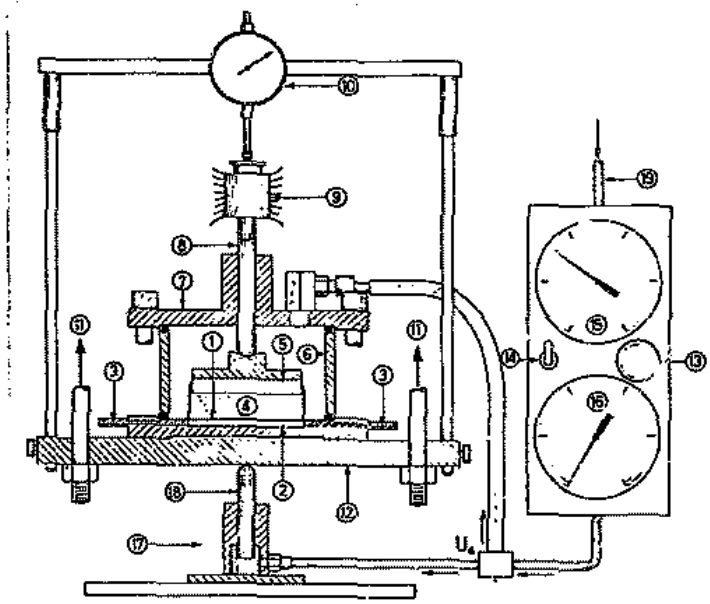

Figure 31. Cross-section of membrane oedometer (Aitchison and Martin 1973).

8.3 Consolidometer developed by Escario and Saez (1973):

A cross-section of this apparatus is given in Figure 32 which shows that the instrument is very similar in construction to the membrane oedometer.

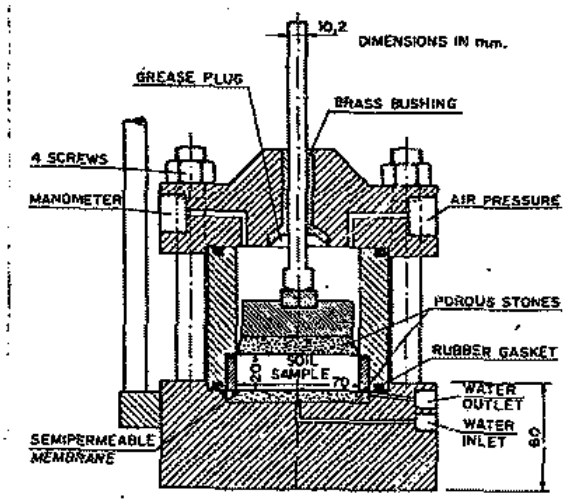

Figure 32. Cross-section of a modified consolidometer developed by Escario and Saez (1973).

This instrument employs the axis-translation technique directly, whereby the pore-water pressure is controlled by an external isotropic air pressure applied to the sample in an enclosed cell. Since the pore-water is always maintained at atmospheric pressure, the internal air pressure is taken as equal to the suction in the sample at some point of equilibrium. In this way suctions of up to pF5,0 can be attained.

Typical results from this instrument are shown in Figure 33. Each curve represents a test with a different sample, each having the same initial density and water content. Initially a vertical load was applied with an air pressure equal to the predetermined suction (17,5 kg/cm^2 in this case). The air pressure was then reduced in steps so as to reduce the suction (the sample was allowed to imbibe water) and the corresponding percent swell was recorded. This curve could be used very effectively to define a modulus because it simulates the conditions under a house foundation quite closely.

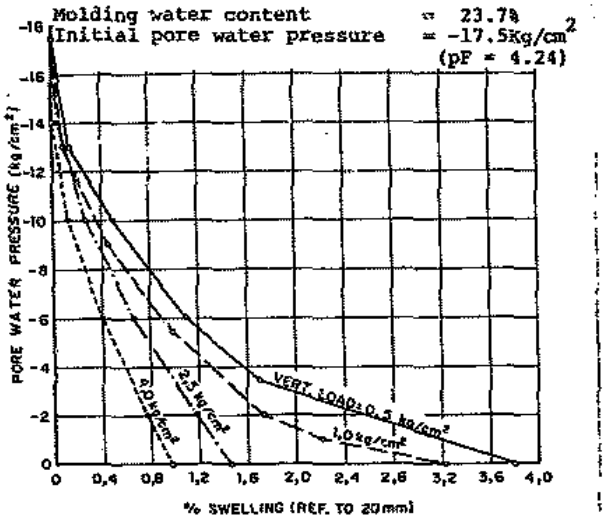

Figure 33. Swelling under constant load and controlled negative pore-water pressure of remoulded clay (Escario and Saez 1973).

8.4 Controlled suction consolidometer developed by Chu and Mou (1973):

The basic layout of this instrument is shown in Figure 34. A suction is developed in the specimen by applying a tension to the de-aired water in the chamber, as indicated in the sketch. The chamber wall is transparent so that air bubbles can be detected below the ceramic plate before the commencement of the test. If air bubbles are present then the vent is used to flush them out.

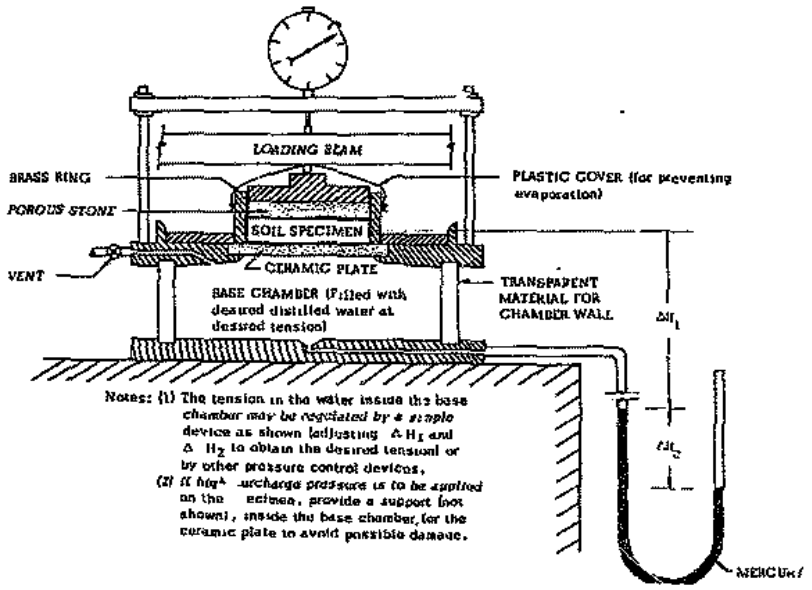

Figure 34. Controlled suction consolidometer developed by Chu and Mou (1973).

Chu and Mou (1973) as well as Mou (1981) have done extensive work with this instrument. Their main interest has been developing a relationship between suction and swelling pressure, and suction and percentage swell (Mou 1981). Some of their more important discoveries in this regard will now be discussed:

1. Tests were conducted where the suction was varied under a constant surcharge. The results of this test are shown in Figure 35 which show that the percent swell is severely reduced after the first cycle of wetting. However, there appears to be a discrepancy in these results because one would expect that the same rebound curve would be followed for both a suction increase and decrease (Blight 1989). Perhaps this discrepancy could be explained by assuming that the initial suction was much greater than the 5 psi that they have assumed and therefore, if the true initial suction was re-established, the percent shrinkage would correlate more closely with the percent swell measured initially.

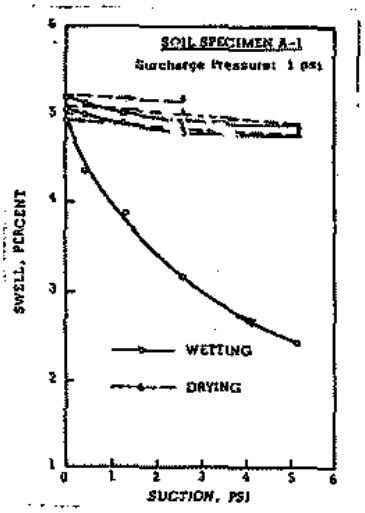

Figure 35. Relationship between suction and swell determined by controlled suction tests (Chu and Mou 1973).

Later work (Mou 1981) showed that most of the swell in a specimen occurs at very low values of suction and is therefore not evenly distributed over a wider suction range (Figure 36). Hence, accurate estimates of potential volume changes (from suction controlled oedometers) require very accurate estimates of the final suction values under the foundation. The validity of (Figure 36) needs to be investigated though because one would suspect that, at the very low suctions quoted in this figure, the water contained in the tank below the sample would cavitate.

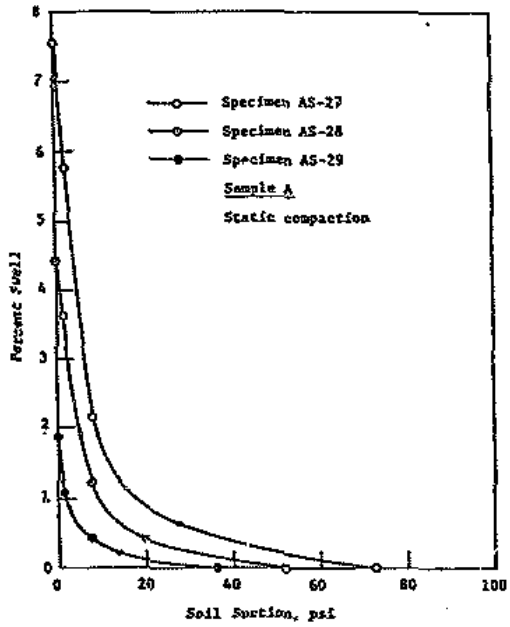

Figure 36. Percent swell vs soil suction relationship for specimens under nominal surcharge (Mou 1981).

2. Chu and Mou (19[illegible]) also conducted standard consolidometer tests whereby the sample was flooded and the resultant swell recorded. They compared these results with those obtained from their modified oedometer under the same conditions, *except that the initial suction was reduced* to zero in various stages. Their findings show that the saturation type test produced substantially greater percentage swell than did the controlled suction test (the results differed by a factor of roughly 5 in some cases).

8.5 Suction controlled consolidometer developed by Richards, Peter and Martin (1984).

This consolidometer is identical in many respects to the membrane oedometer but it is a more compact and sophisticated version as shown in Figure 37.

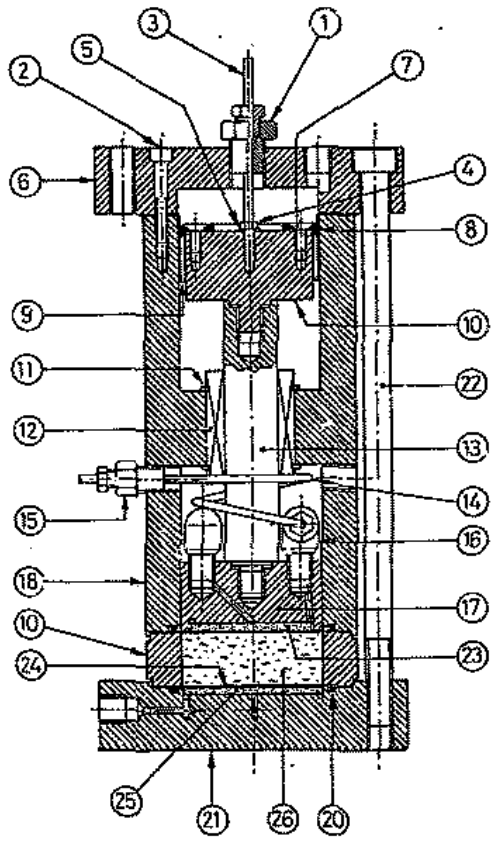

Item	Quantity	Description
1	1	Sliding shaft gland 1/8in dia.
2	4	Socket H'D. Cap screw - M5x0.8x30 Stainless Steel
3	1	Indicator Rod
4	1	Hex nut- No.5. 40 UNC Stainless Steel
5	1	Flat Washer - 1/8in Stainless Steel
6	1	Top end
7	6	Socket Csk. H'D Screw - M4x0.7x12 Stainless Steel
8	1	Diaphram Retainer
9	1	Rolling diaphram seal'Bellofram No.4' 200-162-CBJ
10	1	Air Piston
11	2	External Circlip 1.25in dia.
12	1	Linear bearing 'Barden No.L12'
13	1	Rod
14	2	Nylon pressure tube 1/4in O.D.x0.96in ID. BSC No.NIST4- length to suit
15	2	Adaptor - 1/8in BSP.Tr.Ext.x1/8in Tube - BSC No.-MA-4-4
16	2	Elbow - 1/8in BSP.Tr.Ext.x1/8in Tube - BSC No.B-MEA-4-4
17	1	Consolidator Piston
18	1	Cylinder
19	1	Sample Ring
20	2	'O'-ring - BS 1806: No.228, BSC No.6230/6
21	1	Base end
22	4	Socket H'D. Cap Screw - M10x1.5x200 Stainless Steel
23	1	Porous Stone - Ø $\frac{45.0}{44.9}$x3±0.1 Thick *Aust. Abrasives Grade A 150 kV*
24	1	Visquine permeable membrane size to suit
25	1	Porous stone - Ø $\frac{50.0}{49.9}$x3±0.1 Thick Aust Abrasives
26	0	Sample

Figure 37. Schematic diagram of suction controlled oedometer developed by Richards, Peter and Martin (1984).

The external load is applied through a pneumatically operated piston while the matrix suction is controlled by means of air pressure applied through the top porous stone. This applied air pressure is taken as equal to the soil suction under free draining conditions by virtue of the axis-translation technique. Thus, with this configuration, the actual applied vertical pressure to the sample is assumed to be the pressure applied to the piston less the air pressure applied to the sample. The solute suction of the sample is controlled by means of flushing solute with known suction characteristics under a positive head of 12 kPa through the bottom porous stone. To remove diffused air, the flow of this solution is reversed every 2 minutes. Finally, vertical deformations of the sample are measured by means of a dial gauge on a rod connected to the platen on top of the sample.

This instrument was developed for the express purpose of determining volume changes caused by changes in suction under differing vertical loads. A straight line relationship is assumed to exist between the log of suction (abscissa) and vertical strain (ordinate) (Figure 38). The slope of this line is termed the "Instability Index".

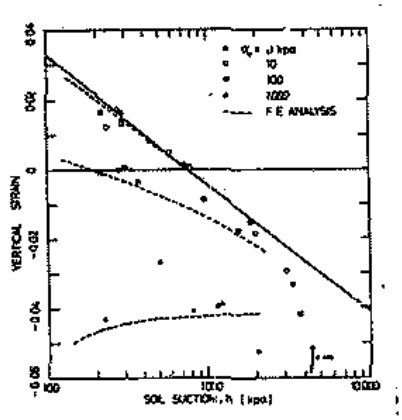

Figure 38. Experimental results from tests on Riverina clay. The results from a finite element analysis have also been included. (Richards et al 1984).

Thus, the instability index is a good indicator of the reactivity of a soil to a known suction change under a given load. Typical values of the instability index for an expansive clay lie in the range of 8-11%. In spite of it's usefulness the instability index approach does suffer from the following shortcomings (Richards et al 1984).

1. For some clays the relationship between percentage swell and log of suction is definitely not linear.

2. The value of the instability index is dependent on the applied vertical stress on the sample.

3. The instability index is dependent on the degree of lateral restraint applied to the sample.

Additional points to note are that the value of the instability index is significantly greater for shrinking than for swelling. This is not surprising when one considers that the soil is in the normally consolidated and overconsolidated range of the e-logp curve when the soil is shrinking and swelling respectively. Also, laboratory determined instability indices have been shown to be three times smaller than those determined in the open field for the same material (Richards et al 1984). This is a surprising result because one would expect that due to the closing up of the macro-cracks in the field there would be less expansion. However Richards

et al (loc. cit.) postulates that in the field long term seasonal swelling occurs while in the laboratory swelling occurs over a much shorter time interval (days).

Of particular interest is the effect of solute suction as well as the type of solute on volume change. Figure 39 shows that, especially for the lower values of the vertical stress, the changes in the solute suction can have a pronounced effect on volume change behaviour. This result could be significant when performing swell-under-load tests as formulated by Brackley (1983) because the indications are that swell could be overpredicted if distilled water is used. Also of interest is the fact that the type of solute used has a significant effect on volume change behaviour with NaCl giving a significantly greater volume change as compared to other solute types (Figure 40).

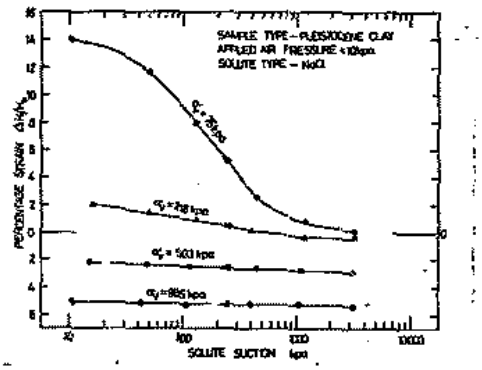

Figure 39. Results of consolidometer tests on pleistocene clay varying the concentration of NaCl in the equilibrating solution. (Richards et al 1984).

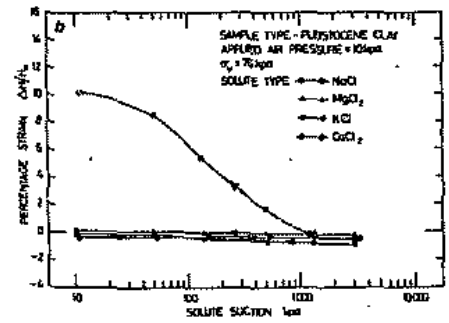

Figure 40. Results of consolidometer tests on pleistocene clay for different solutes in the equilibrating solution. The small volume change occuring on the shrinkage path is due to the expulsion of liquid from the sample *therefore allowing few solutes to enter* the sample (Richards et al 1984).

8.6 Constant-rate-of-strain consolidometers:

A major disadvantage of the conventional incrementally loaded oedometer (abbreviated STD test) is that the time required to complete a test may become excessive. For example, the average test *can take up to 9 days* or longer (Gorman et al 1978). To circumvent this problem constant-rate-of-strain consolidometers (denoted as the CRS test) have been devised. Essentially this instrument is the same as the conventional consolidometer, except that the consolidometer *cell is placed in a triaxial* loading press. Also, to aid in sample saturation, a back pressure lead is sometimes connected to the base and top of the sample while pore pressures are measured at the base of the sample (Wissa et al 1971).

Experience with constant-rate-of-strain consolidometers have shown that they can generate e-log p' curves which are very close to those produced by *conventional consolidometers. This is shown* in Figure 41 which presents the results from STD tests and CRS tests on Boston Blue clay. As further confirmation of the validity of using CRS tests, is the finding that the confined modulus (D) for STD tests and CRS tests correlate very closely (Figure 42).

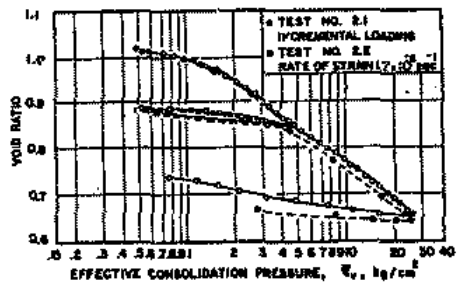

Figure 41. Comparison of stress-strain relations as obtained from incremental loading test and CRS test (Wissa et al 1971).

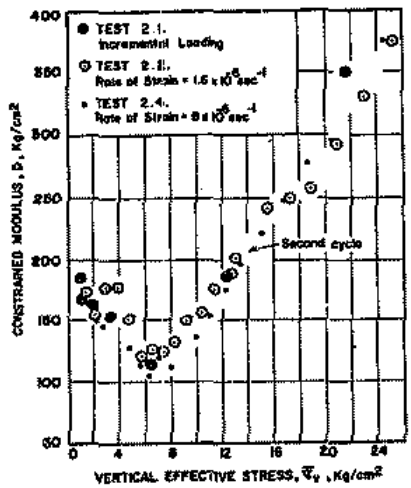

Figure 42. Comparison of constrained moduli.: These results are obtained from an incremental loading test and two constant-rate-of-strain tests (Wissa et al 1971).

A *strain controlled consolidometer* has been developed by Nelson and Porter (1980) for the specific purpose of testing expansive soils. The test procedure consists of initially confining the sample in the loading frame so that no volume change can take place when water is added. Once water has been added the maximum swelling pressure is allowed to develop, whereupon the sample is allowed to swell by a prescribed amount

and the associated swelling pressure is measured. Hence, strain is controlled incrementally and not continuously, as in the previously described tests.

Porter and Nelson (1980) arrived at some interesting conclusions from tests performed on shales from the Western USA. Figure 43A gives a typical curve from a conventional consolidometer apparatus. On the other hand Figure 43B shows typical results from tests on the same shale using the strain controlled consolidometer as described above. If these two curves are superimposed (Figure 43C) then it is found that the points on both curves are coincident (ie. these authors assume that curves 3 and 5 in Figure 30 are co-incident). This has led Porter and Nelson to believe that incremental strain controlled testing can replace the incrementally loaded consolidometer with a concomitant saving in testing time. Whether or not this assumption applies only to this particular material or can be stated generally has yet to be investigated.

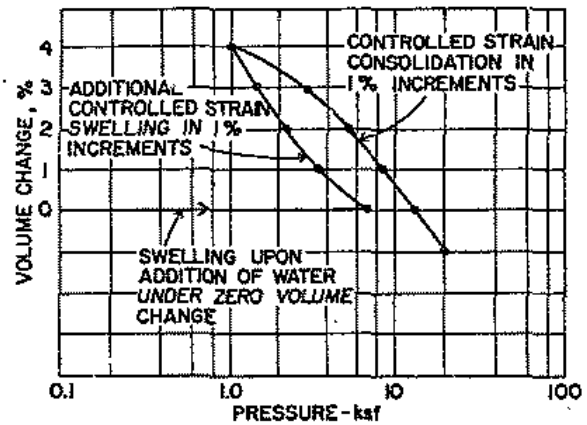

Figure 43A Typical consolidation-swell test results (Porter and Nelson 1980).

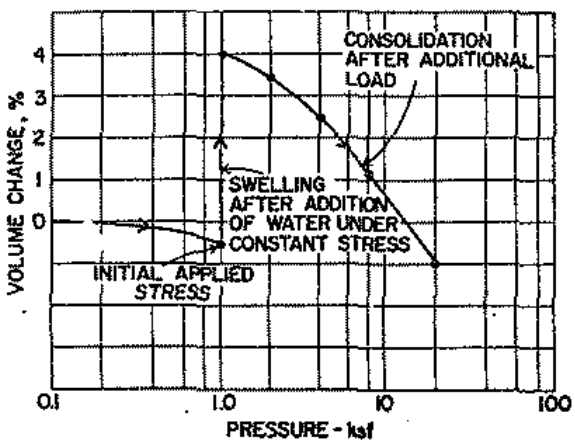

Figure 43B Typical strain controlled swell tests (Porter and Nelson 1980).

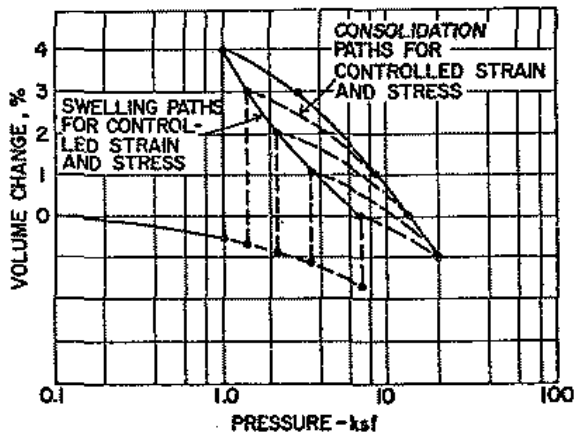

Figure 43c Comparison of controlled strain and consolidation swell test results (Porter and Nelson 1980).

8.7 Corrections to be applied to the Consolidometer results.

The first consolidometer was developed in 1925 by Terzaghi for the specific purpose of establishing the rate of settlement and the ultimate settlement of expansive clays. Thus, when the consolidometer is used to test expansive soils, special procedures and corrections have to be introduded because the consolidometer in its standard form is now no longer being used for its originally intended purpose (Fredlund 1969).

For instance, in the constant volume test (stress path 3, figure 18), the final swelling pressure is highly sensitive to volume changes of the order of 'a fraction of a few percent'(Fredlund 1969). It is therefore obvious that any deformations occuring in the consolidometer apparatus itself can have a significant effect on the value of the final swelling pressure. In fact Fredlund (1969) maintains that, without corrections for apparatus compressibility, the measured swelling pressure can sometimes be underestimated by as much as 100%.

Essentially the correction process consists of accounting for deformations that occur external to the sample but are nevertheless measured on the dial gauge. A description of the main sources of deformation that occur external to the sample can be listed as follows (Fredlund 1969):

1. Compressibility of the apparatus: The compression of the apparatus can be measured by using a steel plug for the sample and performing loading and unloading cycles.

2. Compressibility of the filter paper: The deformations occuring in the filter paper usually placed above and below the sample can be four times as large as the deformations occuring in the apparatus at a load of 100 kPa. For this reason Fredlund recommends that filter paper should not be used when testing expansive soils.

3. Seating of the porous stones and the soil sample: Seating occurs as the peaks from the soil surface fail and fit into the porous stones. Additional seating also occurs due to the levelling out of the roughness on a larger scale. Seating deformations can be reduced by loading the sample to the total vertical pressure existing at the time of sampling.

4. Fredlund (1969) has also noted that, due to friction in the pin connections on the loading arm, a lower load is applied to the sample than actually calculated using moment equilibrium. The error can be of the order of 1.2% for an applied pressure above 20kPa using a Wykeham-Farrance bench model consolidometer. For lower loads, the error increases significantly up to an error of 100% for a load of 1kPa.

8.8 Summary

1. The standard oedometer can be used to follow many different stress paths with regard to sequences of loading, sample volume control and point or time of sample wetting. Conversely, the standard apparatus cannot follow a stress path defined in terms of suction changes. For this reason, modified oedometers have been developed which can measure both matrix and solute suction.

2. Suction controlled oedometers can be used to quantify the instability index which is defined as the slope of of the assumed linear relationship between changes in vertical strain (ordinate) and soil suction (plotted on a log scale). The instability index is a useful index in characterising the volume change properties of a soil and could find application in future computer models of soil structure interaction. However, the relationship between log soil suction and vertical strain is often not linear, and furthermore, it is dependent on the applied vertical pressure.

3. Changes in solute suction as well as solute type can significantly effect swell behaviour especially at lower loads. Thus it appears that the influence of solute suction could have an influence on the swell under load test as proposed by Brackley (1983).

4. Particular care should be taken to account for extraneous deformations in the oedometer such as apparatus compressibility, filter paper compressibility and seating of the porous stone and sample particularly when determining swelling pressures. This is because the final swelling pressure has been shown to be highly sensitive to very small volume changes.

5. Constant-rate-of-strain oedometers give results very similar to those of the conventional oedometers, but can also achieve a large saving in testing times. An incrementally strain controlled oedometer has been developed to test expansive soils. In the conventional oedometer, at least two samples have to be tested to obtain the swell under load curve. However, tests on expansive shale with this incrementally strain controlled oedometer showed that only one sample needs to be tested to obtain this curve and testing times are also shorter.

Presentation of the experimental results

9.0 Explanation of the Experimental Design.

Unfortunately, in the case of soils and particularly expansive soils, it is difficult to describe the material by means of one value of modulus only. As was shown in the literature survey, the behaviour of the material is highly stress path dependent and therefore a whole range of moduli values can be generated depending on the stress path followed. Consequently, the primary aim of this program is to subject the Onderstepoort clay to a number of stress paths in the standard oedometer and triaxial apparatus so as to ascertain the extent of this range. Also, modulus values obtained from these tests will be compared with the value of EEMM recommended by Pidgeon (1988), so as to identify which type of test gives a modulus within the appropriate range for the purposes of raft design. Finally, values of the field moduli determined by Sanders (1989) will be compared with values of the laboratory moduli determined in this experimental program.

In this experimental program, the constants are the type of soil, the initial conditions of the soil with respect to the dry density, and the degree of sample disturbance (ie all the sample will be remolded). On the other hand, the main variable is the stress path followed.

10.0 Material Description.

Only one type of material was used in the entire experimental program. This comprised of highly expansive clay obtained from a site near Onderstepoort north of Pretoria. To the layman this clay is known as a "black-turf" and is a residual soil derived from the in-situ weathering of norite gabbro (Brink 1979).

A typical profile at Onderstepoort is presented in figure 44 which shows that the profile essentially consists of a residual gabbro roughly 3.3m deep overlying gabbro bedrock. This profile developed in a topographic depression which is a common setting for the formation of a deep residual profile of expansive clay (Brink 1979, Ollier 1984). The reason for this is that, in topographic depressions, weathering products are not flushed away which allows for the production of complex clay minerals such as smectite.

Another interesting feature regarding this profile is that a layer of sand consisting of pyroxene and plagioclase interfaces with the bedrock at the base of the profile. This layer has a low swelling potential (Van Der Merwe 1967) and represents an early stage of weathering of the parent material. The absence of a water table is also noteworthy while the absence of a pebble marker indicates that the entire profile consists of residual soil. Not indicated in figure 44 is the fact that the soil mass is highly fissured. Fissures at the surface can reach 100 mm in width (Brink 1979). During the dry season surface material accumulates in these fissures and is subsequently incorporated into the soil mass when the cracks close up again during the rainy season. Consequently the profile is being continually reworked in-situ (Williams and Pidgeon 1983).

A general description of the material used in this experimental program is given in table 1. Of particular importance is the fact that the material is in a remoulded state before testing. As already mentioned, the soil is remoulded in-situ and therefore it is felt that there would be very little difference in behaviour between disturbed and undisturbed material (Williams 1987).

The grading curve for this material is shown in figure 45. The coarse sand and fine gravel fraction arose from the presence of calcium carbonate nodules. The calcium is a weathering product of plagioclase feldspar which is a predominant mineral found in gabbro (Partridge 1988). In general the proportion of calcium carbonate is small which results in the material being very fine indeed.

Figure 46 shows the suction versus moisture content curve for the material. This curve was determined in the laboratory by means of a thermocouple psychrometer placed in a C-52 sample chamber supplied by WESCOR. As shown in this figure, the material displays extremely large suctions even at large moisture contents, which implies that the material will remain relatively moist throughout the year. In fact Williams

and Pidgeon (1983) state that the moisture content of the clay will never drop below the permanent wilting point of the plants which corresponds to a moisture content of 25% in this case. The curve they proposed has also been included as a comparison and confirmation of the results. It was felt that agreement was generally good considering that, in any case, slightly different materials were being tested.

The compaction versus moisture content curve, using a standard Proctor mould and compaction effort, is shown in figure 47. The optimum moisture content is of the order of 25% corresponding to a dry density of approximately 1440kg/m^3. This dry density has been used for all the samples tested in the experimental program so as to obtain a basis of comparison for all the results.

Except for one test, all of the material used in the experiments was taken from a drum in which it was originally placed on site. Therefore, it had never been dried out beyond the point at which it is in equilibrium with the atmosphere (7-9% water content). At a water content of approximately 20% and lower, the material is in a state as described in table 1 (ie it has a shattered crumb structure). However, at higher moisture contents, (say above 25%) the material turns into a highly plastic and workable material. The implication of this is that one is not only testing a material at different moisture contents, but one is also dealing with a material with a greatly varying soil fabric depending on the water content.

A lower limit for the water content has been set at a value corresponding to the lowest water content likely to occur in the field. As has already been discussed, one would not expect the field moisture content to drop below 25% . On the other hand, a water content corresponding to full saturation (at a dry density of 1440 kg/m^3) will form the upper bound value for the laboratory samples which is equal to 33% in this case. Thus the range of water contents that can be used in this experimental program lie in the small range of 25-33%. In practice this range will be extended to include lower water contents in the hope of identifying general trends.

Lastly, all mixing water used was distilled water at ambient temperature. This was so as to avoid changing the salt content of the soil through repeated additions and evaporation of the water.

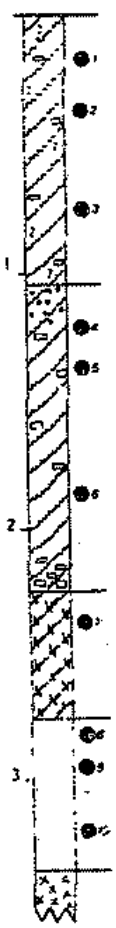

		Liquid limit	Plasticity index	Linear shrinkage	Clay <2µm	Montmorillonite	Specific surface (m²/gm) External	Internal	Total
1	Black, stiff, fissured, slightly sandy clay, with occasional calcrete nodules and fine roots; reworked residual gabbro	75	48	13	49				
						24	160	329	489
						26	189	305	494
	1,1								
2	Dark grey, stiff, fissured, clay with calcrete nodules and with black ferruginous spots towards top of horizon; residual gabbro	98	65	19	52				
						29	210	300	510
	(Concentration of calcite nodules at base of horizon)					51	235	361	596
	2,3								
	Light grey, in profile grey mottled yellow, stiff, shattered and slickensided, clay; residual gabbro	108	67	17	46				
	2,3					59	276	437	713
3	Light yellow, dense but friable sand with angular grains of weathered plagioclase and pyroxene; residual gabbro	42	15	-	12				
						58	160	424	584
	3,4								
	Soft rock weathered gabbro								

Figure 44. Typical soil profile at Onderstepoort (Brink 1979)

TABLE 1 : Material Classification Data

DESCRIPTOR	
Liquid Limit	71%
Plastic Limit	32%
Plasticity Index	39%
Specific Gravity	2.76
Unified Soil Classification System	CH
Potential Expansiveness (Van Der Merwe's Chart)	Very high
Linear Shrinkage	17%
Predominant Clay Mineral	Montmorilonite (Brink 1979)
Soil Description	Dry,dark grey clay with highly shattered crumb structure. Calcium carbonate nodules, 2mm max size, interspersed in clay matrix in small quantities. Residual Gabbro.
% Clay (<2&mu.m)	58%
Depth of Sampling	0.5m
Sampling Procedure	Disturbed

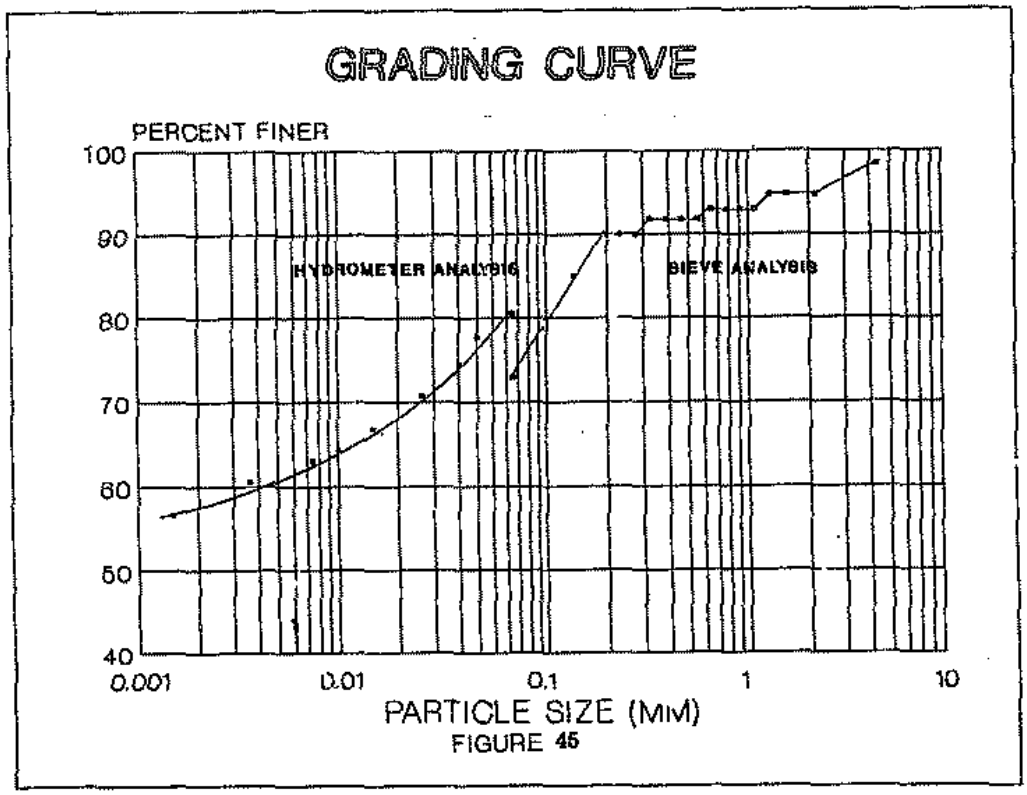

FIGURE 45

SUCTION VS MOISTURE CONTENT

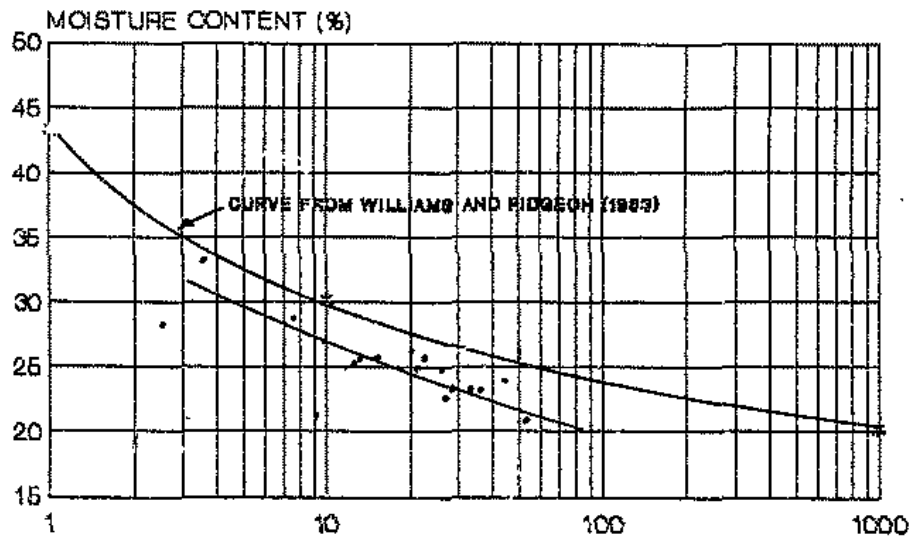

FIGURE 46

COMPACTION CURVE STANDARD PROCTOR COMPACTION EFFORT

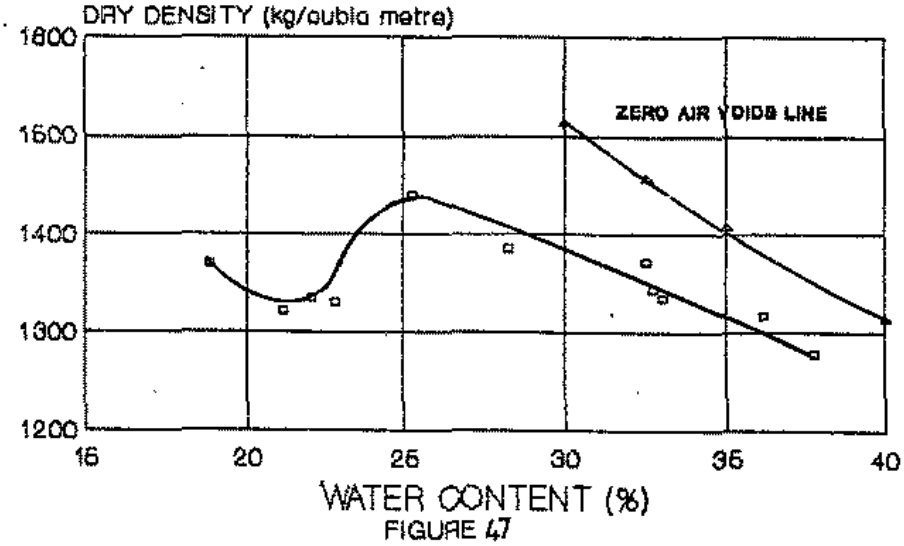

FIGURE 47

11.0 Triaxial Tests.

11.1 Introduction

The triaxial moduli represent the stiffness of the clay as a purely frictional material either in saturated or partially saturated states. In other words,the triaxial modulus is really a measure of the shear stiffness of the material. Obviously, in the behaviour of stiffened rafts, one is primarily concerned with swell and consolidation and hence, it could be argued that the triaxial moduli are not that relevant for raft design purposes. However, the triaxial moduli do serve as a very useful point of reference, as they 'complete the picture' as it were.

In this investigation, two categories of samples were tested:

1. Saturated samples : The purpose of these tests was to determine the moduli of the clay at low effective stresses. It was assumed that this stress range would be relevant when the soil became saturated at shallow depths. Also included in this test series was a stage loading sequence with a view to gaining more data on the validity of this method.

2. Unsaturated samples : These samples were tested at differing initial moisture contents each of which was kept constant throughout the test. One group of samples was tested unconfined while the other group was tested with a confining pressure of 50 kPa. These two conditions of confinement were thought to be the maximum and minimum occuring down to a depth of approximately 4m due to the presence of fissures.

The samples were prepared in a mould (figure 48) to a target dry density of 1440 kg/m^3. Also, a computer program was utilised to process the results which applied a membrane correction as follows (Alexander 1988):

Corrected deviator stress(kPa) = Deviator stress(kPa)-7.5 .(ε)

(ε <2%)

Corrected deviator stress(kPa) = Deviator stress (kPa) - 15kPa

(ε >2%)

Where ε is the percentage strain.

11.2 Triaxial Tests on Saturated Samples

11.2.1 Experimental technique

The samples tested can be listed as follows (see also table 2):

1. Samples T1, T2 and T3: These samples were tested right at the beginning of the experimental program for the purposes of gaining a feel for the triaxial apparatus itself. These tests were therefore not intended to form part of the main experimental program but nevertheless the results do contain some useful information.

2. Samples T4S/1, T5 and T6 were tested undrained at effective consolidation stresses of 10kPa, 35kPa and 50kPa respectively. Note that samples T4S/2 and T4S/3 consist of the same material as sample T4S 1 but these latter two samples have gone through a subsequent stage loading cycle. This implies that, in each case, the samples were not loaded to failure, but rather they were unloaded before failure, following which the effective stress was increased. After a 24 hour equilibrium period, the samples were once again reloaded.

3. Samples T7S/1, T8, T9 and T10 were all tested under drained conditions. In this case sample T7S/1 went through a stage loading cycle.

4. Samples T11, T12 and T13 were all load cycled. This implies that the samples went through a loading and unloading cycle before being loaded to failure to ascertain how much larger the modulus would be on the second load cycle.

To reduce the number of variables, thixotropic effects were not investigated so straight after sample compaction, the samples were mounted in the triaxial cell and consolidated.

For most of the samples an initial water content of 25% was used because, at higher moisture contents, the material has a tendency to stick slightly to the sides of the mould during sample extrusion. Based on preliminary results from Brackely swell under load tests a swelling pressure of 110kPa was assumed (refer to the following section for an explanation of how the Brackely swelling pressure is derived). Thus the cell pressure was chosen as being greater than this value so that the sample would not swell during saturation.

Initially, no c_v value was available from which an estimate of the strain rate for the drained tests could be made. Thus, for the first sample tested under drained conditions, it was decided to make an initial estimate

of the required strain rate and then, during sample shearing, the pore water pressure would be monitored through the bottom drain while the sample was allowed to drain through the top drain. In practice it was found that the initial estimate of the strain rate was too fast - because a slight build-up of pore pressure was detected - and thus the strain rate was reduced by a factor of 3. Both the top and bottom drains were then opened. This reduced strain rate was subsequently used for all the drained samples with the exception of sample T13 (table 4).

In hindsight, now that the c_v value is known (see results quoted in later sections), an estimate of the time to failure by means of the method given by Blight (1963) would be of the order of 12 hours. In the light of this information it was decided to reduce the strain rate for sample 13 as this sample was tested a little later in the experimental program.

The undrained strain rate was based on information given in Bishop and Henkel (1972, pg101) where it was recommended that a strain rate of 0.06% per minute be used.

11.2.2 Discussion of the stress-strain curves.

Table 4 contains the values of all the moduli from the standard tests. The values quoted in this table have been determined by calculating the best fit lines through the first few points. Notice that, in some cases, the curve was initially very steep (ie between the origin and the first point) which could be partly due to ram friction. In these cases a range of modulus values have been given in table 4.

11.2.2.1 The undrained test

The stress-strain curves for the undrained tests are shown in figures 49 to 52. Figures 51 and 52 show the results from the load cycled tests and in the case of figure 52, the curve from sample T6 has also been included for the sake of comparison. A general feature of all the curves is that the initial approximately linear region of the curve falls into a very small strain range. These results therefore confirm the ideas presented in the literature survey regarding the small strains over which the material can be thought to behave in a linear fashion (see for instance figure 11). With regard to figure 49, the initial flat portion of the curves are due to bedding-in effects. At this point it is worth mentioning that if the three curves shown in this figure were normalised by means of the initial consolidation stress, then one single curve would definitely not result. The obvious reason for this is that the peak deviator stress is reached at differing axial strains.Further, it is difficult to explain why the the stiffness of sample T2 is so much greater than T1 even though sample T1 had a much

larger initial effective stress.Thus it would appear that the relationship between effective stress and the initial consolidation stress is not that clearly defined.

The stress-strain curves in figure 51 and to a lesser extent the curve in figure 52 manifests a sharp rise in deviator stress with no strain occuring. This is most probably due to ram friction and is thus not indicative of material behaviour. It is also interesting to note that, upon reloading after the first load cycle, the stress strain curve rejoins the original stress strain trajectory set up by the first load cycle (figure 51 and 52). This behaviour corresponds to the well known e-logp' plot from the oedometer test where the curve rejoins the virgin compression line during the reloading cycle.

Theoretically, the two curves given in figure 52 should correspond a lot more closely, but the difference can be ascribed to the fact that the samples do not have the same initial water contents. Sample T12 was the first sample tested in a new test series of load cycled tests and it was therefore decided to investigate the possibility of raising the initial water contents so as reduce the time required for saturation (usually in the region of 48 hours). It was found that there was not much difference in this time, but, surprisingly, the effect of raising the initial water was to significantly increase the stiffness and strength of the sample. One would be inclined to think that, because both samples were fully saturated before testing, the stress-strain curves should coincide beyond 0.5% strain. On the other hand, perhaps the difference in initial water contents gave the samples differing initial soil fabrics which influenced the shear resistance of the soil.

11.2.2.2 The Drained Tests.

The results from the drained tests are shown in figure 53 and 54. As is shown in these two figures, the shape of the stress strain curve is less linear than in the case of the undrained test. A possible reason could be that, due to the much longer testing times involved, the material has more opportunity to undergo creep.Also, an increase in stiffness only occurs in a very small strain range during the second load cycle. Thereafter, the stiffness is little different from the first load cycle.

The results from figures 50 and 53 are consistent (ie drained samples slighly stiffer and stronger than the undrained samples), but unfortunately this is not the case when one compares the load cycled samples (ie figures 52 and 54). As explained previously this is most probably due to the fact that sample T12 is not exactly the same as the other samples tested in this test series.

11.2.2.3 The Stage Loaded Tests.

The results of the undrained and drained stage loading tests are presented in figures 55 and 56 respectively. On these figures the results from the standard tests (given in figures 50 and 53 respectively) have also been superimposed. A comparison of the stage loaded tests and the standard tests at a particular consolidation stress indicates that agreement between the two tests is poor particularly at large strains. This could be due to the fact that all the clay particles became orientated within a failure zone after the first load cycle.

A comparison of the moduli from the stage loaded tests and the standard tests at the same consolidation stress shows that there is fair correlation between the two moduli values (table 5). More tests are required before any general conclusions can be drawn, but in this case it appears that there is a fair correlation between the initial tangent modulus value from the stage loaded test and the first load cycle modulus from a standard test.

11.2.3 Discussion of the p-q plots

Figure 57 shows the p-q plots for the tests on samples T1, T2 and T3. The shape of the curve (ie a near vertical climb to the K_f line) was typical of all the tests. The fact that the stress-path veers-off in a horizontal direction to the right after having intercepted the K_f line implies that the deviator stress remains constant after failure but, at the same time, the pore water pressure is decreasing. This is a typical stress path for an over-consolidated soil. Also, because the p-q plot lies between $45^0$and 90^0 in its accent towards the K_f line, the 'A' parameter lies between 0 and 0.5. This figure also shows that the K_f line passes near the origin which is what one would expect from a compacted soil.

The p-q plot for the stage loaded test is given in figure 58. The point to notice here is that the curve does not return to it's initial starting point. The difference between the final and the initial value on the p' axis can be ascribed to the pore water pressure build-up du: g the test. Also, the fact that the p'-q plots from the stage loaded tests do not approach the K_f line, indicates that the sample was far from failure at the second and third stage of loading.

Table 2: Sample Preparation Data
for Triaxial Tests on Saturated Samples

SAMPLE NUMBER	DRY DENSITY (kg/cubic m)	INITIAL WATER CONTENT(%)	FINAL WATER CONTENT(%)	TYPE OF TEST	INITIAL CONSOLIDATION STRESS (kPa)
T1	1469	26.3	39.2	CIU	200
T2	1503	25.7	38.6	CIU	100
T3	1515	24.8	39.7	CIU	50
T4S/1	1423	25.1	39.3	CIU+S	10
T4S/2	1423	25.1	39.3	CIU+S	35
T4S/3	1423	25.1	39.3	CIU+S	50
T5	1415	24.7	36.9	CIU	35
T6	1413	24.7	36.4	CIU	50
T7S/1	1445	24.5	38.5	CD+S	10
T7S/2	1445	24.5	38.5	CD+S	35
T7S/3	1445	24.5	38.5	CD+S	50
T8	1431	25.0	36.3	CD	50
T9	1455	25.4	35.9	CD	35
T10	1443	24.5	37.2	CD	18
T11	1493	24.0	38.4	CIU+L	10
T12	1335	33.8	39.0	CIU+L	50
T13	1451	25.1	35.4	CD+L	50

Note : CIU = Consolidated Isotropic Undrained Test.
CIU+S = As above with stage loading.
CIU+L = As above with load cycling.
CD = Consolidated Isotropic Drained Test.
CD+S = As above with stage loading.
CD+L = As above load cycling.

Table 3: Strain-Rate and B values
for Triaxial Tests on Nominally Saturated Samples..

SAMPLE NUMBER	STRAIN RATE (mm/min)	'B' Value
T1	0.035	0.94
T2	0.035	0.80
T3	0.03*	0.80
T4	0.04199	0.92
T5	0.04199	0.90
T6	0.04199	0.95
T7	0.00378	0.96
T8	0.00378	1.00
T9	0.00378	0.95
T10	0.00378	1.00
T11	0.0304	0.96
T12	0.0508	0.98
T13	0.00168	0.98

Table 4 : Tangent and Secant Moduli from Triaxial Tests on Saturated Samples.

SAMPLE	INITIAL EFFECTIVE STRESS (kPa)	TANGENT MODULUS FOR FIRST LOAD CYCLE (MPa)	TANGENT MODULUS SECOND LOAD CYCLE (MPa)	MODULUS FOR LARGE STRAINS (MPa)
T1 (UND-	200	27		
T2 (DRAINED)	100	37		
T3 "	50	14		
T6 "	50	19		
T12 "	50	18	25	6
T5 "	35	19		
T4S/1 "	10	6		
T11 "	10	6-8	14	
T8 (DRAINED)	50	40-12		
T13	50	25-12	42-15	5
T9 "	35	13		
T10 "	18	10		

Table 5 : Comparison of Triaxial Moduli from Stage Loaded and Standard tests.

TYPE OF TEST	SPECIMEN	INITIAL EFFECTIVE STRESS (kPa)	TANGENT MODULUS (MPa)
UNDRAINED	T4S/2	35	15
"	T5	35	19
"	T4S/3	50	24
"	T6	50	19
DRAINED	T7S/2	35	12
	T9	35	13
	T7S/3	50	20
	T8	50	40-12

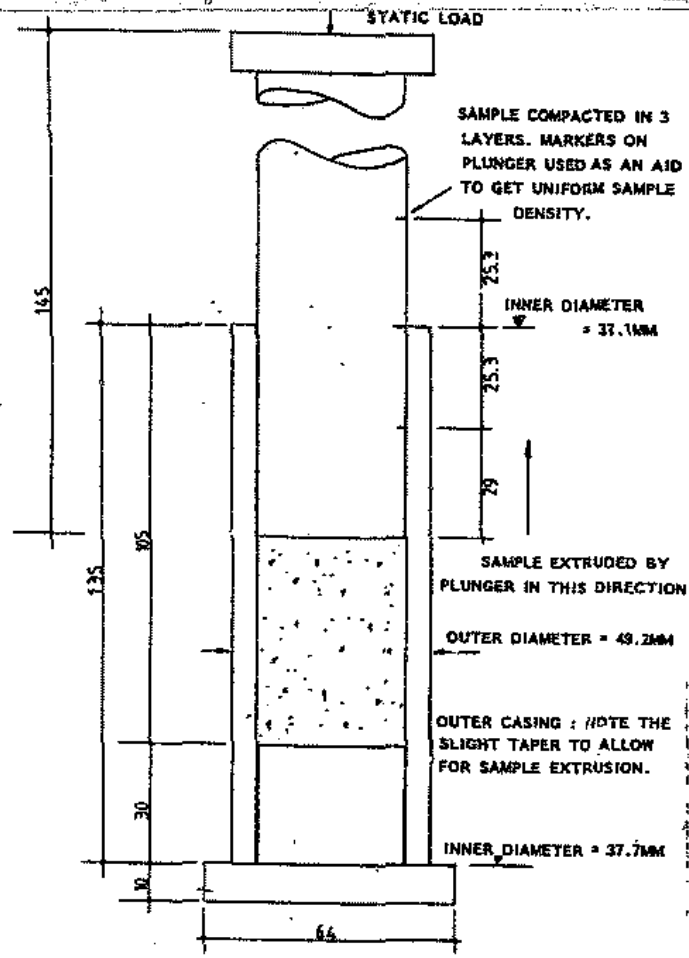

FIGURE 48 : TRIAXIAL SAMPLE MOULD

TRIAXIAL TESTS
UNDRAINED TESTS

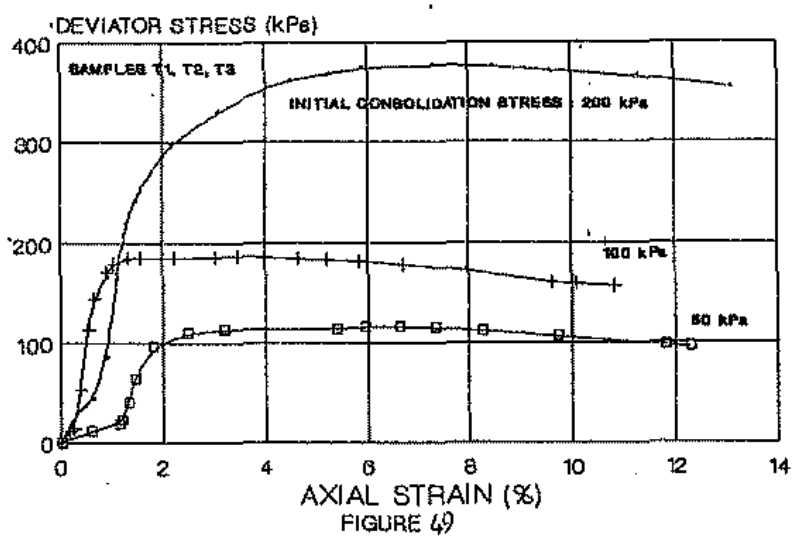

FIGURE 49

TRIAXIAL TEST RESULTS
UNDRAINED TEST

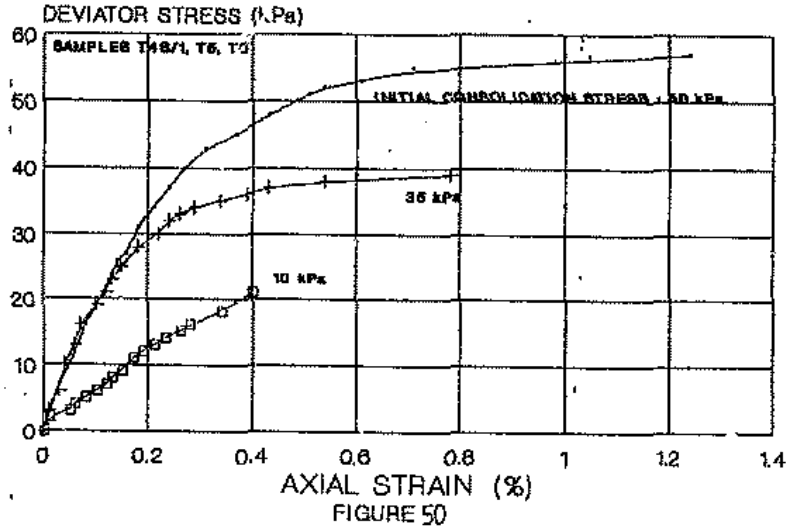

FIGURE 50

UNDRAINED TRIAXIAL TEST WITH LOAD CYCLING

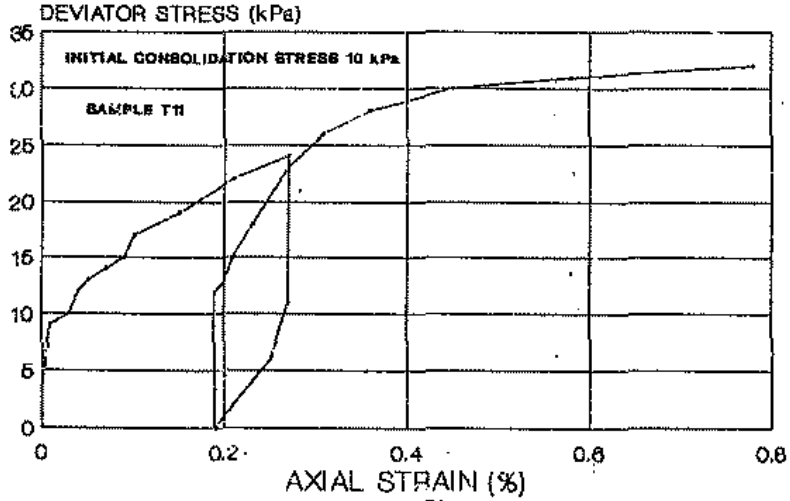

FIGURE 51

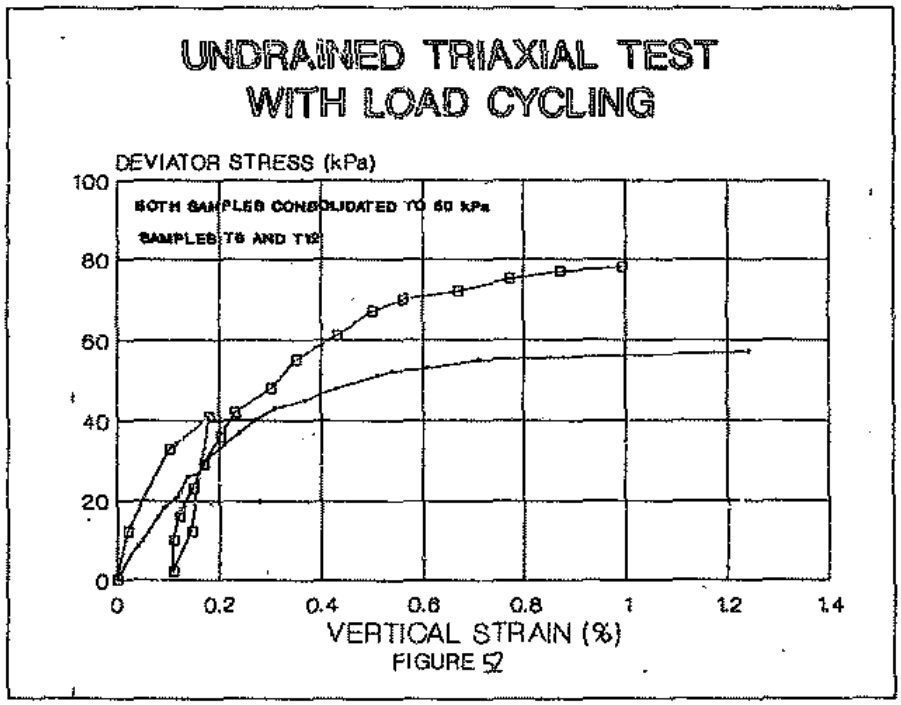

FIGURE 52

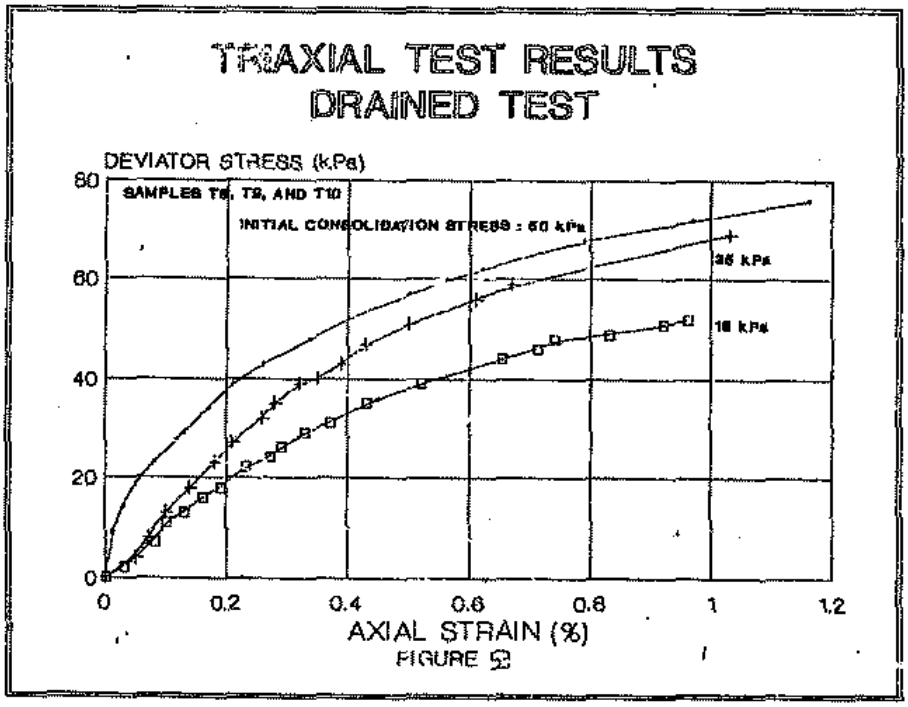

FIGURE 53

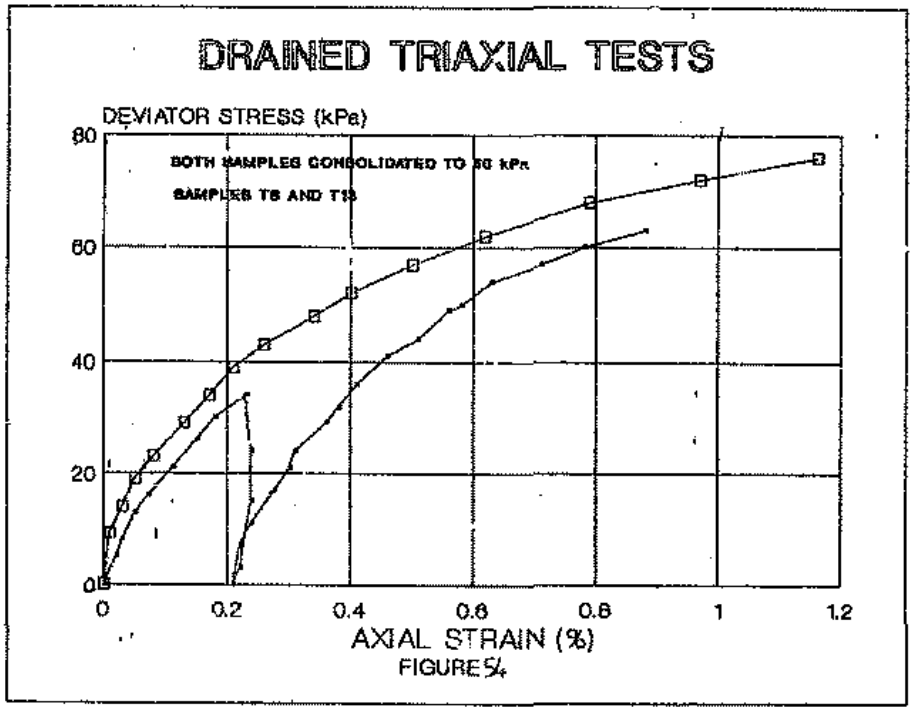

FIGURE 54

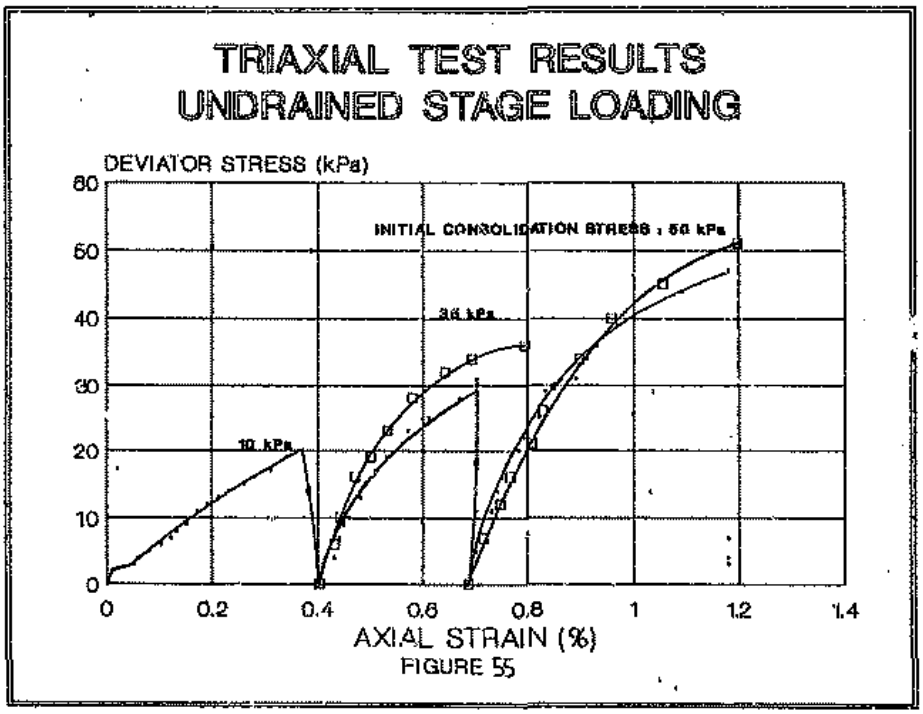

FIGURE 55

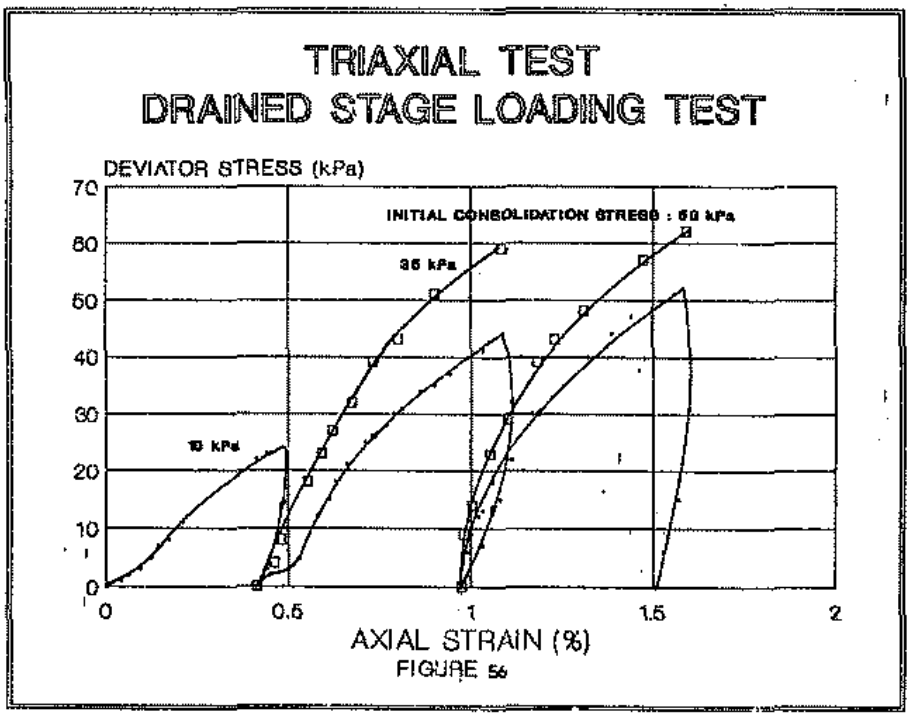

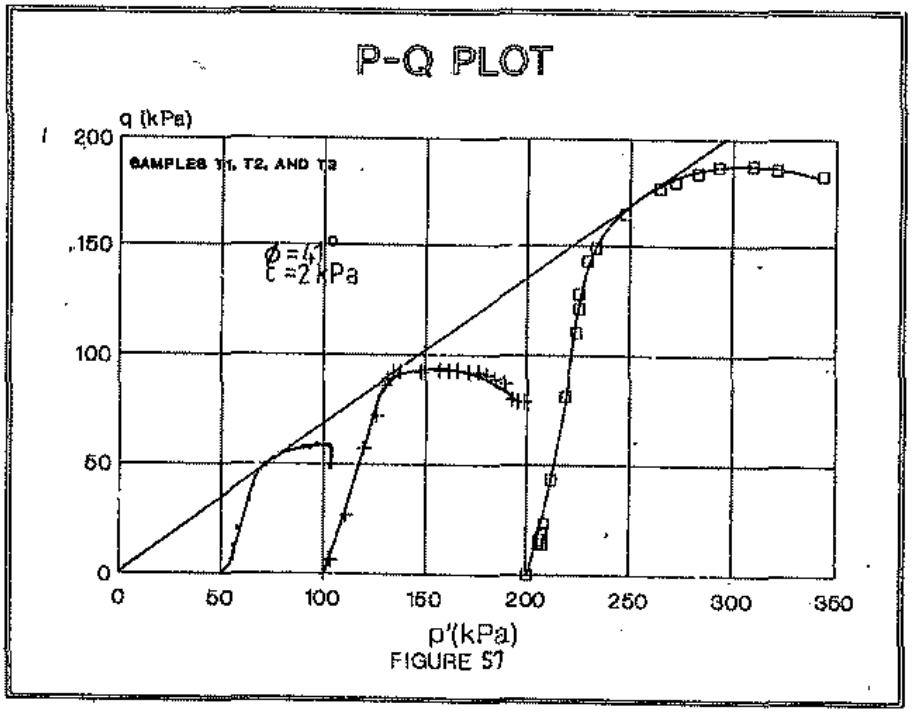

Figure 59. P-Q plot

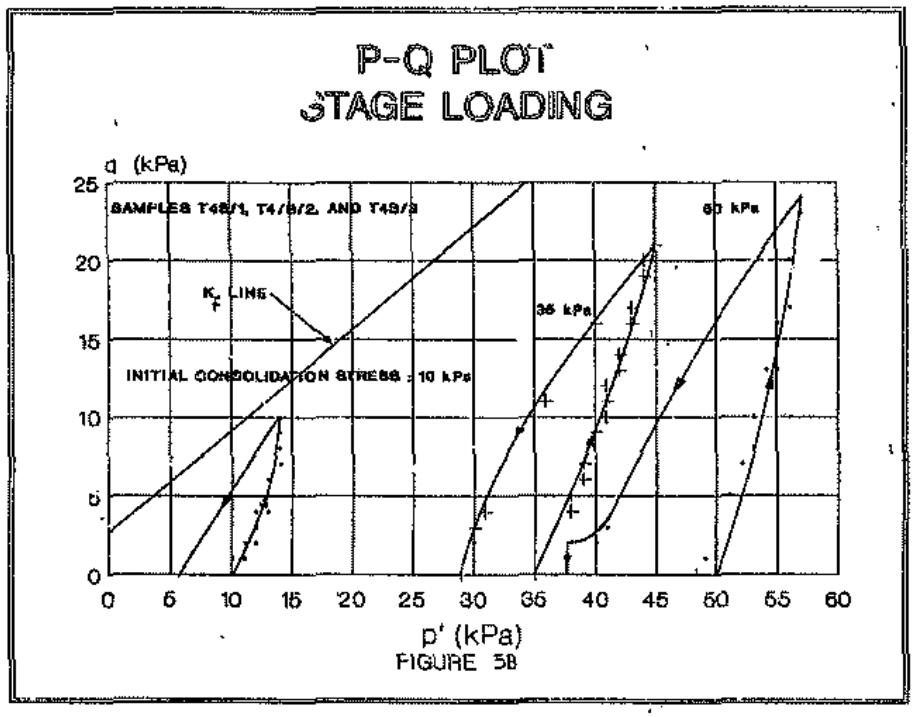
P-Q PLOT
STAGE LOADING
q (kPa)
SAMPLES T4S/1, T4/S/2, AND T4S/3
60 kPa
K_f LINE
35 kPa
INITIAL CONSOLIDATION STRESS : 10 kPa
0
5
10
15
20
25
0
5
10
15
20
25
30
35
40
45
50
55
60
p' (kPa)
FIGURE 5B

11.3 Triaxial Tests on Partially Saturated Samples.

11.3.1 Experimental Procedure.

All the samples were prepared in the triaxial mould to three different target moisture contents of approximately 21%, 26% and 31% respectively. After extrusion from the mould the samples were wrapped in plastic wrapping and allowed to cure for a period of one week to facilitate moisture equilibrium within the sample. The rate of load application was set at 0.06%-0.08% strain per minute which corresponds to the strain rate for undrained loading (Bishop and Henkel 1973). One additional test was undertaken whereby the strain rate was reduced by a factor of 5 to determine the effect of strain rate on the modulus.

11.3.2 Discussion of the results

The sample preparation data for the confined and unconfined test is given in tables 6 and 7 respectively.

At the time of testing, the samples had numerous horizontal cracks which penetrated the cylindrical surfaces of the sample to some depth. These cracks were the result of the original material consisting of a granular mass which was not completely broken down during the compaction process. No doubt the effect of sample extrusion as well as the small degree of drying shrinkage which occurred during the curing period accentuated the size of the cracks.

The stress strain curves for the unconfined and confined tests are given in figures 59 to 61. The material behaviour shown here is consistent with the tests on the saturated samples whereby, after a second load cycle, the curve rejoins the 'virgin compression curve'.

The tangent moduli for the first and second load cycles are shown in table 8. In this table, a modulus over a wider stress range has also been quoted.

In these tests, the modulus for the second load cycle is significantly larger than that for the first cycle. This is most probably due to the closing up of the cracks during the first load cycle, and, with very little elastic recovery during subsequent unloading, the sample is very stiff on the second cycle of loading. The confining pressure had no effect on the modulus and, in some cases, the confined sample had a lower modulus than the unconfined sample. Thus the effect of sample variability masked the effect of the low confining pressure. Further, even at large moisture contents, the sample suction is large relative to the confining pressure - for

example, at a moisture content of 31%, the sample suction is of the order of 600 kPa (see Figure 46). Thus it is not surprising to find that this low confining pressure makes very little difference to the stiffness.

The effect of reducing the strain rate only had an effect on the moduli for the second cycle of loading (table 8). In fact, a reduction in strain rate by a factor of 5, resulted in this modulus being reduced by 62%. Therefore, even though one might expect the stiffness of the sample at a moisture content of 22% to be large, it can be assumed that the very large stiffness recorded in the second load cycle is due to an excessively fast strain rate. In general however, the main compression curve does not appear to be influenced by strain rate.

The influence of fissures on the stiffness is shown by comparing the stress strain curves of the partially and fully saturated triaxial samples respectively. As one would expect, the strains in the case of the partially saturated samples are larger as compared to the fully saturated samples, but it is interesting to note that the stiffness from the second load cycle is more or less the same for the two tests in some cases. For example, there is good agreement between the second cycle modulus for the partially saturated sample at a moisture content of 26,7% (reduced strain rate) and the undrained test at an initial effective consolidation stress of 50 kPa. This indicates that in spite of the large effective stress in the case of the partially saturated sample, its stiffness is equivalent to a sample with no fissures at a much lower effective stress.

Table 6: Confined Triaxial Test data

SAMPLE	INITIAL WATER CONTENT (%)	FINAL WATER CONTENT (%)	DRY DENSITY (kg/cu m)	STRAIN RATE (mm/min)
TRIAX1	22.6	22.4	1416	0.06
TRIAX2	27.8	27.5	1403	0.06

Table 7: Unconfined Triaxial Test Data

SAMPLE	INITIAL WATER CONTENT (%)	FINAL WATER CONTENT (%)	DRY DENSITY (kg/cu m)	STRAIN RATE (mm/min)
TRIAX3	22.4	22.6	1439	0.06
TRIAX4	26.8	26.6	1427	0.06
TRIAX5	31.2	31.0	1368	0.06
TRIAX6	26.7	26.4	1422	0.01%

Table 8: Tangent Moduli from Confined and Unconfined Triaxial Tests.

SAMPLE	TYPE OF TEST	INITIAL WATER CONTENT %	MODULUS FOR FIRST LOAD CYCLE (MPa)	MODULUS FOR SECOND LOAD CYCLE (MPa)	MODULUS OVER 0.5-2.5% STRAIN
TRIAX1	CONFND	22.6	17	34	12
TRIAX2	CONFND	27.5	13	32	5
TRIAX3	UNCONFND	22.4	15	82	10
TRIAX4	"	26.8	13	[illegible]	13-6
TRIAX6	" + SLOW	26.7	10	23	8
TRIAX5	UNCONFND	31.2	7	18	6

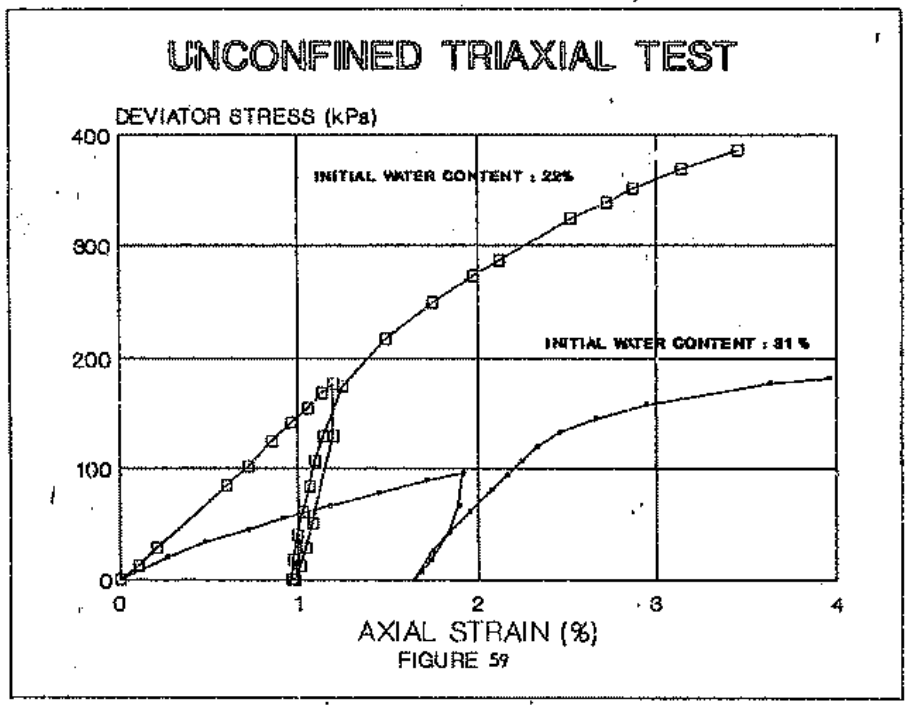

FIGURE 59

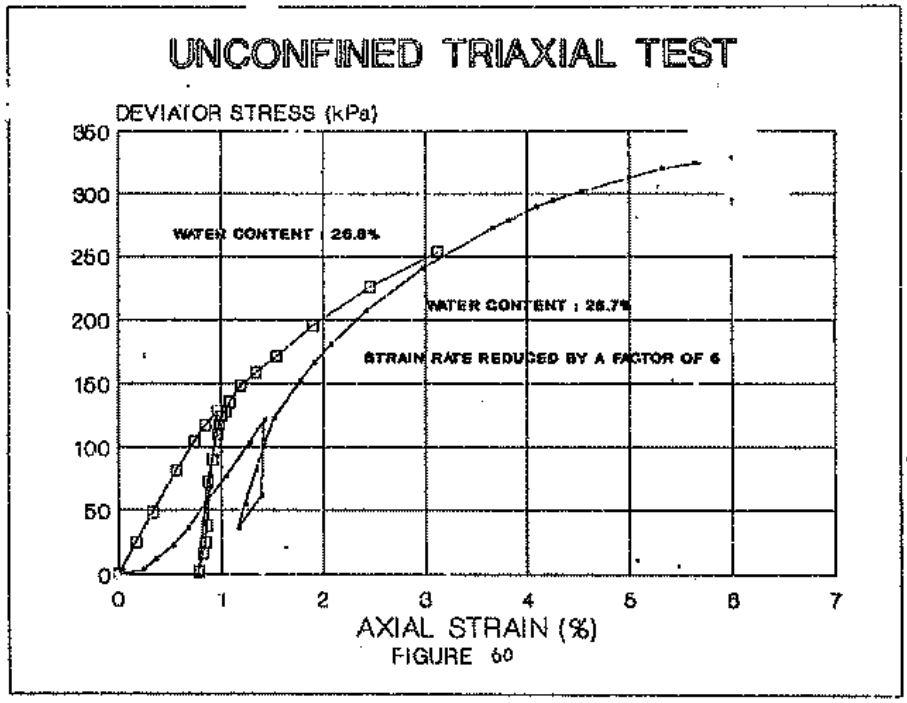

FIGURE 60

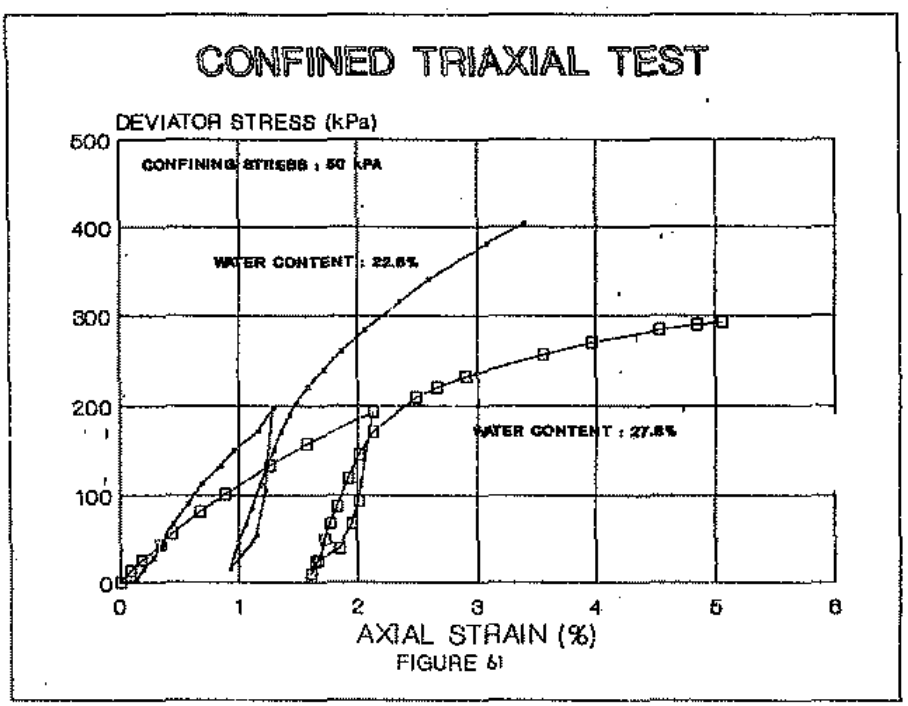
CONFINED TRIAXIAL TEST
DEVIATOR STRESS (kPa)
500
400
300
200
100
0
CONFINING STRESS : 50 kPA
WATER CONTENT : 22.6%
WATER CONTENT : 27.6%
0
1
2
3
4
5
6
AXIAL STRAIN (%)
FIGURE 61

11.4 Measured Triaxial Moduli Related to Stiffened Raft Design

In general, there is large scatter in the triaxial moduli caused by factors such as a high degree of variability in stiffness with strain and differences in modulus measured between the first and second load cycle. This fact makes it difficult to propose a modulus value from the triaxial test within a small range, but it can be said that, even at very low effective stresses, the triaxial moduli measured were much larger than the EEMM value required for raft simulation. For instance, even at a low effective stress of 10 kPa, the modulus value is roughly four times greater than the suggested EEMM value of 2.6 MPa for Onderstepoort clay.

Another point regarding the applicability of the triaxial moduli in raft design, is the question of strains. Particularly in the case of the saturated samples, the strains are very small which is definitely not the case in the field situation.

12.0 THE OEDOMETER TEST

12.1 Introduction

The oedometer moduli are important in that they take into account both swell and consolidation although the true stress path occuring under a raft cannot be followed in the conventional oedometer as mentioned in the literature survey. Thus the standard oedometer moduli can be classified as being either swell or consolidation moduli respectively. For the purposes of raft design, both moduli should ideally be considered because both processes of swell and consolidation are at work under a raft from the time of raft construction onwards.

In this experimental phase the following stress paths were followed to determine the moduli values:

1. Swell under load tests : A group of samples with the same initial water contents are loaded under different surcharges and then saturated after which the swell is monitored.

2. A sample is loaded with a load approximated to the estimated swelling pressure. After sample saturation the equilibrium value of the sample deformation is recorded following which the sample is unloaded. Subsequent reloading is then undertaken.

3. Compression at constant moisture content.

4. Constant rate of strain oedometer tests.

5. Tests with a modified strain controlled oedometer.

All of the samples were statically compacted in a mould as shown in figure 62. Note that the purpose of the porous stone shown in this figure is to act as a filler. Thus, prior to testing, the stone was removed which allowed sufficient room (+/- 5mm) for the sample to swell. In tests where the sample was not to be saturated, the stone was omitted and the sample was compacted to the full height of the ring. The target dry density for all the samples was set at 1440kg/m^3

As stated in the literature survey, static compaction as opposed to kneading compaction may instil a larger total suction in the soil. Therefore, one might expect different material behaviour depending on the technique used for sample compaction. However, if a basic procedure is used for the samples, then a basis for comparison is established.

After sample compaction the samples were sealed in plastic wrapping and allowed to cure for a period of 4 days. The minimum curing time was established on the basis of Mov (1981) as presented in the literature survey. In the cases were the sample was not prepared to the full height, a narrow steel plate of known height was placed on the top surface of the oedometer ring and this plate was then used as a platform for sample height measurements. Height measurements were then taken by means of a pair of vernier callipers which had a maximum resolution of 0.05mm.

The samples were compacted with filter paper included between the soil and the two plungers of the mould. This was done to prevent the soil from sticking to the plunger surfaces when the sample was removed from the mould. Before testing it was impossible to remove the filter paper from the soil sufaces without undue disturbance so therefore all the samples were tested with the inclusion of filter paper. This goes contrary to what was stated in the literature survey but it was thought that the compressibility of the filter paper could be taken into account by means of a correction curve.

This correction curve was established by replacing the soil specimen with a steel plug together with filter paper which was placed on the top and bottom surfaces of the steel plug. Loading and unloading curves were then plotted for the case of wet and dry filter paper respectively (figure 63). This figure shows that, when the first load was applied, a large deflection occurred which is a general characteristic of the apparatus. For this reason, it is very difficult to establish, with any accuracy, the initial dial gauge reading associated with the initial height of the sample. Therefore, when the first load was applied to a sample, the initial reading on the dial gauge was recorded (ie that reading which corresponds to the initial sample height) only once this instantaneous deformation had taken place. Consequently, all the oedometer results have been corrected on the basis of shifting up the correction curve so that it passes through the origin.

12.2 Swell under load tests.

12.2.1 Introduction

Besides using this test to determine the magnitude of the swell stiffness at different initial water contents, this test is also useful in determining the Brackley swell pressure as well as a measure of the free swell (ie swell under no load). There is also great value in comparing the percentage swell calculated from the formula presented by Brackley (1983) and those measured in this investigation.

12.2.2 Experimental Technique

One of the main problems experienced with this test was that, after curing, the samples had an irregular surface. This was most probably due to the fact that water was not equally distributed in the sample during the compaction stage, and thus, during the curing period, the clay swelled locally in the process of moisture migration. The magnitude of these irregularities was such that the error in the initial sample height measurements was of the order of 0.4%.

Once loaded in the oedometer, the samples were inundated after approximately 5 minutes. This procedure differs from the one used by Brackley (1983) who left the samples for two hours under the load before inundation. In this case it was felt that by doing this, the sample would be dried out excessively because it was usually warm and dry in the laboratory. Also, the porous stones in the oedometer were kept initially dry because in this way it was felt that close control over the initial water content could be maintained

The dial gauge reading corresponding to the initial sample height was taken just before inundation. However, to be strictly correct, the procedure should be one of determining the dial gauge reading before and after load application. This would then allow one to reduce the initial sample height based on the extent of the deformations under the applied load. Unfortunately, the surface irregularities mentioned previously made this procedure impossible because it was felt that any deformation occuring under the load was largely the result of compression of the irregularities. Thus no correction to the initial sample height was applied. Correction for oedometer compressibility was also not applied because the zero reading was taken after the deformation due to oedometer compressibility had taken place.

After inundation some of the samples underwent a collapse settlement before undergoing swell particularly under the higher loads. This can only be ascribed to the softening of the small irregularities on the surface of the sample before the sample wetted up. The order of magnitude of this settlement was in the order 1% in the extreme case and it is debatable as to whether or not this should be added to the final percent swell. In this case this was not done for the sake of applying a consistent procedure to all of the samples.

The samples were allowed to undergo swell for a period of two days as suggested by Brackley (1983).

12.2.3 Discussion of the results

The sample preparation data is given in tables 9 and 10.

Figure 64 displays the swell versus time relationships for various samples at different water contents under

a load of 22kPa. Most of the swell takes place in under 7 hours (approximately 400 minute [illegible] of the sample at an initial water content of 16.7%, some swell is still evident even after a period [illegible] (the last point on the curve).

The percent swell versus log pressure relationships are shown in figures 65 and 66.

The first few tests were performed with material that was oven dried to a condition of zero water content. This was done because it was thought that sample preparation would be made easier if the material that one is starting with has a fixed known water content. However, it was later found out that oven drying the soil even at temperatures below 110° alters the material. In the light of this new knowledge, material straight from a storage bin was used, and the tests were repeated. A comparison of the percentage swell from each of these two tests shows that the material is indeed altered because distinctly different swell lines are generated (see figure 66).

When one examines the data presented in table 9 then it is apparent that, given two samples with the same initial conditions, totally different values of swell are recorded. For example, [illegible] samples at an initial water content of 25% and loaded to 11 kPa, [illegible] that, for the three [illegible] of 6.1%, 3.7% and 2.3% were measured respectively. How[illegible] the average of the [illegible] seems to give a more reasonable estimate of the swell relative to the [illegible] under [illegible] loads.

Best fit lines have been fitted through the data by means [illegible] regression (table 11). Where more than one estimate of swell exists at a particular load, an [illegible] of swell was used in the regression analysis.

In spite of the experimental difficulties mentioned earlier there is still a good straight line correlation between percent swell and log pressure. This table also shows that if a natural scale is used instead of the log scale, then an equally good fit can be obtained in most cases. If Brackley's assumption is correct (ie that all the lines should pass through the same point on the percent swell vs log pressure curve) then it is evident that by using a non-log plot one can predict this point with greater consistency (table 12). Also, the percent free-swell for the log plot is consistently double that of the natural plot. Thus it seems clear that the way the results are plotted can give different values of the output parameters.

Table 13 compares values of percentage swell derived from this experimental program with those derived from the equation proposed by Brackley (1983) ie:

$$\%swell = (5.3-147.e/PI-\log p)(0.525.PI + 4.1-0.85.w) \quad (3)$$

Where e = Original void ratio of sample

PI = Plasticity Index of the whole sample

p = Applied pressure in kPa

w = Original sample moisture content (%)

In this case the original void ratio was set at 0.96 which was the average value of the void ratio for all the samples prepared. The PI used in the calculation was 39. In general, agreement is very poor and it appears as if the Brackley equation under-predicts the percentage swell. However, the equation is extremely sensitive to changes in PI Brackley (1983), and it was found that if a PI of 42 was used then the predicted percentage swell was roughly doubled and therefore better agreement could be obtained. In this case the PI was varied to gain a better fit because the PI of the sample can obviously vary within a given soil body. Thus, to make proper use of of this equation, one would definitely need a good estimate of the variation of the PI within the soil mass. Perhaps then an average value of the PI could be used to calculate the percentage swell.

In theory, the pressure required to prevent swell can be calculated by simply setting equation (3) equal to zero. This yields the following equation for the swelling pressure :

$$\log p_s = 5.3 - 147.e/PI$$

Where p_s is the swelling pressure

Using this formula with a void ratio of 0.96 and a PI of 39%, a swelling pressure of only 50 kPa is is calculated. This is obviously an underestimate but if the PI is changed by only 10% (to give a value of 43%) then a difference in swelling pressure of roughly 100% results.

The modulus values have been given in table 11 for each of the best fit lines. These values are simply the inverse of the slope of the best-fit lines and thus reflect an increase in modulus with an increase in moisture content.

TABLE 9: Sample Preparation Data and Percent Swell for Swell under Load Tests

SAMPLE NO	INITIAL WATER CONTENT (%)	FINAL WATER CONTENT (%)	INITIAL DRY DENSITY (kg/cu m)	INITIAL VOID RATIO	LOAD kPa	SWELL %
OD15/1	15.0	42.8	1483	0.86	11	16.3
OD15/2	15.4	38.2	1450	0.90	50	6.2
OD15/3	14.9	36.2	1477	0.87	100	3.5
OD15/4	13.8	37.0	1383	0.99	96	3.4
OD15/5	15.4	42.5	1442	0.91	11	14.6
OD15/6	15.2	38.1	1450	0.90	50	8.4
OD15/7	14.6	37.8	1453	0.90	75	6.8
OD15/8	14.9	39.6	1396	0.95	25	10.1
OD20/1	19.5	38.0	1421	0.96	100	2.0
OD20/2	20	40.4	1425	0.94	11	8.8
OD20/3	20.4	37.7	1357	1.03	50	3.0
OD20/4	19.5	36.0	1440	0.92	25	3.9
OD20/5	19.8	35.8	1394	0.97	100	0.5
OD20/6	19.5	39.4	1404	0.97	25	5.8
OD20/7	19.8	39.3	1389	0.98	25	5.7
OD25/1	24.6	38.3	1396	0.99	11	2.3
OD25/2	24.3	36.2	1406	0.96	50	1.7
OD25/3	24.5	34.4	1406	0.94	100	0.5
OD25/4	25.3	39.5	1390	1.00	11	6.1
OD25/5	25.3	35.6	1403	0.97	100	0.5
OD25/6	24.6	37.3	1450	0.90	11	3.7
OD25/7	23.7	33.5	1416	1.03	25	4.4
OD25/8	24.2	35.6	1373	1.04	50	1.5
OD25/9	24.9	34.9	1393	1.00	75	1.2
OD30/1	29.8	37.0	1361	1.08	11	2.5
OD30/2	29.4	34.4	1353	1.07	50	1.0
OD30/3	29.1	33.7	1414	0.97	100	0.5

TABLE 10: Sample Preparation Data and Percent Swell for Swell under Load Tests. Material was initially Oven Dried.

SAMPLE No	APPLIED VERTICAL LOAD (kPa)	INITIAL WATER CONTENT (%)	FINAL WATER CONTENT (%)	DRY DENSITY (kg/cum)	INITIAL VOID RATIO	SWELL %
OD25/1x	11	25.9	36.9	1405	0.96	6.6
OD25/2x	35	25.8	35.3	1431	0.95	4.1
OD25/3x	65	26.3	34.9	1439	0.92	2.6
OD25/4x	100	25.0	33.8	1374	1.02	2.3

TABLE 11: Equations of Best Fit Lines for Swell-Under-Load Tests.

WATER CONTENT (%)	BEST FIT EQUATION	COEFF OF CORRELATION	SLOPE OF LINE (kPa)
15	%swell=-11.79(log p)+27.42	0.98	
15	%swell=-0.116.(p)+14.71	0.95	8.9
20	%swell=-7.55(log p)+15.88	0.97	
20	%swell=-0.07.(p)+7.567	0.86	1.4
25	%swell=-4.21(log p)+8.93	0.91	
25	%swell=-0.045.p+4.676	0.94	2.2
30	%swell=-2.064(log p)+4.58	0.99	
30	%swell=-0.021.p+2.464	0.93	4.8

Note: The units of applied pressure p are kPa.

TABLE 12: Predicted Swelling Pressure and Free Swell from Best Fit Lines.

WATER CONTENT (%)	LOG PLOT		NORMAL PLOT	
	SWELLING PRESSURE (kPa)	FREE SWELL (%)	SWELLING PRESSURE (kPa)	FREE SWELL (%)
15	212	27	126	15
20	127	16	107	6
25	147	9	104	5
30	166	5	116	2

TABLE 13: Comparison of Predicted Swell and Measured Swell.

WATER CONTENT %	APPLIED LOAD (kPa)	AVERAGE PERCENT SWELL	PREDICTED SWELL BRACKLEY (1963)	
			PI=39%	PI=43%
15	11	15.5	7.6	13.4
15	50	7.3	0.0	4.2
15	100	3.5	0.0	0.0
20	11	8.8	5.0	10.0
20	50	3.0	0.0	3.0
20	100	1.3	0.0	0.0
25	11	4.0	2.2	5.3
25	50	1.6	0.0	1.7
25	100	0.5	0.0	0.0
30	11	2.5	0.0	1.5
30	50	1.0	0.0	0.5
30	100	0.5	0.0	0.0

KEY: 1)TOP PLUNGER
2)OUTER CASING
3)SOIL SAMPLE
4)TOP OF OEDOMETER RING
5)BOLTS SPACED AT 120 PLAN VIEW
6)POROUS STONE
7)BASE OF OEDOMETER RING
8)BOTTOM PLUNGER
9)FILTER PAPER

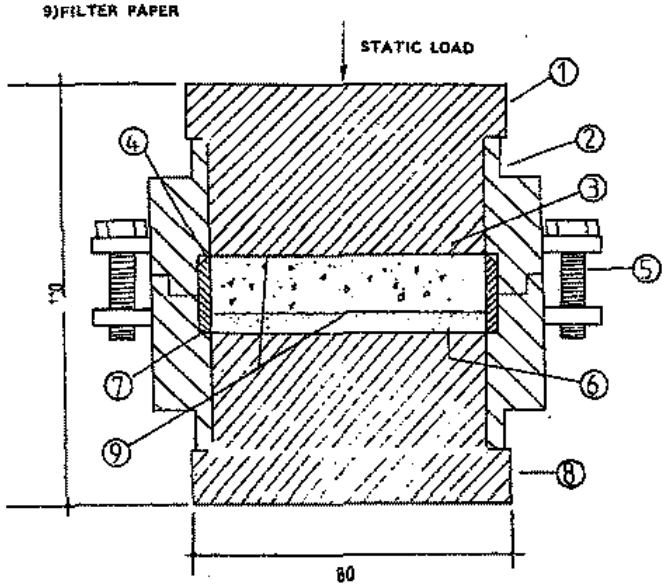

FIGURE 62: SKETCH OF MOULD FOR OEDOMETER SAMPLES

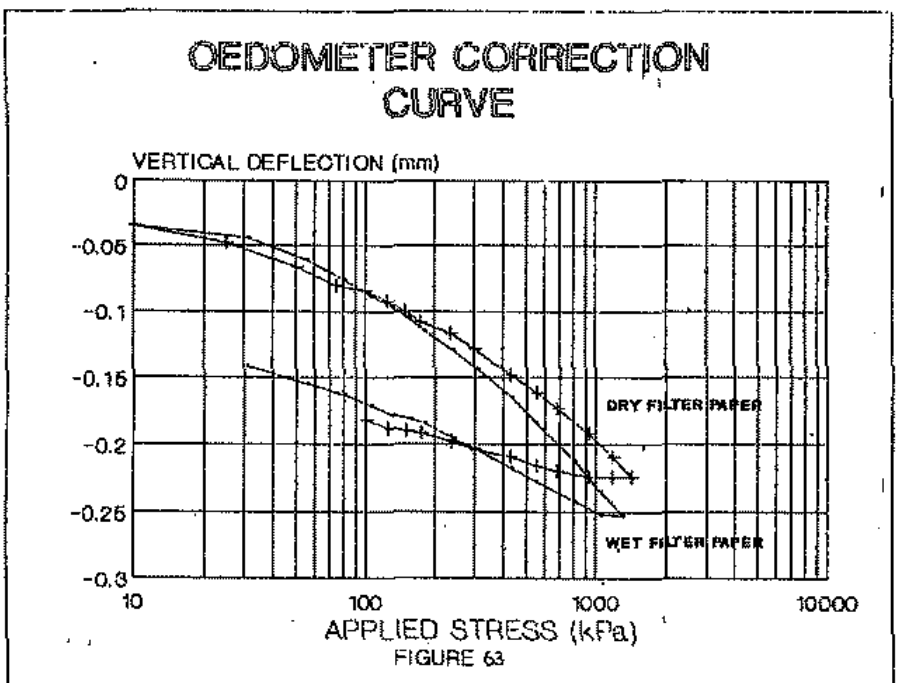

FIGURE 63

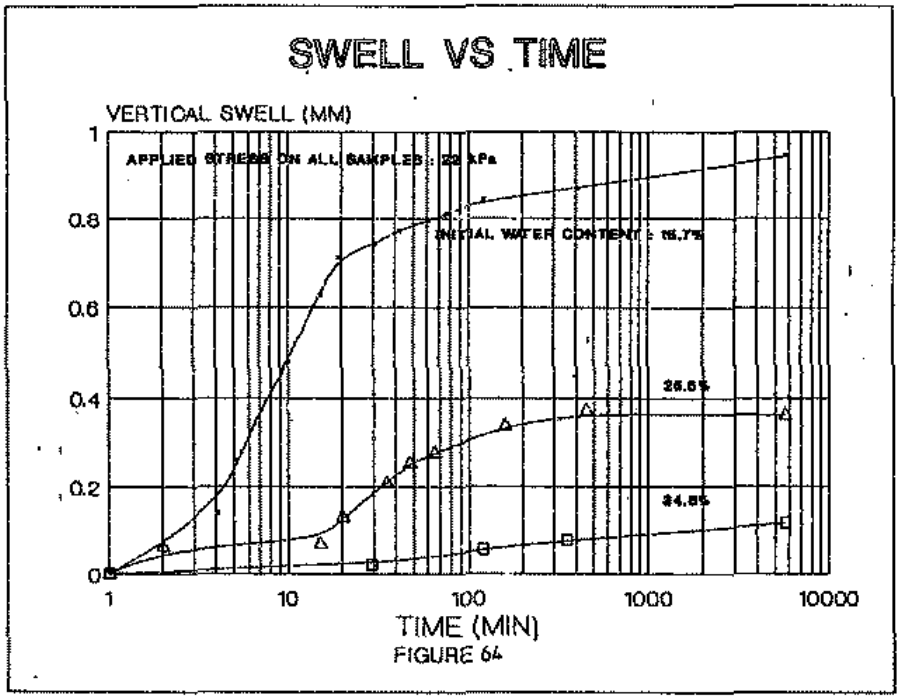

FIGURE 64

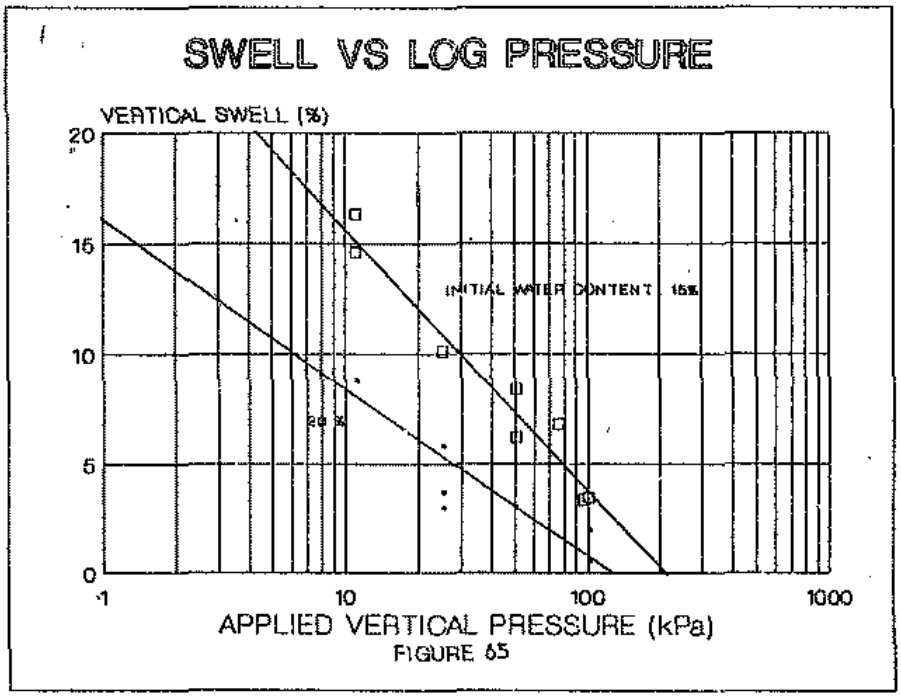

FIGURE 65

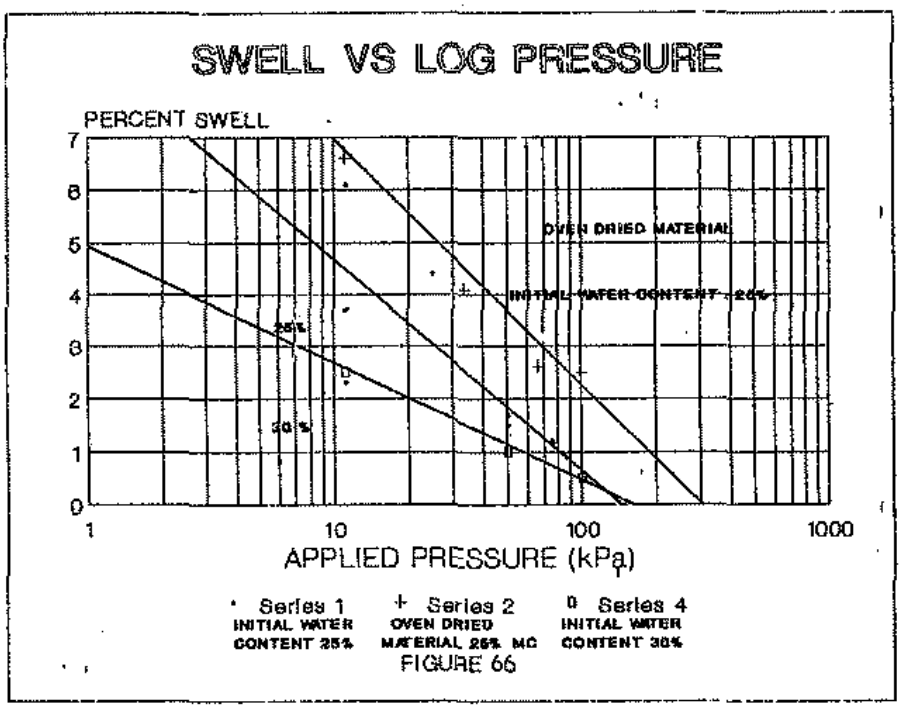
SWELL VS LOG PRESSURE
PERCENT SWELL
7
6
5
4
3
2
1
0
1
10
100
1000
APPLIED PRESSURE (kPa)
OVEN DRIED MATERIAL
INITIAL WATER CONTENT = 25%
25%
30%
Series 1 INITIAL WATER CONTENT 25%
Series 2 OVEN DRIED MATERIAL 25% MC
Series 4 INITIAL WATER CONTENT 30%
FIGURE 66

12.3 *Oedometer tests on saturated samples*

12.3.1 Test Objective.

The object of this test is to determine the following three moduli from tests on saturated samples:

1. Modulus in the normally consolidated stress range.

2. Modulus in the overconsolidated stress range

3. Unloading modulus.

12.3.2 Experimental Procedure

Three samples were prepared at target water contents of 15, 20 and 25 % respectively. After a 4 day curing period the samples were loaded in the oedometer up to a load of 120 kPa. This was assumed to be the approximate value of the swelling pressure based on the swell under load curves. In this case the problem of the uneven sample surface straight after curing was circumvented by recompressing the samples to give them a flat surface before mounting them in the oedometer cell. After mounting the samples in the oedometer cell the samples were inundated and after a period of 2 days the samples were unloaded. Each load was applied for a period of 24 hours, and after the unloading cycle was completed the samples were reloaded again. The sample preparation data for the samples tested here are given in table 14 while the stress strain curves for each sample are plotted in figures 67, 69 and 70 respectively. Figure 68 is a duplicate of figure 65 except that a log plot is used.

12.3.3 Discussion of the results.

The first point to notice is that all the samples showed varying degrees of swell under the estimated swelling pressure load. This demonstrates that it is very difficult to define a swelling pressure with accuracy. A comparison of the two methods of plotting the data (figures 67 and 68) shows the advantages of using the log scale because the effect of giving a linear plot in the over-consolidated range. However, this is misleading as far as modulus is concerned because on the linear plot there is a slight degree of non-linearity in this region.

Values of the different moduli pertaining to the different regions of the curves are given in table 15. The fact that the moduli from all the tests agree fairly well for each of the comparable regions on the curves was to be expected because all the samples were in a saturated state once the first unloading cycle commenced. A

comparison of the values in this table will also show that when unloading from the virgin compression curve, the modulus is much greater than that of the first unloading cycle straight after inundation. The probable reason for this is that in the former case one is dealing with an elastic response while in the latter case the initial release of suction has a role to play.

TABLE 14 : Sample Preparation Data
for Oedometer Tests on Saturated Samples.

SAMPLE	INITIAL WATER (%)	FINAL WATER CONTENT (%)	DRY DENSITY (kg/cu m)
OD15/9	15.3	32.0	1445
OD20/8	20.1	31.8	1430
OD25/10	25.1	31.6	1383

TABLE 15 : Summary of Oedometer Modulus D from
Oedometer Compression of Saturated samples.

SAMPLE NUMBER	UNLOADING FROM POINT OF INUNDATION (MPa)	OVERCONSOLIDATED REGION (MPa)	UNLOADING FROM VIRGIN COMPRESSION CURVE (MPa)	VIRGIN COMPRESSION CURVE (MPa)
OD15/9	5	10	35	5
OD20/8	4	12	32	6
OD25/10	Non-linear	12	38	6

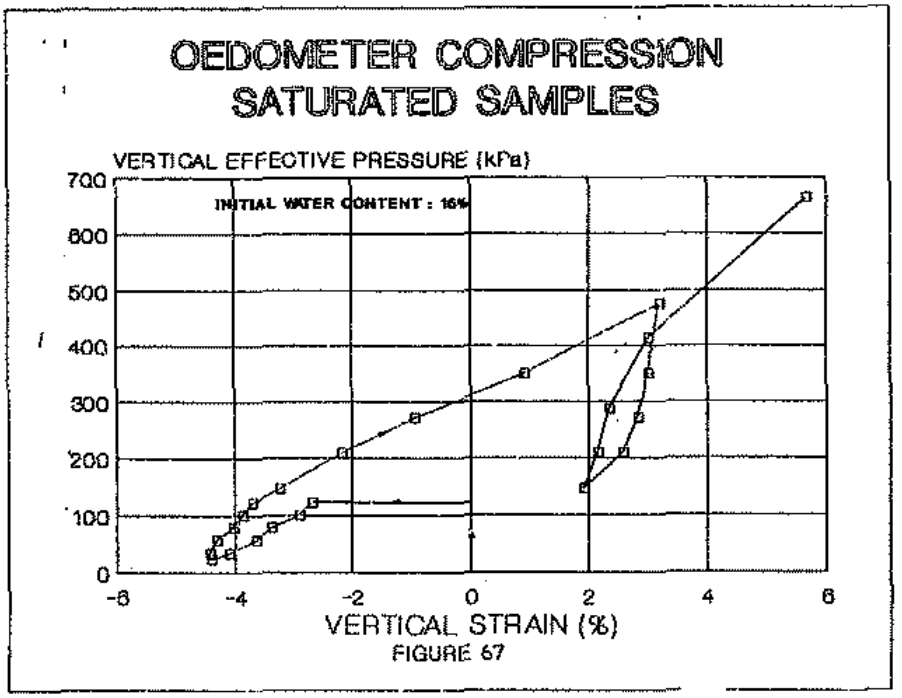

FIGURE 67

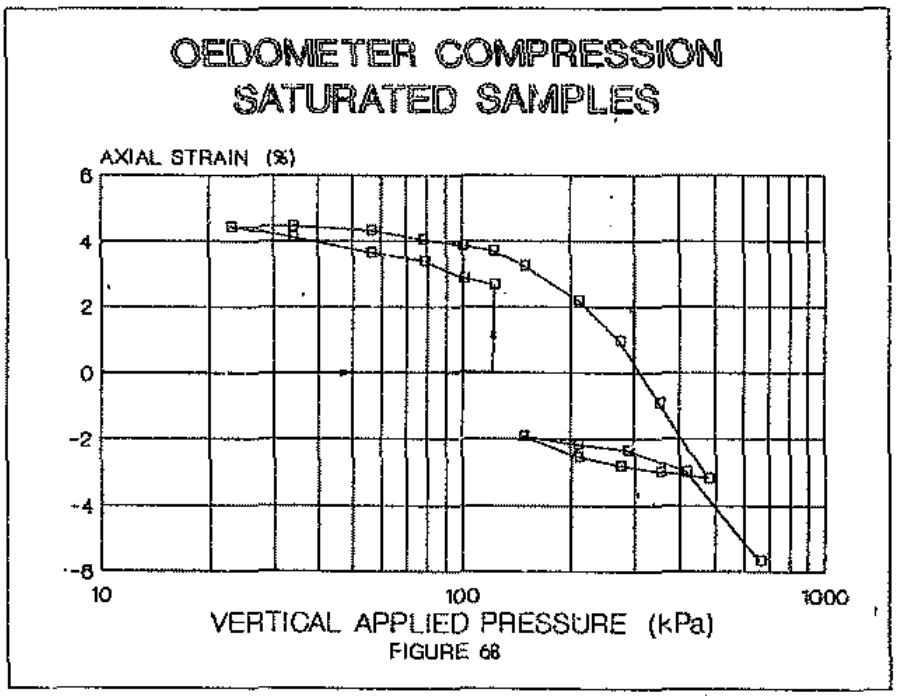

FIGURE 68

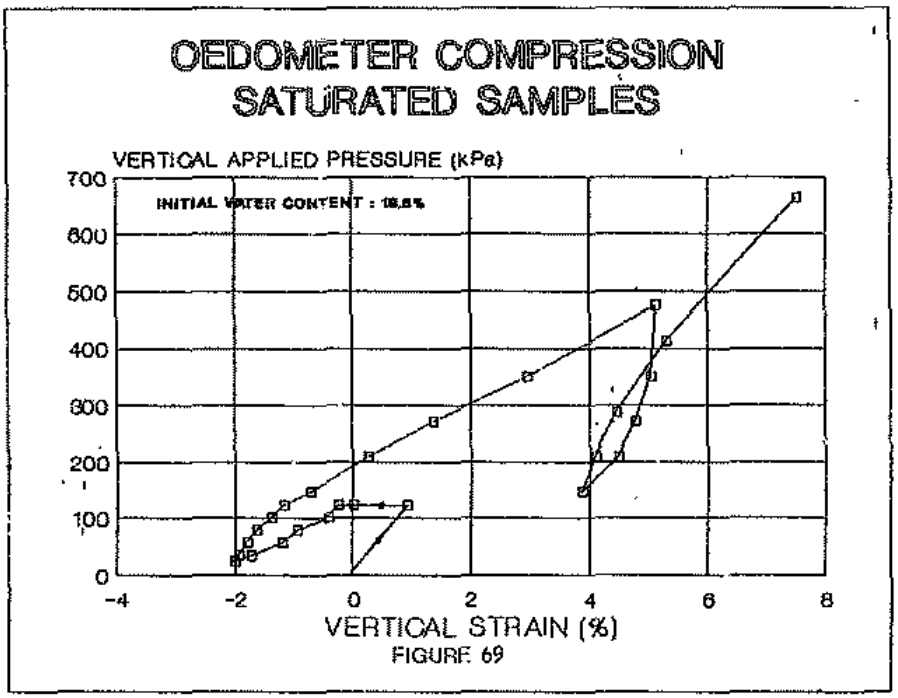

FIGURE 69

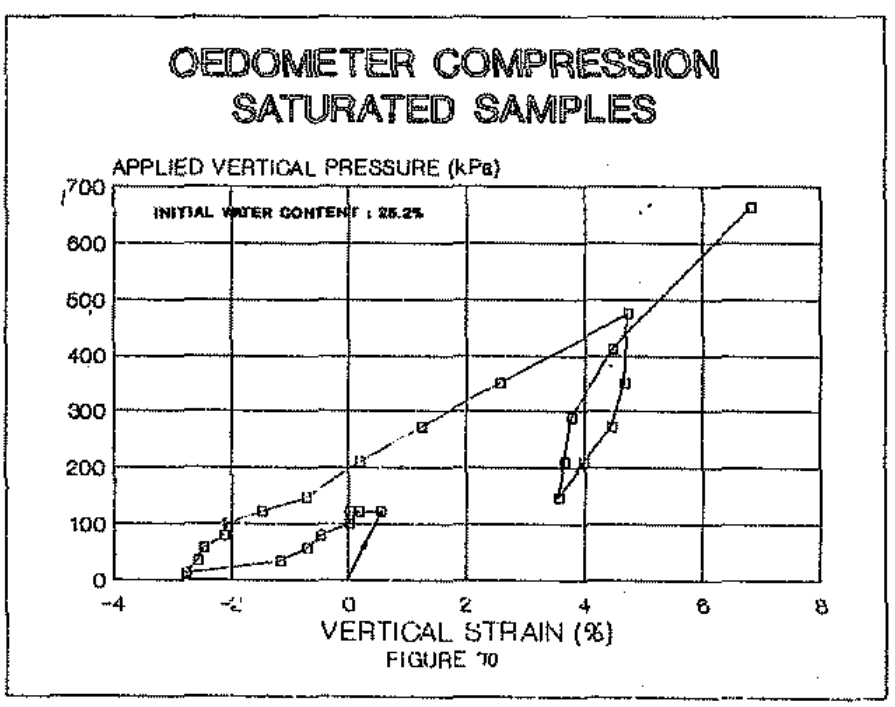

FIGURE 70

12.4 Oedometer Compression Tests at Constant Moisture Content

12.4.1 Experimental Technique

The aim of this series of tests was to determine the moduli obtained when the samples were compressed at constant moisture content.

All the samples were statically compacted in the mould as shown in figure 62, but in this case the porous stone was omitted and the samples were thus compacted to the full height of the ring. After compaction, the samples were sealed in plastic wrapping and allowed to cure for a period of four days. As usual, after the curing period, the sample had an uneven surface which necessitated sample recompaction to obtain smooth surfaces. Once the oedometer was mounted in the oedometer cell, the whole cell was sealed by means of a plastic bag, the opening of which, was taped to the sides of the oedometer cell. As a further precaution - to prevent moisture loss - moist strips of filter paper were also sealed in with the sample.

As in the case of the unconfined triaxial tests, samples with target initial water contents of 20%, 25% and 33% respectively were tested. The sample preparation data is given in table 16. Lastly, all the results were corrected for the effects of apparatus and filter paper deformations as previously described.

12.4.2 Discussion of the Results

Unfortunately, as indicated in table 16, sample OD33/2 lost an appreciable amount of water during the test, but if one assumes that only half of the moisture was lost during the initial load cycle, then the moisture loss cannot be considered to be too significant with regard to the calculated first load cycle modulus.

Figures 71 and 72 show the consolidation curves for the samples at water contents of 25% and 33% respectively. These curves show that a load duration of 24 hours may not be sufficient especially at lower loads. It was therefore decided to repeat the test at a moisture content of 33%, but this time a load duration of 48 hours would be used (figure 73). As expected, the curve with the longer load duration lies below that of the curve with the shorter load duration and furthemore, the shape of the two curves appears to be different.

Figure 74 presents the stress strain curves from the samples at water contents of roughly 20% and 26% and, as evident from these curves, there are two distinct regions to the stress strain curves. The first region occurs in the low stress range and is non-linear. No doubt, in this region, bedding-in effects have also had an influence on the results. The second region is linear and occurs at much larger stress ranges. This finding is consistent with the work of Fredlund (1969) who ascribes the linear behaviour to the compression of the air voids within the partially saturated soil. In the case of the sample at a water content of 33%, the normally and overconsolidated regions are more or less indistinct from each other particularly in the case of the samples which had a 48 hour load duration.

With regard to the sample at a water content of 20% it seems reasonable to conclude that the soil is still in the non-linear region and that perhaps at higher applied stress levels , the soil would also display a linear stress strain relationship. A C_v value has been calculated from the load deformation curves in the large stress range for the sample at an initial water content of 33% (figure 75). This sample was chosen for the C_v calculation because its initial water content corresponded to that of full saturation. As is expected, the C_v values are very small indeed.

Table 17 contains estimates of the moduli for the initial non-linear region of the curve as well as the linear region of the curve. Most of the samples are extremely stiff in the non-linear range which implies that the soil skeleton can take the load without deforming much itself. However, when more load is applied, the soil skeleton starts to deform appreciably whith a consequent reduction in stiffness.

It is interesting to note that in the case of the samples at a moisture content of 33%, the modulus is actually slightly less for a shorter load duration when working in the linear region over a comparable stress range. However, this difference could also be influenced by variations in the samples themselves.

It appears that, as far as the modulus corresponding to the linear region is concerned, it is not greatly affected beyond a water content of 25% by changes in water content. This may also be true for lower moisture contents as well, but unfortunately, the sample at a moisture content of 20 % was not loaded to a sufficiently high enough load to ascertain this fact.

TABLE 16 : Sample Preparation Data for Oedometer Compression at Constant Moisture Content.

SAMPLE	INITIAL WATER CONTENT (%)	FINAL WATER content (%)	DRY DENSITY (kg/cubic m)	LOAD DURATION (hrs)
OD33/2	33.6	27.6	1443	48
OD25/11	27.7	23.1	1443	48
OD20/9	19.7	19.3	1469	24
OD33/1	33.3	30.4	1432	24

TABLE 17: Oedometer Modulus D from Oedometer Compression at Constant Moisture Content.

SAMPLE	AVERAGE MODULUS IN NON-LINEAR REGION	MODULUS CALCULATED FROM LINEAR PORTION IN NORMALLY CONSOLIDATED RANGE.
OD20/9	36	-
OD33/1	17	12
OD33/2	8	16
OD25/11	27	10

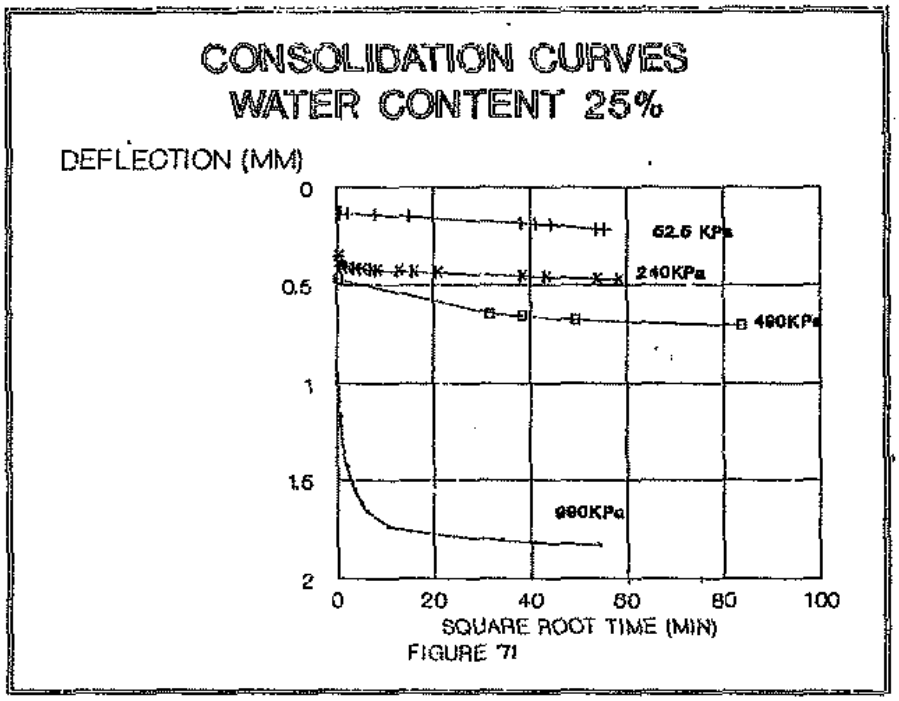

FIGURE 71

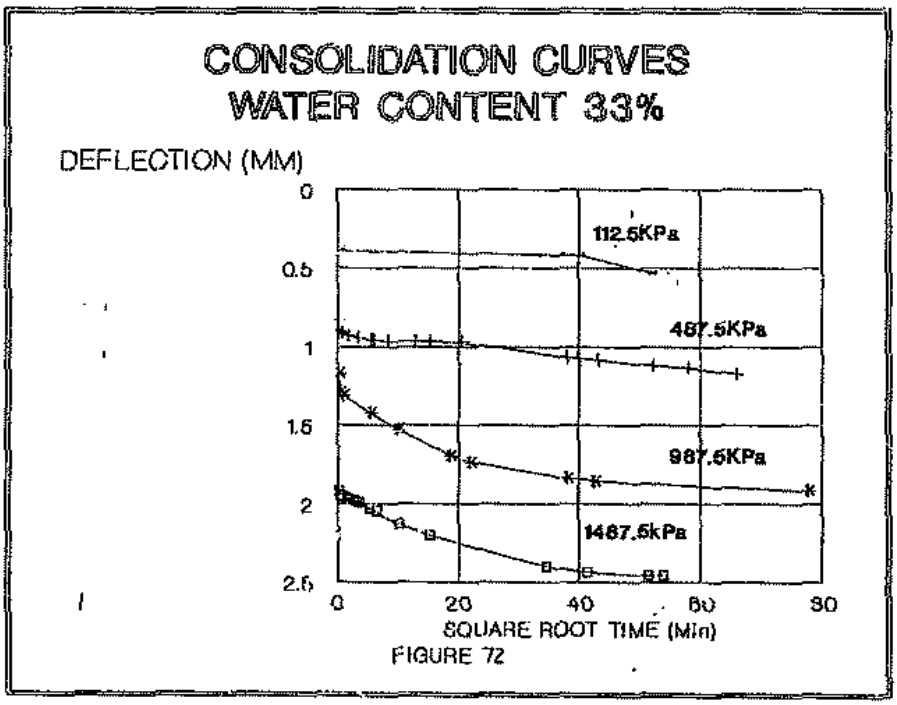

FIGURE 72

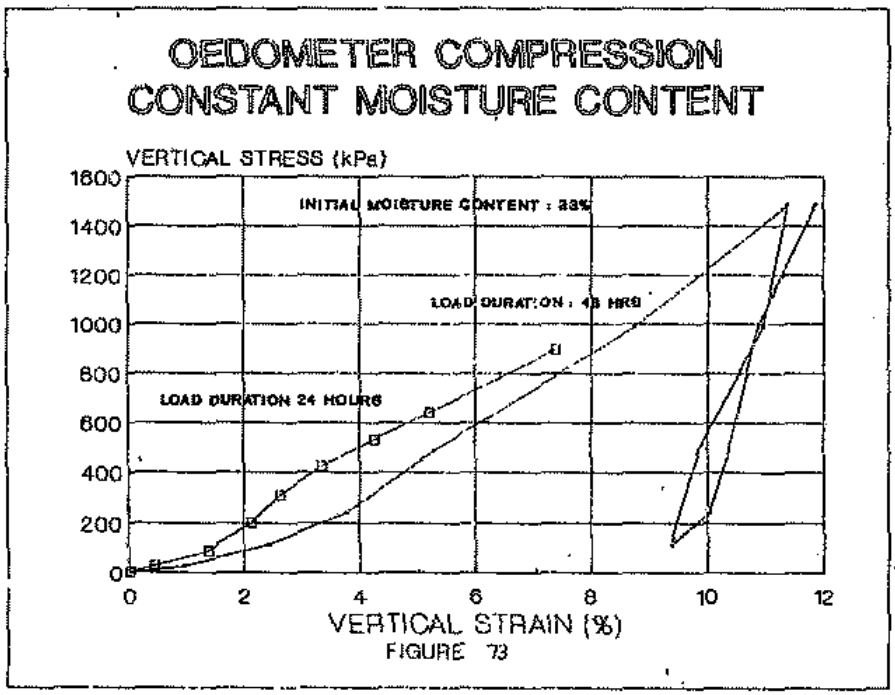

FIGURE 73

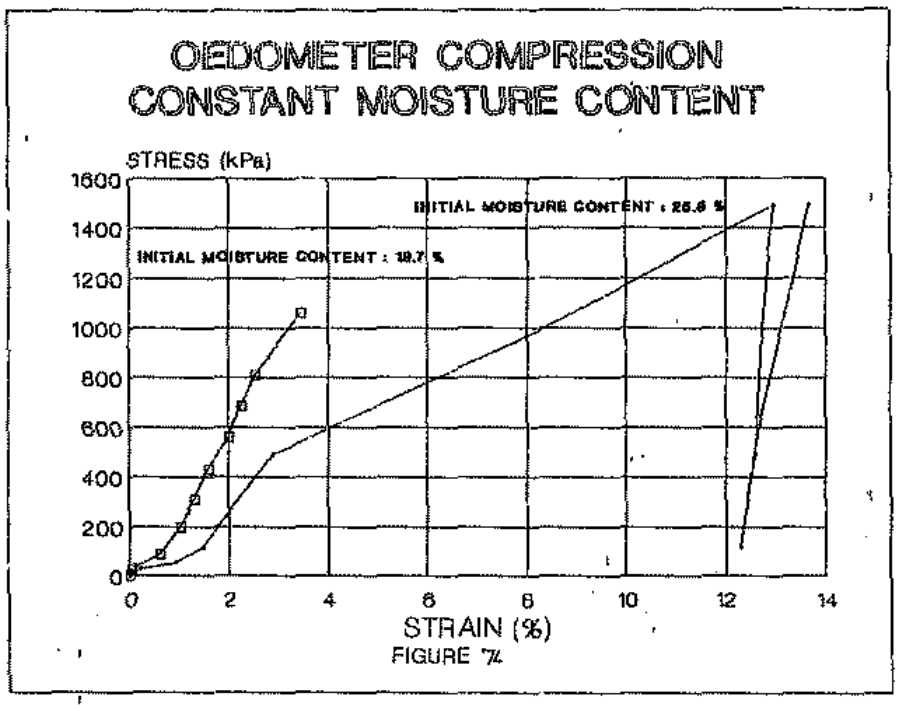

FIGURE 74

CONSOLIDATION CURVE
INITIAL WATER CONTENT 33%

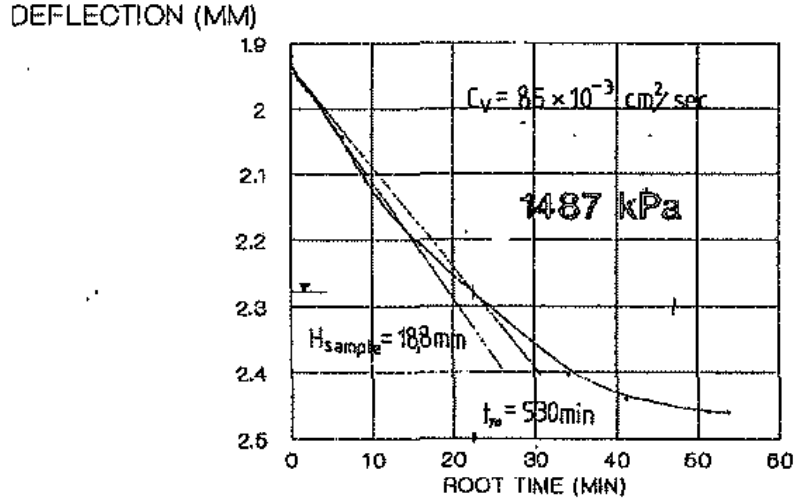

FIGURE 75

12.5 *Constant Rate of Strain Oedometer.*

12.5.1 Experimental Procedure.

This test series is the same as the constant moisture content tests in the oedometer, the only difference being that the method of loading was changed. As the name implies, the oedometer samples were loaded at a constant rate of strain. This was easily achieved by mounting the oedometer cell in the triaxial apparatus which was adapted slightly for the purpose. This adaption consisted of screwing a bar into the the base of the proving ring so that a connection was formed between the proving ring and the oedometer cell. The sample preparation technique was exactly the same as in the previous section so it will not be repeated here. However in this testing series, a slurry specimen was also prepared.

Before any samples were tested, a test was undertaken to determine how much deformation was actually due to the to deformations in the apparatus itself. In this test a steel plug together with filter paper was substituted for the sample in the oedometer cell and a stress strain curve for this arrangement was then plotted out. The results from this test showed that, after a bedding-in region, the stress strain curve was linear, having a slope of 90 MPa and 104 MPa for the wet and dry filter paper respectively. The bedding-in region extended from 0 to 0.2% strain which is an interesting finding because it shows that bedding-in effects are still significant even when the surfaces are relatively smooth. The actual curve that was used to correct the results was drawn through the origin because the amount of bedding-in varies with each different sample and thus cannot be corrected for.

Estimates of the required strain rate were based on data presented by Salfords (1975) who showed that strain rates in the wide range of 0.0006 to 0.02 mm/min would not generate significantly different stress strain curves for highly plastic saturated clays.

12.5.2 Presentation of the results

The sample preparation data is given in table 18. The first samples to be tested were samples OD20/10, OD25/12 and the slurry specimen (figures 76 and 77). The results from sample OD25/12 indicated that the stiffness was extremely large so it was therefore decided to repeat the tests at slower strain rates because it was suspected that the large stiffness was as a result of the excessively fast strain rates.

The results of these tests are shown in figure 78. The reason why the stress strain curve for the sample at a moisture content of 26% is so devoid of points is because the test was not slowed down during the evening.

On this figure, the results from the standard oedometer tests have also been plotted. In the case of the sample at a moisture content of 25% and tested under CRS conditions, the stress strain curve does not appear to show the two distinct regions as evident in the results from the standard test. Perhaps this is due to the fact that there are too few points on the curve as well as because the applied stress is not large enough to take the sample into the overconsolidated range. However, agreement between the two tests seems to be much better in the case of the sample at 33% moisture content.

The moduli are given in table 19. These moduli have were calculated by means of fitting a best-fit line through the points after bedding-in effects. In practice this was achieved by extrapolating a line backwards from the last point on the graph. In the case of the slurry specimen, a minimum and maximum modulus has been quoted to take into account the effects of non-linearity.

If one compares the moduli values from sample OD25/12 and OD25/13 then it turns out that the effect of reducing the strain rate by a factor of 13 was to reduce the modulus by a factor of 1.75. It would have been interesting to have repeated the test with an even slower strain rate, but the point has been made that it is preferable to use as slow a strain rate as possible.

TABLE 18: Sample Preparation Data for Constant Rate of Strain Oedometer.

SAMPLE	INITIAL WATER CONTENT (%)	FINAL WATER CONTENT (%)	DRY DENSITY (kg/cubic m)	STRAIN RATE (mm/min)
OD20/10	22.5	21.8	1464	0.0198
OD25/12	27.1	25.5	1406	0.00838
OD25/13	25.8	25.0	1469	0.00064
OD33/3	33.8	32.2	1465	0.00064
SLURRY	-	32.0	-	0.00838

TABLE 19: Moduli Values Determined from Constant Rate of Strain Oedometer Tests.

SAMPLE	MODULUS MEASURED AFTER POINT OF BENDING IN (MPa)
OD20/10	42
OD25/12	35
OD25/13	20
OD33/3	11
SLURRY	2-11

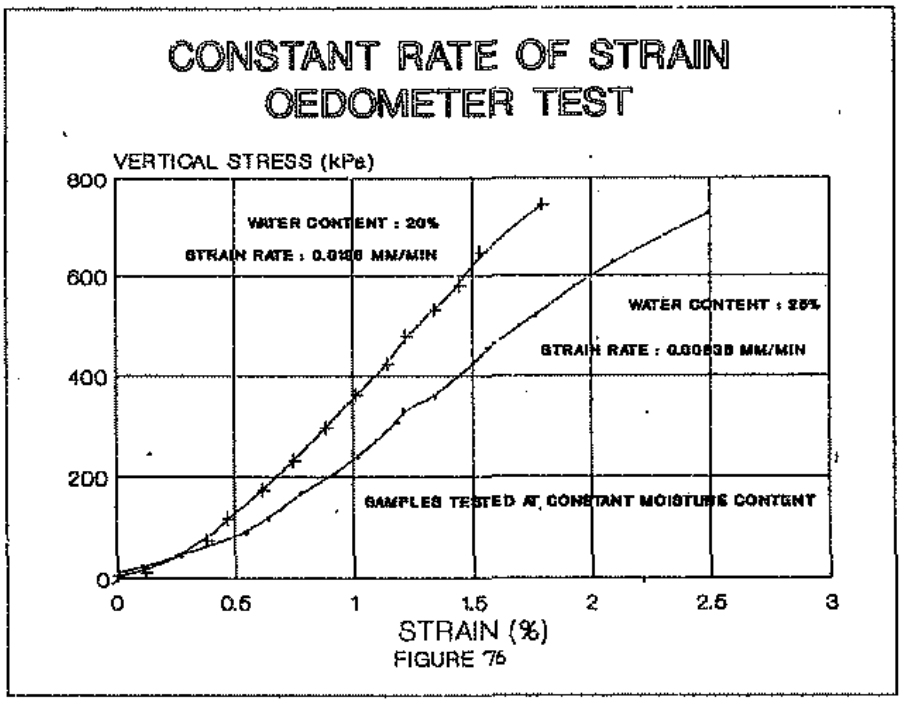

FIGURE 76

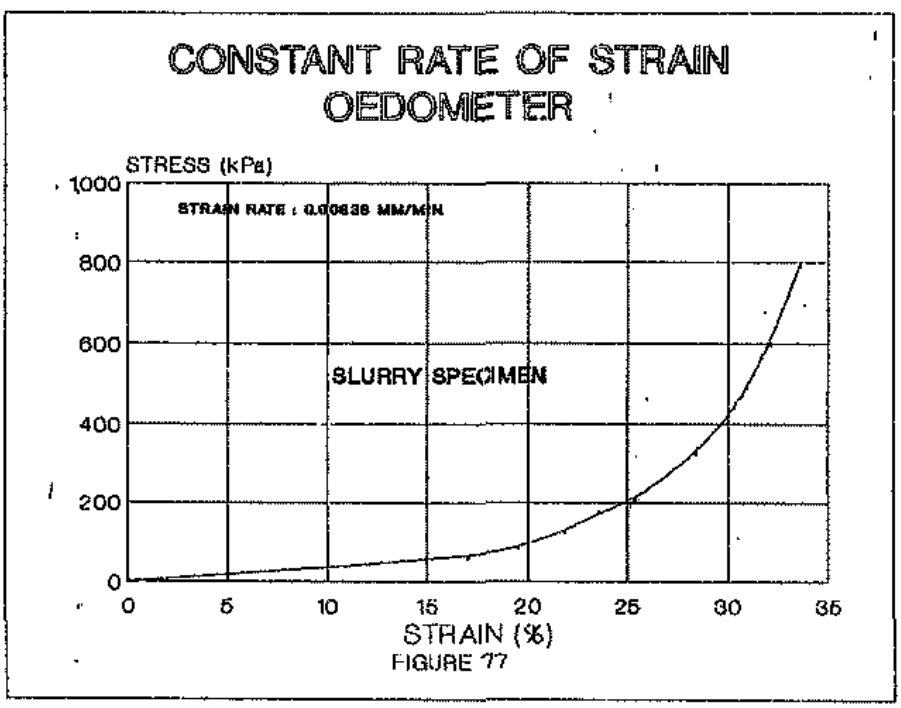

FIGURE 77

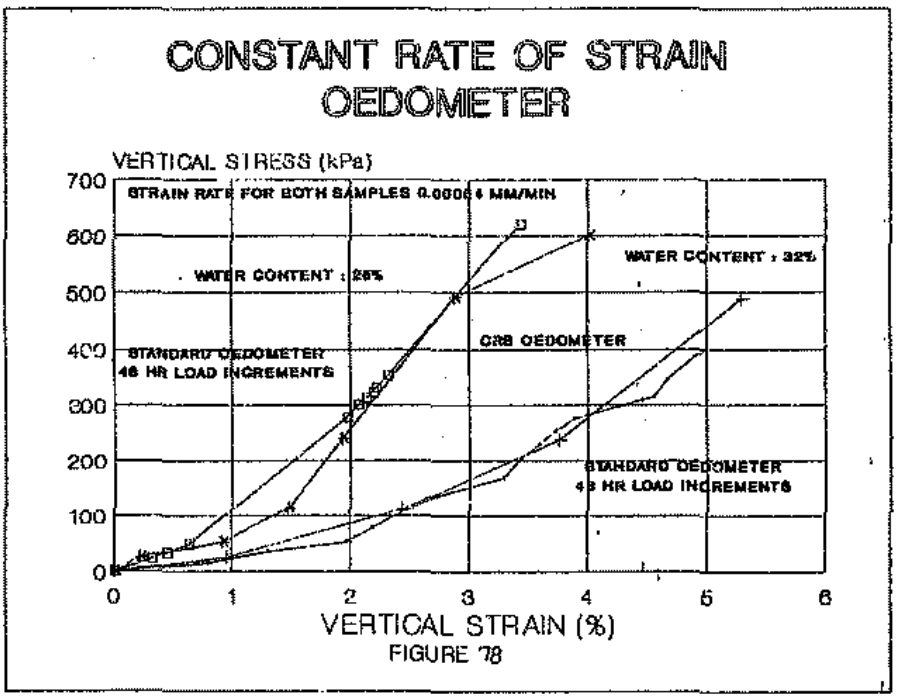
CONSTANT RATE OF STRAIN
OEDOMETER
VERTICAL STRESS (kPa)
700
600
500
400
300
200
100
0
STRAIN RATE FOR BOTH SAMPLES 0.0006 MM/MIN
WATER CONTENT : 28%
WATER CONTENT : 32%
STANDARD OEDOMETER
48 HR LOAD INCREMENTS
CRS OEDOMETER
STANDARD OEDOMETER
48 HR LOAD INCREMENTS
0
1
2
3
4
5
6
VERTICAL STRAIN (%)
FIGURE 78

12.6 Measured Oedometer Moduli Related to Raft Design.

The swell under load moduli determined here (table *11*) agree very well with the results from the Sanders (1989). For instance, at an initial moisture content of 22%, Sanders (loc. cit.) calculated a swell under load modulus of 1.76 MPa while the result obtained here is 1.72 MPa. Interestingly, Sanders used a much higher density of roughly 1800 kg/m^3 which seems to indicate that the swell under load modulus is not greatly effected by density. As was mentioned in the literature survey, it appears as if the value of the EEMM from the swell under load oedometer tests can be used directly in the evaluation of the EEMM where there is a deep residual layer of expansive clay. Alternatively, the swell under load oedometer tests can be used to define the swelling pressure and free swell of each soil layer, and equation 3 and 4 is then applied to calculate the EEMM.

The consolidation moduli belong to two well known regions, namely the overconsolidated region and the normally consolidated region respectively. In most cases, the overconsolidated modulus was of the order of twice the normally consolidated modulus. It is also evident that if swell is allowed to occur prior to consolidation, then lower moduli values are measured. For instance, the normally consolidated modulus is 16 MPa when the sample is consolidated from a saturated state, while it is only 6 MPa when the sample is consolidated from a point after swell has taken place.

In any event, the consolidation moduli are generally too large to be used in the raft design program developed by Pidgeon (1988). However, the moduli from the virgin compression curves of the samples that underwent swell, approach the low moduli values required for correct raft design simulation. But of course these values are only applicable at very large applied stresses which are not relevant to the field situation.

Conclusions and Recommendations

13.0 Laboratory and Field Moduli Compared.

The moduli from the field and laboratory are plotted in figure 79. The field results are taken from figure 40a while in the case of the laboratory tests, representative values for each type of test have been plotted. In this plot, the moduli values have been plotted against applic l stress simply because the applied stress range over which the moduli were measured is known for both the field and laboratory tests. It can of course be argued that the different moduli have been measured under such divergent conditions that they are not directly comparable. However, the purposes of this graph is to illustrate the large scatter in the results, rather than to establish some strict relationship between the variables.

It must be noted that the laboratory moduli have been plotted as a single point, whereas in reality, the moduli value is applicable over a wider stress range in some cases. For example, in the constant moisture content oedometer test, the normally consolidated modulus is applicable in the range 450-1400 kPa. Consequently, only the midpoint of the stress range is shown for the purposes of simplifying the plot and to gain a neater diagram. Also, in the case of the triaxial moduli, only the initial tangent moduli have been plotted for the second load cycle to represent the upper limit of modulus for this type of test. However, the true initial tangent moduli are probably even larger because the compliance of the apparatus itself was not accounted for.

The only correlation shown in the plot is a weak tendency for the results to fall into three groups. Group A represents values of modulus measured at low stresses and, even within this group, there is a large scatter. Besides the very good agreement between the field and laboratory swell under load test discussed previously, there is also fair agreement between the partially saturated triaxial modulus (water content 31%) and the CRP plate modulus. One would presume that the effect of fissures in he soil was responsible for reducing the modulus in the case of the CRP plate test.

Group C represents low values of modulus measured at high stresses. The values are low because either the high stresses force the soil into the normally consolidated range in the case of the oedometer, or because the soil was approaching failure in the case of the plate test.

Group B contains values of moduli which are relatively large at intermediate values of stress. Generally, oedometer moduli values from the overconsolidated range fall into this region. There appears to be good agreement between the pressuremeter modulus and the constant moisture content oedometer modulus at a water content of 25%. However, this ma' be partly coincidental because the two moduli values have been measured under vastly different conditions.

Finally, because the overall picture is one of large scatter in the results, it appears as if the laboratory and field moduli are poorly correlated, but more tests are required before this can be stated as a general fact. Perhaps, if it were possible to relate the moduli values to strain, then possibly a better correlation could be obtained. However, the swell under load laboratory and field tests agree very well which is extremely significant in the case of stiffened raft design as has been previously mentioned.

14.0 Reccomended Procedure to Determine the Modulus.

This work attempted to draw together the many estimates of modulus for the Onderstepoort clay. It has been shown that the scatter in the results is very large indeed, and this is partly due to the many different circumstances under which the modulus was measured. However, the large variation in the modulus must also surely be due to the complex nature of the material itself.

Thus, one cannot simply talk about 'a modulus' for a soil. One always needs to consider which modulus is most appropriate to the particular application to which the modulus is to be put. To illustrate this point, this project has clearly shown that the modulus for Onderstepoort clay can be anything between 1MPa and 145 MPa depending on the technique employed for it's measurement.

However, in the case of stiffened raft foundation design, back analysis of full scale experimental rafts as well as field swell under load tests have shown that a modulus as low as 2.6 MPa is applicable for Onderstepoort clay. Not surprisingly, the laboratory swell under load tests are the only tests which give moduli values within this range. For this reason, as well as the fact that the field and laboratory swell under load tests showed good agreement, it can be recommended that this test be used to determine the modulus or EEMM value required in the design program developed by Pidgeon (1988) where there is a deep residual soil layer. In the case where there are distinctly different soil layers with different soil properties, an analytical analysis using equations 3 and would have to be used. Also, the swell under load test is the only test which incorporates the process of swell which implies that this test emulates the field stress path a little more closely than all the other laboratory tests. On the other hand, it must also be stressed that the "modulus" derived from this test is not really a modulus in the true sense of the word. The fact that the swell under load modulus increases with decreasing water content illustrates this point.

The point to note is that, if it weren't for the back analysis of the raft it would be difficult to recommend an appropriate value of the modulus. Perhaps, without any other information, one would use a modulus somewhere between a consolidation modulus and a swell under load modulus. An analysis of this sort would yield a modulus of roughly 6 - 8 MPa for Onderstepoort clay. This happens to be of the order of four times the required modulus for accurate raft simulation for design purposes and therefore, the computer model requires some sort of "calibration" as it were. Perhaps it could be argued that this calibration process is required because the design model deviates so much from reality by using the "plate on mound" approach in the first place. No doubt if a different modelling approach was used (for instance a swell under load model), a different range of moduli values would be applicable.

In any case, it has been shown that, because of the large scatter in the modulus values, back analysis are definitely required in computer models to gain some idea of what the input values should be, and also what test correctly predicts this value.

15.0 Other General Conclusions

Other more general conclusions emanating from this work can be listed as follows:

1. With regard to the triaxial tests, it was found that at the same initial effective consolidation stress, there was reasonable agreement between the initial tangent modulus measured from the first load cycle in a standard test, and that measured in the stage loaded test. However, the shear strength of the stage loaded samples seemed to be reduced especially in the case of the drained tests.

2. The Brackley equation could be used to calculate the value of swell stiffness if the water content, PI and void ratio of the relevant soil layers are known. However, it has been shown that the equation is very sensitive to small changes in PI which makes it less useful in practise. Also, from the limited data presented here, it is evident that a normal plot instead of a log plot could be used to present the data from the swell under load tests because the coefficient of correlation using a normal plot is not significantly reduced as compared to using a log plot. Also, by using a normal plot, the Brackley swelling pressure can be more accurately defined.

3. At relatively low stress levels (say 0 to 500 kPa), the CRS oedometer and conventional oedometer produced stress strain curves which were relatively similar to each other for samples at water contents of 25% and 32% respectively. The correlation between the two tests at larger stresses cannot be commented upon because the CRS oedometer tests were only conducted to a stress of roughly 500 kPa.

16.0 Suggestions For Further Research

The next step in stiffened raft foundation design techniques, is the development of a design package which models the suction changes occuring under a raft and then quantifies the the resultant swell by means of a parameter similar to the Instability Index. Such an approach is described in detail by Pidgeon (1980c) but a design technique of this nature will not prove successful until stiffness is related to changes in suction. Obviously suction controlled oedometers would have to be used to quantify such a relationship.

I also believe that the effect of the use different solute types and concentrations in laboratory tests on expansive clays needs to be investigated further. The findings of such an investigation may show that the free swell and swelling pressure in the Brackley swell under load test is significantly influenced when the sample is inundated with a solution as opposed to distilled water.

MODULUS VS APPLIED PRESSURE

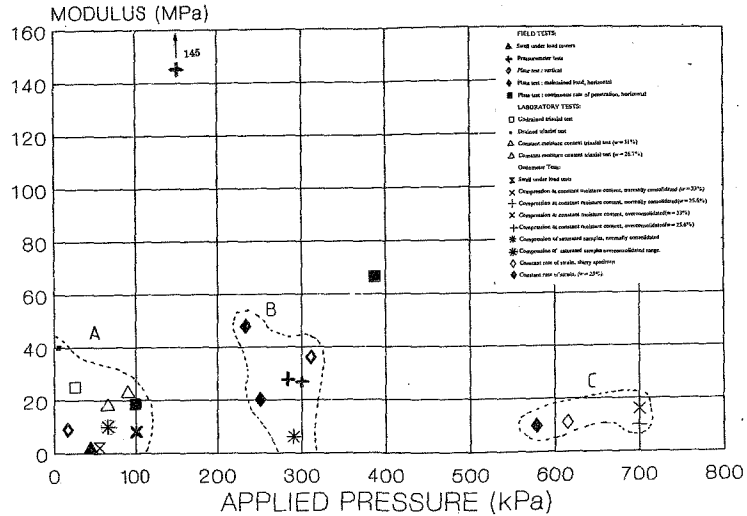

FIGURE 79

16.0 REFERENCES.

AITCHISON, G.D. (1973), Preface to a set of papers on the quantitative description of the stress-deformation behaviour of expansive soils. Proc. of the Third Int. Conf. on Expansive Soils, Haifa, Israel.

AITCHISON, G.D. and PETER, P. (1973), The measurement of *matrix suctions in expansive* clays, using the membrane oedometer. Proc. of the Third Int. Conf. on Expansive Soils, Haifa, Israel.

AITCHISON, G.D. and *WOODBURN, M.E. (1969), Soil suction* in foundation design. Proc. of the Seventh Int. Conf. on SM. and FE., Vol 2, p.7, Mexico City.

AITCHISON, G.D. and MARTIN, R. (1973), A membrane oedometer for complex stress-path studies in expansive clays. Proc. of the Third Int. Conf. on Expansive Soils, Haifa, Israel.

AITCHISON, G.D. and RICHARDS, B.G. (1965), A broad-scale study of moisture conditions in pavement subgrades throughout Australia. Moisture Equilibria and Moisture Changes in Soils Beneath Covered Areas. A Symposium in print. Butterworths. Australia

ALEXANDER, N.(1988),Personal Communication.

BISHOP, A.W. and BLIGHT, G.E.B. (1963), Some aspects of effective stress in saturated and partly saturated soils. Geotechnique, Vol 13, pp177- 197.

BISHOP, A.W. and HENKEL, (1972), The measurement of soil properties in the triaxial apparatus. Edward and Arnold, Second Edition.

BISHOP, A.W. and DONALD, I.B. (1961), The experimental study of partly saturated soils in the triaxial apparatus. Proc. of the Fifth Int. Conf. on *SM. and FE., Paris.*

BLIGHT, G.E.(1963),The effect of nonuniform pore pressure on laboratory measurements of the shear strength of soils. Laboratory *Shear testing of Soils. ASTM Special* Tech. Pub. 361.

BLIGHT, G.E. (1965), A study of effective stresses for volume change. Moisture Equilibria and Moisture Changes in *Soils Beneath Covered Areas. A Symposium* in print. Butterworths, Australia.

BLIGHT, G. E. (1989), Personal Communication

BOCKING, K.A. and FREDLUND, D.G. (1980), Limitations of the axis-translation technique. Proc. of the Fourth Int. Conf. on Expansive Soils. Denver, Colarado.

BRACKLEY, I.J.A. (1983), The effect of density, moisture content and loading on swelling of clays. National Building Research Institute, CSIR, Pretoria. Report number Bov 66 1983.

BRACKLEY, I.J.A. (1971), Partial collapse in unsaturated expansive clay. National Building Research Institute. South African Council for Scientific and Industrial Research, Pretoria. R/Bou 379 1971.

BRINK, A.B.A. (1979), Engineering Geology of Southern Africa. Volume 1. Building Publications, Pretoria.

BURLAND, J.B. (1965), Some aspects of the mechanical behaviour of partly saturated soils. Moisture Equilibria and Moisture Changes in Soils Beneath Covered Areas. A Symposium in print, Butterworths, Australia.

CHU, T.Y. and MOU, C.H. (1973), Volume change characteristics of expansive soils determined by controlled suction tests. Proc. of the Third Int. Conf. on Expansive Soils, Haifa, Israel.

De BRUIJN, C.M.A. (1973), Moisture Distribution and Soil Movements at Vereeniging (Transvaal). Proc. of the Third Int. Conf. on Expansive Soils, Haifa, Israel.

De BRUIJN, C.M.A. (1965), Annual redistribution of soil moisture suction and soil moisture density beneath two different surface covers and the associated heaves at the Onderstepoort test site near Pretoria. Moisture Equilibria and Moisture Changes Beneath Covered Areas. A Symposium in print. Butterworths, Australia.

ESCARIO, V. and SAEZ, J. (1973), Measurement of the properties of swelling and collapsing soils under controlled suction. Proc. of the Third Int. Conf. on Expansive Soils, Haifa, Israel.

FRASER, R.A. and WARDLE, L.J. (1975), The analysis of stiffened raft foundations on expansive soils. Symposium on recent developments in the analysis of soil behaviour and their applications to geotechnical structures. July 1975.

FREDLUND, D.J. (1969), Consolidation test procedural factors affecting swell properties. Proc. of the Second Int. Conf. on Expansive Soils.

GORMAN, C.T., HOPKINS, T.C., DEEN, R.C. and DRNEVICH, V.P., Constant-rate-of-strain and controlled-gradient consolidation testing. Geotechnical Testing Journal, GTJODJ, Vol 1, No.1, March 1978, pp3-15.

HAMBERG, D.J. and NELSON, J.D. (1984), Prediction of floor slab heave. Proc. of the Fifth Int. Conf. on Expansive Soils, Adelaide, Australia.

HO, D.Y.F. and FREDLUND, D.G., A multistage triaxial test for unsaturated soils. Geotechnical Testing Journal, GTJODJ, Vol 5, No.1/2, March/June 1982, pp18-25.

HOFMEYER, A. (1988), Personal Communication

HOLLAND, J.E. and RICHARDS, J. (1984), The practical design of foundations for light structures on expansive clays. Proc. of the Fifth Int. Conf. on Expansive Soils, Adelaide, Australia.

JARDINE, R.J., SYMES, M. J. and BURLAND, J. R. (1983), The measurement of soil stiffness in the triaxial apparatus. Geotechnique Vol34, No3 pp323-340

JENNINGS, J.E.B. and BURLAND, J.B. (1962), Limitations to the use of effective stresses in partly saturated soils. Geotechnique, Vol 12.

LADD, C.C. (1964), Stress-strain modulus of clay in undrained shear. Journal of the Soil Mechanics and Foundation Division, ASCE, No SM5, pp103-132, September 1964.

LAMBE, W.J. and WHITMAN, R.U. (1969), Soil mechanics. John Wiley and Sons Inc.

LEE, K.L., WHITE, W., and INGLES, O.G. (1983), Geotechnical Engineering. Pitman Books Limited.

Louw, H. H., (1980), How to avoid cracking in a house in heaving soils- a layman's guide. South African Geotech. Conf.

LYTTON, R.L. and MEYER, K.T. (1971), Stiffened mounts on expansive clay. Journal of the SM. and FE.. ASCE, July 1971, No.SM7.

MITCHELL, P.W. (1980), The structural analysis of footings on expansive soil. Kenneth W.G. Smith and Associates. Research Report No.1. Second Edition, March 1980.

MITCHELL, P.W. (1984), A simple method of design of shallow footings on expansive soil. Proc. of the Fifth Int. Conf. on Expansive Soils, Adelaide, Australia.

MOU, C.H. (1981), Soil suction approach for the evaluation of swelling potentials of expansive clays. PhD Thesis, University of South Carolina.

OLLIER, C. (1984), Weathering. Second Edition.Longman Group Limited

OLSON, R.E. and LANGFELDER, L.J. (1965), Pore-water pressures in unsaturated soils. Journal of the Soil Mechanics and Foundations Division, Proc. of the American Society of Civil Engineers, Vol 91, No.SM4, July 1965.

O'NEILL, W.M. and POORMOAYED, N. (1980), Methodology for foundations on expansive clays. Journal of the Geotechnical Engineering Division, ASCE, GT12, pp1345-1367.

PARTRIDGE, T. (1988) - Personal Communication

PELLISIER, J.P. (1987), Factors influencing rational stiffened raft design of heaving clays. Internal Report. CSIR. Pretoria, South Africa.

PELLISIER, J.P. (1987), Factors influencing rational stiffened raft design on heaving clays. Report for the National Building Research Institute, CSIR, Pretoria.

PELLISIER J, P (1989) - Personal Communication

PETER, P. (1979), Soil moisture suction. Footings and Foundations for Small Buildings in Arid Climates with Special Reference to Adelaide in South Australia, June 1979, pp46-62.

PETER, P.B. (1979), Soil moisture suction. Footings and Foundations in Arid Climates with Special Reference to Adelaide in South Australia. Fargher, P.J.; Woodburn, J.A. and Selby, J. Ed.

PIDGEON, J.T. (1980a), The interaction of expansive soil and a stiffened raft foundation. Seventh Regional Conf. for Africa on SM. and FE., Accra.

PIDGEON, J.T. (1980b), A comparison of existing methods for the design of stiffened raft foundations on expansive soils. Seventh Regional Conf. for Africa on SM. and FE., Accra.

PIDGEON, J.T. (1980c), The rational design of raft foundations for houses on heaving soil. Seventh Reg. Conf. for Africa on SM and FE., Accra

PIDGEON, J.T. (1987a), The results of a large scale field experiment aimed at studying the interaction of raft foundations and expansive soils. ENPC/DFCAI Conf. on Soil/Structure Interactions, Paris, France, 1987.

PIDGEON, J.T. (1987b), Personal communication.

PIDGEON, J.T. (1987c), The behaviour of an L-shaped raft subject to non-uniform support conditions. ENPC/DFCAI Conf. on Soil/Structure interactions, Paris, France 1987.

PIDGEON, J.T. (1988).Guide to the universal method for the rational design of stiffened raft foundations for small structures. Lecture notes for Course on the Design of Stiffened Raft Foundations and Articulated Structures on Expansive Clay soils, CSIR, Pretoria, 24-25 Aug 1988.

PILE, K.C. and McINNES, D.B. (1984), Laboratory technology for measuring properties of expansive clays. Proc. of the Fifth Int. Conf. on Expansive Soils, Adelaide, Australia.

PILE, K.C. (1984), The deformation of structures on reactive clay soils. Proc. of the Fifth Int. Conf. on Expansive Soils, Adelaide, Australia.

PORTER, A.A. and NELSON, J.D. (1980), Strain controlled testing of expansive soils. Proc. of the Fourth Int. Conf. on Expansive Soils, Denver, Colorado.

RICHARDS, B.G., PETER, P., and MARTIN, R. (1984), The determination of volume control properties of expansive soils. Proc. of the Fifth Int. Conf. on Expansive Soils, Adelaide, Australia, May 1984.

RPUG (1989). Raft Program User Group Newsletter, Sept 1989. Published by the CSIR Pretoria.

RUSSAM, K. and COLEMAN, J.D. (1961), The effect of climatic factors on subgrade moisture conditions. Geotechnique 11 (1), 22-28.

SANDERS, P.J. (1989), Test Analysis for the Equivalant Elastic Mound Modulus (EEMM). An Appraisal of Techniques. Division of Building Technology, CSIR, Pretoria. Int. Rep. 89/4

SNETHEN, R.D. (1969), Characterisation of expansive soils using soil suction data. Proc. of the Fourth Int. Conf. on Expansive Soils, Denver, Colorado, Vol I, pp54-75.

VAN DER MERWE, D.H. (1967), The composition and physical properties of the clay soils on the mafic rocks of the Bushveld Igneous Complex. Proc. of the Fourth Reg. Conf. for Africa on SM and FE, Cape Town, Vol 1

WALSH, P.F. (1984), Concrete slabs for houses. CSIRO Aust. Div. Bldg. Res. Tech. Pap. (Second series) No.48, pp1-23.

WALSH, P.F. (1978), The analysis of stiffened rafts on expansive clay. Division of Building Research Technical Paper (Second series) N0.23, CSIRO Australia.

WILLIAMS, A.A.B. and PIDGEON, J.T. (1983), Evapo-transpiration and heaving clays in South Africa. Geotechnique 33 (2), 1983.

WILLIAMS, A.A.B., PIDGEON, J.T. and DAY, P.W. (1985), Expansive soils. State of the Art Report, The Civil Engineer in South Africa, July 1985.

WILLIAMS, A. A. B (1987), Personal Communication

WISSA, A.Z., CHRISTIAN, J.T., DAVIES, E.H., and HEIBERG, S. (1971), Consolidation of constant rate of strain. Journal of the Soil Mechanics and Foundation Division, Proc. of the ASCE, Vol 97, SMIO, Oct. 1971.

WOODBURN, J. (1979), Design of footings on clay soils. Footings and Foundations for Small Buildings in Arid Climates. Fargher, P.J., Woodburn, J., and Selby, J. Editors.

Author David Richard
Name of thesis The Laboratory Determination Of Young's Modulus For An Expansive Clay With Particular Reference To Stiffened Raft Foundation Design. 1989

PUBLISHER:
University of the Witwatersrand, Johannesburg
©2013

LEGAL NOTICES:

Copyright Notice: All materials on the University of the Witwatersrand, Johannesburg Library website are protected by South African copyright law and may not be distributed, transmitted, displayed, or otherwise published in any format, without the prior written permission of the copyright owner.

Disclaimer and Terms of Use: Provided that you maintain all copyright and other notices contained therein, you may download material (one machine readable copy and one print copy per page) for your personal and/or educational non-commercial use only.

The University of the Witwatersrand, Johannesburg, is not responsible for any errors or omissions and excludes any and all liability for any errors in or omissions from the information on the Library website.